Tungsten-acetylene hydratase from *Pelobacter acetylenicus* and molybdenum-transhydroxylase from *Pelobacter acidigallici*: Two novel molybdopterin and iron-sulfur containing enzymes

Dissertation submitted to

Fachbereich Biologie, Universität Konstanz, Germany

for the degree of

Doctor of Natural Sciences

by

Dipl.-Biol. Dietmar Josef Abt

Konstanz, July 2001

Dissertation der Universität Konstanz
Datum der mündlichen Prüfung: 10. September 2001

Referent: Prof. Dr. P.M.H. Kroneck
Referent: Prof. Dr. B. Schink

Für meine Eltern

“... to boldly go where no man has gone before.“

(Star Trek)

Table of Contents

Zusammenfassung ..... **IV**

Summary ..... **VII**

1. Introduction 1

1.1. Physical and chemical properties of molybdenum and tungsten 1
1.2. The mononuclear molybdenum and tungsten enzymes 3
1.3. The molybdenum cofactor 6
1.4. Iron-sulfur centers 7
1.5. *Pelobacter acetylenicus* acetylene hydratase 9
1.5.1. Acetylene metabolism 10
1.5.2. Molecular properties of acetylene hydratase 11
1.6. *Pelobacter acidigallici* transhydroxylase 12
1.6.1. Metabolism of gallic acid by *Pelobacter acidigallici* 12
1.6.2. Molecular properties of transhydroxylase 13
1.7. Scope of the study 15

2. Materials and Methods **16**

2.1. Chemicals and biochemicals 16
2.2. Organisms 17
2.2.1. *Pelobacter acetylenicus* 17
2.2.2. *Pelobacter acidigallici* 18
2.3. Cultivation of bacteria 18
2.3.1. *Pelobacter acetylenicus* 18
2.3.2. *Pelobacter acidigallici* 22
2.4. Glycerol cryo-cultures 23
2.5. Enzyme purification 23
2.5.1. Acetylene hydratase 24
2.5.2. Transhydroxylase 25
2.6. Enzyme activity 26
2.6.1. Acetylene hydratase 26
2.6.2. Transhydroxylase 27
2.6.3. Alcohol dehydrogenase 28
2.7. UV/Vis spectroscopy 28
2.8. EPR spectroscopy 29
2.9. Crystallization 29
2.10. Sequencing of the acetylene hydratase gene 30
2.10.1. N-terminal amino acid sequencing 30
2.10.2. Cyanogen bromide digestion 31
2.10.3. DNA preparation 31
2.10.3. Primers for polymerase chain reaction 32
2.10.4. PCR techniques 32
2.10.5. Sequencing 35
2.10.6. Cloning 36
2.10.7. Computer programs and Internet websites 37

2.10.8. Sequence handling and phylogenetic analysis 38
2.11. Analytical methods 38
2.11.1. ICP-MS 38
2.11.2. Protein 39
2.11.3. Polyacrylamide gel electrophoresis 39
2.11.4. Agarose gels 39

3. Results 40

3.1. Acetylene hydratase of *Pelobacter acetylenicus* 40
3.1.1. Growth of *Pelobacter acetylenicus* under various conditions 40
3.1.2. Purification of acetylene hydratase 41
3.1.3. Thermostability of acetylene hydratase, Y-ADH, and S-ADH 45
3.1.4. Long-term study on acetylene hydratase activity 47
3.1.5. Metal content of acetylene hydratase 47
3.1.6. UV/Vis spectra of acetylene hydratase 48
3.1.7. EPR spectra of acetylene hydratase 49
3.1.8. Identification, amplification, and sequencing of the acetylene hydratase gene structure via PCR based techniques 53
3.1.9. Crystallization and three-dimensional structure of acetylene hydratase 61
3.1.10. Acetylene hydratase activity in *Archaeoglobus fulgidus* 62
3.2. Transhydroxylase of *Pelobacter acidigallici* 63
3.2.1. Growth of *Pelobacter acidigallici* 63
3.2.2. Purification of transhydroxylase 63
3.2.3. UV/Vis spectra of transhydroxylase 65
3.2.4. EPR spectra of transhydroxylase 66
3.2.5. Crystallization and three dimensional structure of transhydroxylase 68
3.3. Phylogenetic analysis of acetylene hydratase and transhydroxylase 69
3.3.1. The DMSO-reductase family 69
3.3.2. The DMSO-reductase subfamily 73

4. Discussion 76

4.1. Molybdenum *versus* tungsten in enzymes 76
4.2. Cultivation of the bacteria and enzyme purification 77
4.2.1. *Pelobacter acetylenicus* 78
4.2.2. *Pelobacter acidigallici* 79
4.3. Spectroscopic properties of acetylene hydratase and transhydroxylase 80
4.3.1. UV/Vis spectroscopy 80
4.3.2. EPR-spectra of acetylene hydratase 81
4.3.3. EPR-spectra of transhydroxylase 83
4.4. Evolution of the DMSO-reductase family 85
4.4.1. Relationships of the tree domains of life 85
4.4.2. The DMSO-reductase subfamily 88
4.5. Towards the reaction mechanisms of acetylene hydratase and transhydroxylase 90
4.5.1. Acetylene hydratase 90
4.5.2. Transhydroxylase 91
4.5.3. Is there a tyrosine at the active site? 97

5. References **100**

6. Appendix **109**

6.1 Abbreviations 109
6.2. Amino acids 110
6.3. Nucleic acid bases 111
6.4. International System of Units (SI) 111
6.5. Acknowledgements 112
6.6. Curriculum vitae 114
6.7. Publications 115
6.8. Conference abstracts 116

Zusammenfassung

1. Acetylenhydratase aus *Pelobacter acetylenicus*

P. acetylenicus ist ein mesophiles, strikt anaerob lebendes Bakterium, das in der Lage ist, auf Acetylen als einziger Kohlenstoff- und Energiequelle zu wachsen. Die Metabolisierung von Acetylen wird durch das W/Fe-S abhängige Enzym Acetylenhydratase eingeleitet, wobei in einer ungewöhnlichen Reaktion Acetylen zu Acetaldehyd hydratisiert wird.

Das Enzym Acetylenhydratase wurde aus *P. acetylenicus* zur Homogenität gereinigt. Es handelt sich um ein Monomer mit einer molekularen Masse der Aminosäurekette von 81.9 kDa. Das Enzym gehört zur Familie der DMSO-Reduktasen. Acetylenhydratase ist ein thermostabiles Enzym, dessen Temperaturoptimum im Bereich von 50 bis 55°C liegt. In einer Stickstoff/Wasserstoff Atmosphäre bei 6°C konnte das Enzym 3 Monate gelagert werden, ohne daß ein Aktivitätsverlust festgestellt wurde. Obwohl die Acetylenhydratase keine Redox-Reaktion katalysiert, enthält sie ein [4Fe-4S] Zentrum und einen W-bisMGD Kofaktor. Mittels ICP/MS, EPR und UV/Vis wurde gezeigt, daß *P. acetylenicus* in der Lage ist, sowohl Wolfram als auch Molybdän in den bisMGD Kofaktor einzubauen. Das hochaktive W-Enzym (42,3 U mg^{-1}, 50°C) enthält 3,5 Eisen und 1,1 Wolfram. Molybdän hingegen war nicht vorhanden. Das Mo-Isoenzym enthält 3,1 Eisen, 0,5 Molybdän und praktisch kein Wolfram. Die spezifische Aktivität (16,7 U mg^{-1}, 50°C) ist signifikant geringer als die spezifische Aktivität des W-Enzyms. Eine Vanadium-abhängige Acetylenhydratase konnte nicht erhalten werden. Das gereinigte Enzym der Vanadium-Anzucht enthielt praktisch kein Vanadium und nur wenig Wolfram und Molybdän (beide etwa 0,05 mol pro mol Acetylenhydratase). Die spezifische Aktivität war sehr gering (2,6 U mg^{-1}, 50°C). Die EPR-Spektren Dithionit-reduzierter Acetylenhydratase aus den Wolframat, Molybdat und Vanadat Anzuchten zeigten typische Signale von [4Fe-4S] Zentren bei $g_{av} = 1{,}97$. Das mit $[Fe^{III}(CN)_6]^{3-}$ oxidierte Enzym der Wolframat und Vanadat Anzucht zeigte Resonanzen eines W(V) Zentrums, das Enzym der Molybdat (^{95}Mo) Anzucht die eines ^{95}Mo(V) Zentrums. Im UV/Vis Spektrum erkennt man die breiten Absorptionsschultern der Eisen-Schwefel Zentren bei etwa 400 nm und Schwefel→Wolfram Ladungstransfer Übergänge um 600 nm.

Kristalle der W-Acetylenhydratase wurden in Anwesenheit und in Abwesenheit (N_2 : H_2 = 94 : 6 v/v) von Luftsauerstoff erhalten. Dithionit-reduziertes Enzym ergab, unter Ausschluß von Luftsauerstoff, Kristalle, die am Deutschen Elektronen Synchrotron (DESY) in Hamburg vermessen wurden und bis zu Auflösungen unter 2,5 Å streuten. Die Verfeinerung der Kristallisationsbedingungen und die Strukturlösung wird im Moment am Max-Planck-Institut für Biochemie und an der Universität Konstanz, in Zusammenarbeit mit Dipl. Biol. Holger Nießen (Universität Konstanz) und Dr. Oliver Einsle (Max-Planck-Institut für Biochemie, Martinsried), weitergeführt.

Die Sequenzierung von etwa 6000 Basen der Acetylenhydratase-Genregion ergab, daß direkt vor der Acetylenhydratase ein offenes Leseraster (orf) liegt, welches für ein Protein kodiert, dessen Primärstruktur keine signifikante Homologie zu anderen Proteinen aufweist. Vor diesem orf liegt ein weiteres Leseraster, das ansequenziert wurde. Es weist eine signifikante Homologie zu Genen von Reverse Transkriptase/Maturase-Proteinen auf. Phylogenetische Untersuchungen auf Aminosäureebene zeigten, daß die Acetylenhydratase zur Familie der DMSO-Reduktasen gehört. Diese Familie unterteilt sich in sieben Unterfamilien: Die DMSO-Reduktasen, eine Unterfamilie von Oxidoreduktasen mit unbekannten Aktivitäten, die Polysulfid/Thiosulfat-Reduktase-Unterfamilie, die Acetylenhydratase-Unterfamilie, die Nitrat-Reduktase-Unterfamilie und die Formatdehydrogenase-Unterfamilie. Eine Oxidoreduktase mit unbekannter Aktivität aus *Streptomyces coelicolor* ist der einzige Vertreter der siebten Unterfamilie.

2. Transhydroxylase aus *Pelobacter acidigallici*

P. acidigallici ist ein strikt anaerob lebendes Bakterium, das in der Lage ist, mit Gallussäure (3,4,5-Trihydroxybenzoesäure), Pyrogallol (1,2,3-Trihydroxybenzol), Phloroglucin (1,3,5-Trihydroxybenzol) oder 2,4,6-Trihydroxybenzoesäure als einziger Kohlenstoff- und Energiequelle zu leben. Ein entscheidender Schritt während der Metabolisierung von decarboxylierter Gallussäure (Pyrogallol) ist die Transhydroxylierung des Pyrogallols zum Phloroglucin. Diese Reaktion wird von dem Mo/Fe-S abhängigen Enzym Transhydroxylase (Pyrogallol:Phloroglucin Hydroxyltransferase E.C. 1.97.1.2) katalysiert.

Mittels eines neuen Reinigungsverfahrens wurde das Enzym Transhydroxylase aus *P. acidigallici* zur Homogenität gereinigt. Es handelt sich um ein Heterodimer, das aus einer großen Untereinheit (100,4 kDa) und einer kleinen Untereinheit (31,3 kDa) besteht. Das Enzym ist eng mit Mitgliedern der DMSO-Reduktase Familie verwandt. Obwohl die Gesamtreaktion der Transhydroxylase keine Redoxreaktion ist, enthält das Enzym einen Mo-bisMGD Redoxkofaktor und verschiedene Eisen-Schwefel Zentren. Im EPR-Spektrum des „as isolated" Enzyms erkennt man ein Mo(V) Zentrum mit einem g_{av} = 1,98. Das mit Dithionit reduzierte Enzym zeigt Signale von verschiedenen [4Fe-4S] Zentren. Die Anwesenheit von [2Fe-2S] Zentren kann nicht ausgeschlossen werden. Im UV/Vis Spektrum erkennt man die Absorptionsschulter der Eisen-Schwefel Zentren um 400 nm und die von Schwefel→Molybdän Ladungstransfer Übergängen bei 700 nm.

Mit BLASTP Suchen wurde gezeigt, daß 12 der 13 Cysteine der kleinen Untereinheit der Transhydroxylase hochkonserviert sind. Einige davon sind als [4Fe-4S] Ferredoxine beschrieben worden. Die 15 Cysteine der großen Untereinheit lassen sich nicht mit den Cysteinen anderer Proteine abgleichen. Aus diesem Grund ist es wahrscheinlich, daß die Eisen-Schwefel Zentren sich auf der kleinen Untereinheit befinden.

Kristallisationsexperimente und der Beginn der Strukturaufklärung wurden in Zusammenarbeit mit Dipl. Biol. Holger Nießen und Dr. Oliver Einsle durchgeführt. Experimente mit „as isolated"-Transhydroxylase führten zu Kristallen, die im Röntgenstrahl nicht beugten. Die Kristallisation von Dithionit-reduzierter Transhydroxylase unter den anoxischen Bedingungen einer Stickstoff/Wasserstoff-Atmosphäre führte zu Kristallen, die zunächst bis 3,4 Å streuten. Durch Verfeinerungen der Kristallisationsbedingung konnten Kristalle erhalten werden, die mit Synchrotonstrahlung bis zu einer Auflösung unter 2,5 Å streuten.

Phylogenetische Untersuchungen auf Aminosäureebene zeigten, daß die Transhydroxylase ebenfalls zur Familie der DMSO-Reduktasen gehört. Im Gegensatz zur Acetylenhydratase gehört sie zur Unterfamilie der DMSO-Reduktasen, die sich in fünf Gruppen aufteilt: Die Gruppe der *Rhodobacter* DMSO-Reduktasen, die Gruppe der TMAO-Reduktasen, die Gruppe der BSO-Reduktasen, die Gruppe der DMSO-Reduktasen der Proteobakterien und in die Transhydroxylase-Gruppe.

Summary

1. Acetylene hydratase from *Pelobacter acetylenicus*

P. acetylenicus is a strictly anaerobic and mesophilic bacterium that is able to grow on acetylene as single energy and carbon source. The first step in the metabolization of acetylene is the transformation of acetylene to acetaldehyde. This addition of water is catalyzed by the W/Fe-S dependent enzyme acetylene hydratase.

Acetylene hydratase from *P. acetylenicus* was purified to homogeneity. It is a monomer with a molecular mass of the amino acid chain of 81.9 kDa. BLASTP searches revealed that the enzyme is highly similar to enzymes of the DMSO-reductase family. Acetylene hydratase is a thermostable enzyme with a temperature optimum between 50 and 55°C. It is a very stable enzyme when stored under exclusion of dioxygen in a nitrogen/hydrogen atmosphere at 6°C. Within three months, there was no detectable loss of acetylene hydratase activity from tungstate-grown *P. acetylenicus*. Although acetylene hydratase catalyzes no redox reaction, it contains one [4Fe-4S] center and one W-bisMGD as redox-cofactors. ICP/MS, EPR, and UV/Vis-spectroscopy revealed that *P. acetylenicus* is able to insert tungsten as well as molybdenum into the bisMGD cofactor of acetylene hydratase. The highly active W-enzyme (42.3 U mg^{-1}, 50°C) contained 3.5 mol iron and 1.1 mol tungsten per mol acetylene hydratase, whereas molybdenum was absent. The Mo-isoenzyme contained 3.1 mol iron, 0.5 mol molybdenum, and practically no tungsten per mol enzyme. The specific activity (16.7 U mg^{-1}, 50°C) was significantly lower than the specific activity of the W-enzyme. A vanadium containing acetylene hydratase was not obtained. The purified enzyme from the corresponding vanadate cultivation contained practically no vanadium and only little amounts of tungsten and molybdenum (each ≈ 0.05 mol per mol acetylene hydratase). The specific activity was detectable but very low (2.6 U mg^{-1}, 50°C). EPR-spectroscopic investigation of dithionite reduced acetylene hydratase from tungstate, molybdate (^{95}Mo), and vanadate cultivation showed signals of [4Fe-4S] centers with $g_{av} = 1.97$. The $[Fe^{III}(CN)_6]^{3-}$ oxidized enzymes from tungstate and vanadate cultivations exhibited resonances of a W(V) center. The enzyme from molybdate (^{95}Mo) cultivation showed resonances of a ^{95}Mo(V) center. UV/Vis spectra showed absorption shoulders resulting from the iron-sulfur clusters around 400 nm and from sulfur-to-tungsten charge-transfer transitions around 600 nm.

Crystals of W-acetylene hydratase were obtained both in the presence and in the absence of dioxygen (N_2 : H_2 = 94 : 6 v/v). The crystals, grown under exclusion of dioxygen in the presence

of dithionite, diffracted to a resolution better than 2.5 Å. Crystallographic data were obtained at the Deutsche Elektronen Synchrotron (DESY) and were processed in collaboration with Dipl. Biol. Holger Nießen (Universität Konstanz) and Dr. Oliver Einsle (Max-Planck-Institut für Biochemie, Martinsried).

Sequencing of about 6000 bases of the acetylene hydratase gene-region showed an open reading frame (orf) in front of the acetylene hydratase gene that codes for a protein whose primary structure has no significant similarity to any other enzymes. In front of this orf there is another orf that was partially sequenced. It showed significant similarity to genes of reverse transkriptase/maturase proteins. Phylogenetic analyses, based on amino acid sequences, revealed that acetylene hydratase belongs to the family of the DMSO-reductases. This family can be divided into seven subfamilies, namely the DMSO-reductase subfamily, the oxidoreductases with unknown activity subfamily, the polysulfide/thiosulfate-reductase subfamily, the acetylene hydratase subfamily, the nitrate reductase subfamily, and the formate-dehydrogenase subfamily. An oxidoreductase with unknown activity from *Streptomyces coelicolor* is the only member of the seventh subfamily.

2. Transhydroxylase from *Pelobacter acidigallici*

P. acidigallici is a strictly anaerobic bacterium that is able to live on gallic acid (3,4,5-trihydroxybenzoic acid), pyrogallol (1,2,3-trihydroxybenzene), phloroglucinol (1,3,5-trihydroxy-benzene), or 2,4,6-trihydroxybenzoic acid. A crucial step in the fermentation of decarboxylated gallic acid (pyrogallol) is the transhydroxylation of pyrogallol to phloroglucinol. This reaction is catalyzed by the Mo/Fe-S dependent enzyme transhydroxylase (pyrogallol:phloroglucinol hydroxyltransferase E.C. 1.97.1.2).

Transhydroxylase from *P. acidigallici* was purified to homogeneity by a new purification protocol. It is a heterodimer consisting of a large subunit (100.4 kDa) and a small subunit (31.3 kDa). BLASTP searches showed that the large subunit is closely related to enzymes of the DMSO-reductase family. Although the overall reaction of transhydroxylase is no redox reaction it contains different iron-sulfur centers and one Mo-bisMGD as redox-cofactors. EPR-spectroscopic investigation of transhydroxylase in the “as isolated” state showed typical signals of a Mo(V) center with $g_{av} = 1.98$. The dithionite reduced enzyme showed signals of different [4Fe-4S] centers. The existence of [2Fe-2S] centers was not explicitly demonstrated. UV/Vis spectra showed absorption shoulders resulting from the iron-sulfur centers around 400 nm and

from sulfur-to-molybdenum charge-transfer transitions around 700 nm. The specific activity of transhydroxylase (4.5 U mg^{-1}) was about 50% higher than previously reported.

BLASTP searches with the small subunit of transhydroxylase as template showed that 12 of the 13 cysteines are highly conserved within related enzymes. Some of them are referred to as [4Fe-4S] ferredoxins. The 15 cysteines of the big subunit do not align with the cysteines of related iron-sulfur proteins. Therefore, it is unlikely that an iron-sulfur center is located on the large subunit. It is more likely that there are three [4Fe-4S] clusters located on the small subunit.

Crystals were obtained both in the presence and in the absence of dioxygen (N_2 : H_2 = 94 : 6 v/v). The crystals, grown under exclusion of dioxygen in the presence of dithionite, diffracted to a resolution better than 3.4 Å. Refinement of the crystallization conditions led to crystals which diffracted to resolutions better than 2.5 Å with synchrotron radiation. The crystallographic investigation of transhydroxylase was done in collaboration with Dipl. Biol. Holger Nießen (Universität Konstanz) and Dr. Oliver Einsle (Max-Planck-Institut für Biochemie, Martinsried).

Phylogenetic analyses of the large subunit of transhydroxylase (based on amino acid sequences) revealed that transhydroxylase also belongs to the family of the DMSO-reductases. In contrast to acetylene hydratase, transhydroxylase belongs to the subfamily of the DMSO-reductases that consist of at least five distinct groups: The group of the *Rhodobacter* DMSO-reductases, the group of the TMAO-reductases, the group of the BSO-reductases, the group of the DMSO-reductases of the proteobacteria, and the transhydroxylase group.

1. Introduction

Molybdenum and tungsten are the only elements of the second and third row transition series to have known biological functions (Pilato and Stiefel, 1999; Johnson *et al.*, 1996). Molybdenum has been recognized since the 1930s for its role in nitrogen fixing enzyme systems (Stiefel, 1997). From 1953 on it was realized that molybdenum is essential for diverse aspects of metabolism in a wide range of organisms (De Renzo *et al.*, 1953). Tungsten was first identified in 1983 in the NADP-dependent formate dehydrogenase from the thermophilic organism *Clostridium thermoaceticum* (Yamamoto *et al.*, 1983) and has been extensively studied in bacteria and hyperthermophilic archaea since then.

Molybdenum and tungsten enzymes are found throughout the biological world and catalyze critical reactions in the metabolism of purines, aldehydes, carbon monoxide, as well as nitrogen– and sulfur containing compounds (Hille, 1999; Stiefel, 1997). With the exception of nitrogenase, the molybdenum and tungsten enzymes share a structural unit at their catalytic sites. This component is called the molybdenum cofactor (moco, Figure 1.2 A) and binds molybdenum as well as tungsten.

There are now a large series of molybdenum and tungsten enzymes with known three-dimensional structures, and this new structural information has provided the basis for an increasingly detailed understanding of the reaction mechanisms of these enzymes.

An overview of the diverse structures and functions of the molybdenum and tungsten-enzymes is given in a number of recent publications: Hille, 2000; Pilato and Stiefel, 1999; Kisker *et al.*, 1999; Hille *et al.*, 1999; Hille, 1999; Rees *et al.*, 1997; Stiefel, 1997; Johnson *et al.*, 1996; Kletzin and Adams, 1996; Hille, 1996.

1.1. Physical and chemical properties of molybdenum and tungsten

Although the chemistry of molybdenum and tungsten is variable and complex because of the range of possible oxidations states (-II to +VI), only the +IV, +V, and +VI oxidation states of both elements appear biologically relevant (Kletzin and Adams, 1996). The similarity in their chemical properties is well established (Table 1.1). The atomic radii of Mo and W, as well as their electron affinity, are virtually the same. Radioactive isotopes suitable for biological

research are available for both elements (^{99}Mo and ^{185}W), as well as stable nuclear spin isotopes for the study of hyperfine interactions by various spectroscopic techniques (^{95}Mo, I = 5/2 and ^{183}W, I = 1/2).

Both, W and Mo, are relatively rare in nature. The abundance in the earth's crust is only 1.2 ppm for both elements. The concentrations in seawater are ≈ 100 nM for Mo and ≈ 1 pM for W. In freshwater, the Mo concentration is in the range of 5 – 50 nM and the W concentration is less than 500 pM (Table 1.1).

Molybdenum is mostly present in jordesite and molybdenite (both $Mo^{IV}S_2$) and seldom in the +VI oxidation state as wulfenite ($PbMoO_4$) or powellite ($Ca(Mo,W)O_4$, Greenwood and Earnshaw, 1990).

Tungsten is usually found in oxo-rich minerals (oxidation state +VI) either as scheelite ($CaWO_4$) or wolframite ($[Fe/Mn]WO_4$), whereas the more reduced tungstenite ($W^{IV}S_2$) is very rare, in part because WS_2 is readily solubilized (Eq. 1):

$$WS_2 + 4H_2O \rightleftharpoons WO_4^{2-} + 2H_2S + 4H^+ + 2e^- \quad (1)$$

	Molybdenum (Mo)	**Tungsten (W)**
Atomic number	42	74
Average atomic weight	95.94	183.85
Electronic configuration of the outer shell	$4d^5\ 5s^1$	$4f^{14}\ 5d^4\ 6s^2$
Atomic radii (Å)	1.40	1.40
Ionic radii for +IV oxidation state (Å)	0.65	0.66
Ionic radii for +V oxidation state (Å)	0.61	0.62
Ionic radii for +VI oxidation state (Å)	0.59	0.60
Electronegativity	1.8	1.7
pK_a of oxo acid (MO_4^{2-}/HMO_4^-)	3.87	4.60
Concentration in seawater	≈ 100 nM	≈ 1 pM
Concentration in freshwater	≈ 5 – 50 nM	≈ 500 pM
M = O bond length (Å)	1.76	1.76

Table 1.1 Physical and chemical properties of molybdenum and tungsten.
Compiled from Kletzin and Adams (1996) and Greenwood and Earnshaw, (1990).
M represents Mo or W.

1.2. The mononuclear molybdenum and tungsten enzymes

Since the discovery of the first molybdenum enzyme, over 50 mononuclear molybdenum or tungsten enzymes have been found (Hille *et al.*, 1999). They catalyze a variety of hydroxylations, oxygen atom transfer, and other oxidation-reduction reactions, and share the unique molybdenum cofactor.

In the nitrogen cycle both molybdenum enzymes nitrogenase and nitrate reductase are key enzymes. In the metabolism of N-heterocycles a large family of molybdenum enzymes encompasses a range of substrate specifities that allow hydroxylation of carbon centers in strategic regiospecificity. In the sulfur cycle, molybdenum-dependent sulfite oxidation and dimethyl sulfoxide (DMSO) reduction play crucial roles. In carbon metabolism, both in the formation of methane and oxidation of formate, carbon monoxide, and various aldehydes, the molybdenum enzymes again have a prominent position (Stiefel, 1997).

The tungsten enzymes are involved in carbon metabolism and usually have functions related to those of their molybdenum counterparts (Stiefel, 1997).

Table 1.2 shows some stoichiometric formulations for substrate reactions of molybdenum enzymes. In table 1.3 a list of molybdenum and tungsten enzymes is given sorted according to their melabolic roles.

Several alternative classification schemes have been suggested:

Hille (1996, 1999) differentiated three families based on the structure of the molybdenum center in the oxidized Mo(VI) state plus one family for the tungsten containing enzymes (Figure 1.1). According to Dobbek and Huber (2001) the Mo/Cu CO-dehydrogenase from *Oligotropha carboxidovorans* belongs to the xanthine oxidase family.

Based on sequence similarities Kisker *et al.* (1997) divided the moco containing enzymes into four different families, namely the dimethyl sulfoxide reductase (DMSOR), xanthine oxidase, sulfite oxidase, and aldehyde ferredoxin oxidoreductase (AOR) families. Some phylogenetic aspects of the DMSO reductase family will be discussed in the chapters 3.3 and 4.4.

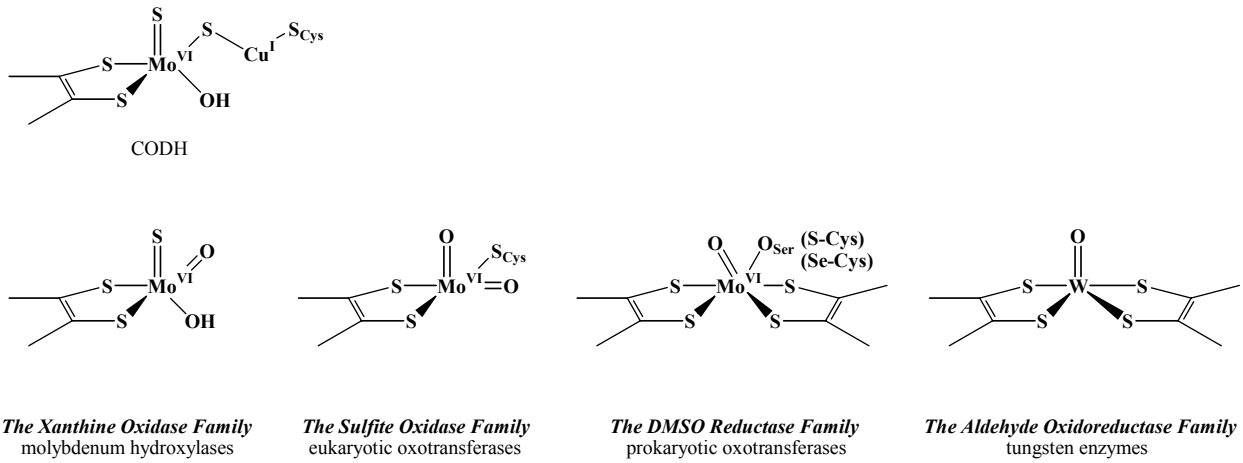

Figure 1.1 The families of mononuclear molybdenum enzymes (Hille, 1996; Hille, 1999; Hille *et al.*, 1999). Note that the recently discovered molybdenum-containing Carbon monoxide dehydrogenase (CODH) from *Oligotropha carboxidovorans* contains the first binuclear metal center (Dobbek and Huber, 2002).

Enzyme	**Reaction**
Dimethyl sulfoxide reductase	$(CH_3)_2SO + 2H^+ + 2e^- \rightarrow (CH_3)_2S + H_2O$
Trimethylamine N-oxide reductase	$(CH_3)_3NO + 2H^+ + 2e^- \rightarrow (CH_3)_3N + H_2O$
Nitrate reductase	$NO_3^- + 2H^+ + 2e^- \rightarrow NO_2^- + H_2O$
Sulfite oxidase	$SO_3^{2-} + H_2O \rightarrow SO_4^{2-} + 2H^+ + 2e^-$
Formate dehydrogenase	$HCOOH \rightarrow CO_2 + 2H^+ + 2e^-$
Polysulfide reductase	$^-S\text{-}(S)_n\text{-}S^- + 2H^+ + 2e^- \rightarrow {}^-S\text{-}(S)_{n-1}\text{-}S^- + H_2S$
Arsenite oxidase	$As^{III}O_2^- + 2H_2O \rightarrow As^{V}O_4^{3-} + 4H^+ + 2e^-$
CO oxidoreductase	$CO + H_2O \rightarrow CO_2 + 2e^- + 2H^+$
Acetylene hydratase	$C_2H_2 + H_2O \rightarrow CH_3CHO$
Transhydroxylase	1,2,3 trihydroxybenzene → 1,3,5 trihydroxybenzene

Table 1.2 Stoichiometric formulations for substrate reactions of selected molybdenum and tungsten enzymes.

Molybdenum enzymes	Tungsten enzymes
Nitrogen cycle	Aldehyde oxidoreductase (carboxylic acid reductase)
Nitrogenase (only molybdenum enzyme not containing the pterindithiolene ligand)	Formate dehydrogenase
Nitrate reductase (assimilatory)	Formaldehyde ferredoxin oxidoreductase
Nitrate reductase (dissimilatory)	*N*-Formyl methanofuran dehydrogenase
Nitrate oxidase	Acetylene hydratase
Trimethylamine *N*-oxide reductase	
N-Heterocyclic metabolism	
Isonicotinic acid hydroxylase	
Nicotinic acid hydroxylase	
Nicotine hydroxylase	
Picolinic acid dehydrogenase	
Pyrimidine oxidase	
Isoquinoline oxidoreductase	
Quinaldic acid 4-oxidoreductase	
Quinoline oxidoreductase	
Xanthine dehydrogenase	
Xanthine oxidase	
Acid and aldehyde reactions	
Aldehyde oxidase (retinal oxidase)	
Aldehyde dehydrogenase	
Pyridoxal oxidase	
Carbon metabolism	
Formate dehydrogenase	
Carbon monoxide oxidoreductase	
N-Formyl methanofuran dehydrogenase	
2-Furoyl dehydrogenase	
Sulfur metabolism	
Polysulfide reductase	
Sulfite oxidase	
Biotin sulfoxide reductase	
Dimethyl sulfoxide reductase	
Tetrathionate reductase	
Miscellaneous	
Pyrogallol phloroglucinol transhydroxylase	
Arsenite oxidase	
Chlorate reductase	

Table 1.3 Molybdenum and tungsten enzymes (Stiefel, 1997).

1.3. The molybdenum cofactor

The mononuclear molybdenum and tungsten enzymes share a similar structural unit at their catalytic sites that distinguishes them from other enzymes (Stiefel, 1997). This component is called the molybdenum cofactor or molybdopterin (moco, Figure 1.2 A) although it is not a cofactor in the classical sense of being dissociable from the enzyme during turnover. The dithiolate portion of the pterin-ene-dithiolate binds molybdenum as well as tungsten and is modifying and, presumably, enhancing their properties (Stiefel, 1997).

The Mo or W ion that binds to the moco is found to be coordinated by three types of ligands: (i) sulfur atoms provided by the moco; (ii) non-protein oxygen or sulfur species, such as oxo, water or sulfido; (iii) (optionally) amino acid side chains (Rees *et al.*, 1997). In bacteria, additional variability of the moco is achieved by conjugation of one of the nucleotides guanosine, adenosine, inosine, or cytidine-5'-monophosphate to the phosphate group of the moco (Figure 1.2 B). The name of the resulting molecule is abbreviated e.g. as MGD (molybdopterin-guanosine-dinucleotide). One or two molecules of e.g. MGD can complex the molybdenum or tungsten atom (Figure 1.2 C).

Enzymes with the molybdenum cofactor often incorporate additional cofactors or prosthetic groups like heme, coenzyme B_{12}, or iron-sulfur centers (Stiefel, 1997).

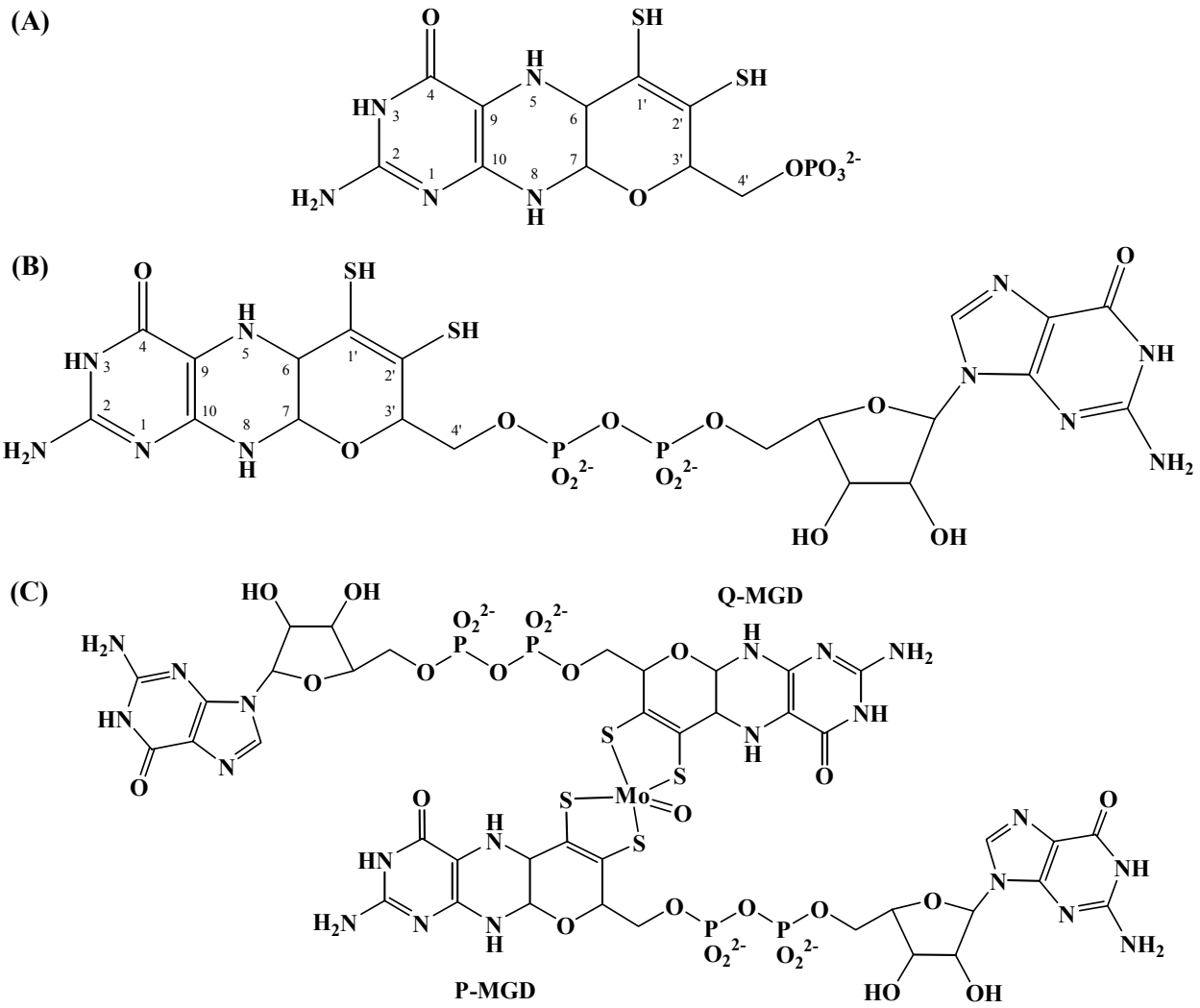

Figure 1.2 Cofactors of molybdenum and tungsten enzymes.
(A) Molybdenum cofactor = molybdopterin = moco. The tricyclic form was observed in all crystal structures of enzymes containing this cofactor (Kisker *et al.*, 1999).
(B) Molybdopterin guanosine dinucleotide (MGD) form as found in some bacterial enzymes (Stiefel, 1997).
(C) Extended molybdenum cofactor (bisMGD) as found in *Alcaligenes faecalis* arsenite oxidase (Ellis *et al.*, 2001).

1.4. Iron-sulfur centers

Iron-sulfur centers constitute one of the most ancient, ubiquitous, structurally, and functionally diverse class of biological prosthetic groups (Cammack, 1992; Beinert *et al.*, 1997). In some molybdopterin-containing enzymes like acetylene hydratase, transhydroxylase, or xanthine oxidase iron-sulfur centers were also found.

In the simplest case the iron atom is tetrahedrally coordinated by four cysteinyl residues, whereas in the more complex centers several iron atoms are bridged by inorganic sulfide (S^{2-}), the so-called acid-labile sulfur. In a scenario of the origin of life in hot environments (Achenbach-

Richter *et al.*, 1987; Wächtershäuser, 1988) the conversion of FeS (Eq. 2) was postulated to serve as the first energy source of primordial life (Wächtershäuser, 1988). Therefore, the iron-sulfur centers found today in proteins might represent remainders of the early past. The most common types of iron-sulfur centers comprise [2Fe-2S], [3Fe-4S], and [4Fe-4S] cores with cysteinyl residues serving as fourth ligand of each iron atom (Figure 1.3).

$$FeS + HS^- \rightarrow FeS_2 + H^+ + 2e^- \qquad E^{\circ\prime} = -620\ mV \qquad (2)$$

The iron-sulfur proteins fall into two major categories: simple iron-sulfur proteins that contain only one or more iron-sulfur centers, and the complex iron-sulfur proteins that bear such additional active redox centers as flavin, molybdenum, or heme.

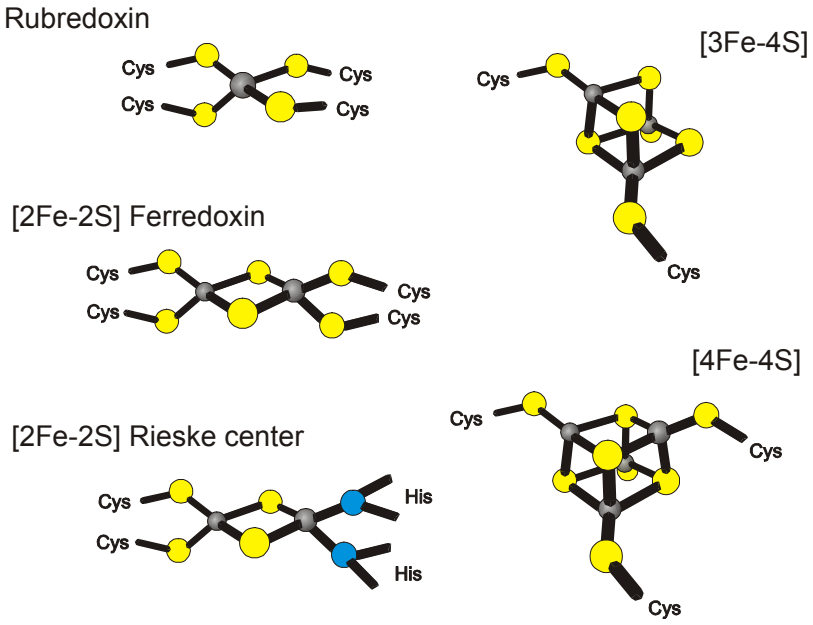

Figure 1.3 Structures of the most common types of iron-sulfur centers.
Iron atoms are colored in gray, sulfur in yellow, and nitrogen in blue.

The functions of iron-sulfur proteins include electron and proton transfer, Lewis acid-base catalysis, structural determinant, and gene regulation (Johnson, 1994). The optical absorption bands of all iron-sulfur proteins are rather broad and featureless and not suitable for obtaining structural information. On the other hand, electron paramagnetic resonance (EPR) spectra of iron-sulfur centers are distinctive (Figure 1.4). From the spectra one can conclude on the nuclearity and redox state of the iron-sulfur centers (Cammack *et al.*, 1985).

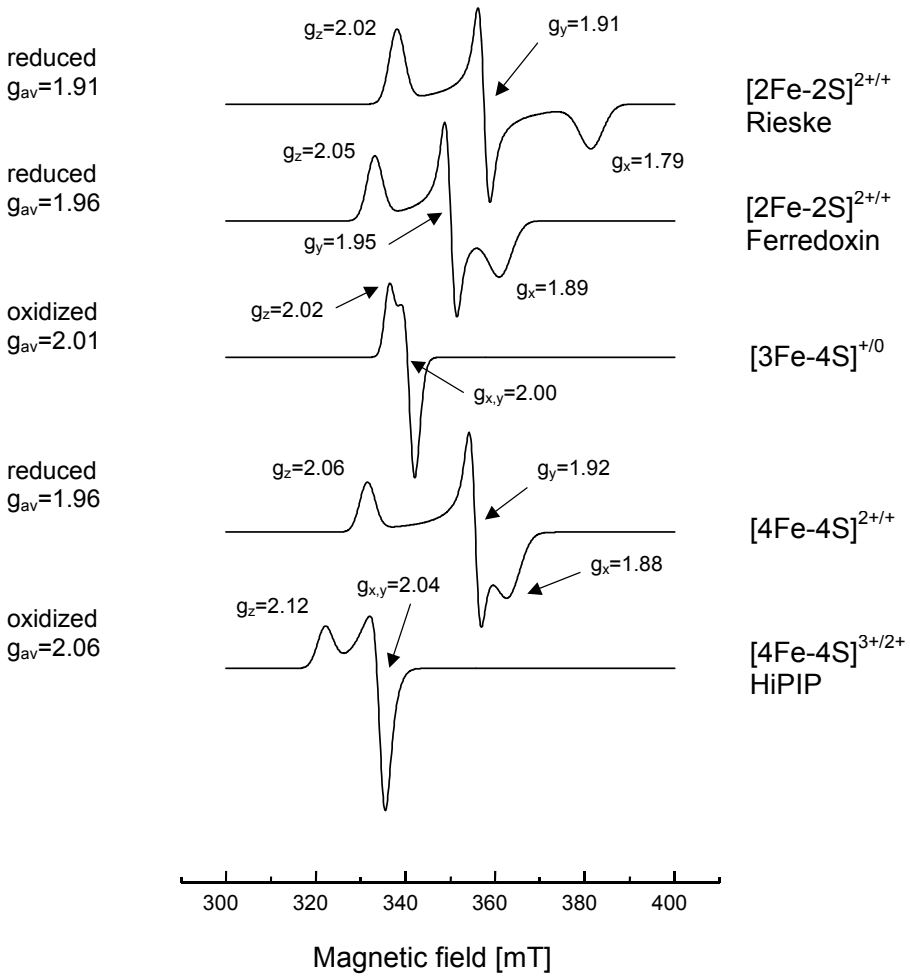

Figure 1.4 Comparison of EPR properties of different types of iron-sulfur centers.
The spectra of different types of iron-sulfur centers differ in shape and *g*-values. According to (Cammack *et al.*, 1985). HiPIP = high potential iron-sulfur protein.

1.5. *Pelobacter acetylenicus* acetylene hydratase

Pelobacter acetylenicus strain WoAcy 1 (DSM 3246) is a strictly anaerobic, chemoorganotroph, and gram-negative bacterium that is able to grow on acetylene as sole carbon and energy source (Schink, 1985). It was isolated from a freshwater creek sediment near Konstanz. The cells are rod-shaped with 0.6 – 0.8 x 1.5 – 4 µm in size. The DNA base ratio is 57.1 ± 0.2 mol% G + C (Schink, 1984).

1.5.1. Acetylene metabolism

Acetylene is so far the only known hydrocarbon that is metabolized in the absence and presence of molecular oxygen in the same manner (Schink, 1985). *P. acetylenicus* hydrates acetylene to acetaldehyde. The further disproportionation of acetaldehyde leads to acetate and ethanol. Though the hydration of acetylene to acetaldehyde is a highly exergonic reaction (Eq. 3; Schink, 1985), studies on cell yield show that only the free energy of the acetate kinase reaction (0.5 mol ATP per mol acetylene) is used for growth (Schink, 1985).

$$C_2H_2 + H_2O \rightarrow [H_2C{=}C(OH)H] \rightarrow CH_3CHO \qquad \Delta G^{0'} = -111.9 \text{ kJ mol}^{-1} \qquad (3)$$

The acetylene degradation pathway of *P. acetylenicus* is shown in figure 1.5.

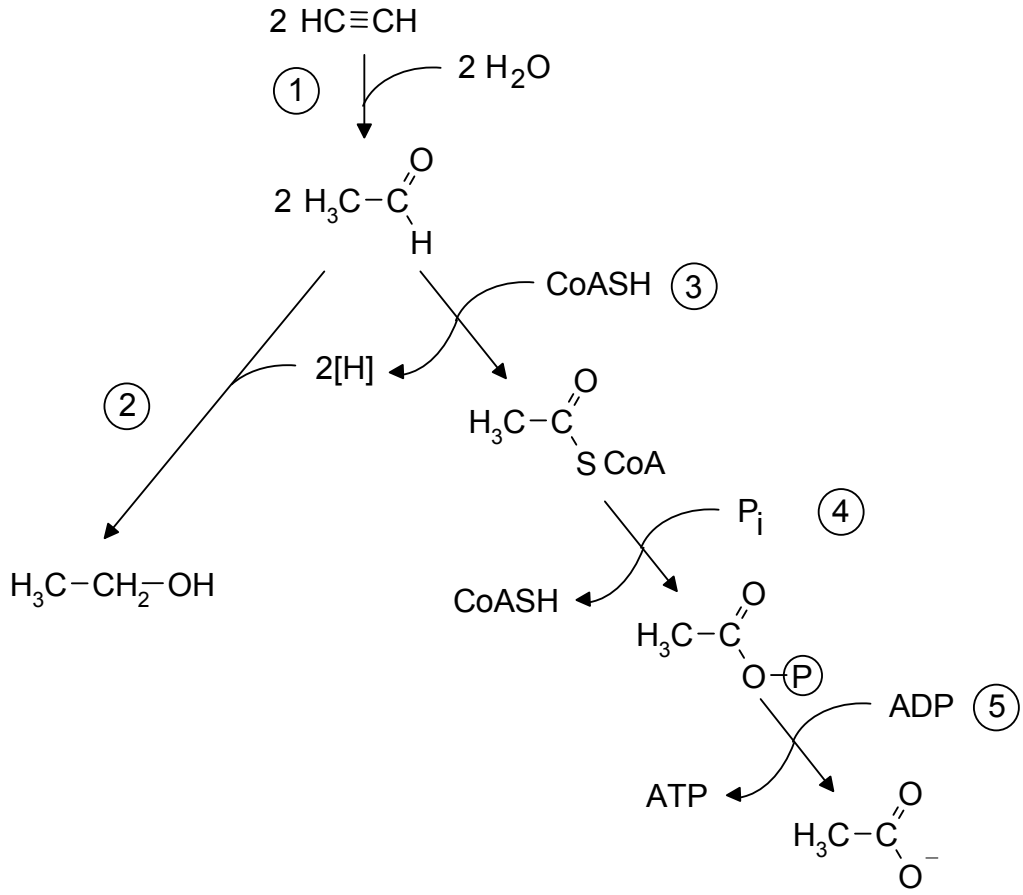

Figure 1.5 Acetylene degradation pathway of *P. acetylenicus* (Rosner 1994, Schink, 1985). (1) Acetylene hydratase, (2) Alcohol dehydrogenase, (3) Aldehyde dehydrogenase, (4) Phosphate acetyltransferase, (5) Acetate kinase.

1.5.2. Molecular properties of acetylene hydratase

Acetylene hydratase has been isolated as a monomeric enzyme with a molecular mass of 72 kDa (SDS-PAGE) *versus* 85 kDa (MALDI-MS). The N-terminus of the protein shows a sequence motif C-x-x-C-x-x-x-C that could represent a motif for a Fe-S site (Rosner and Schink, 1995). 4.4 ± 0.4 mol Fe and 0.5 ± 0.1 mol W (ICP/MS), 3.9 ± 0.4 mol acid labile sulfur, and 1.3 ± 0.1 mol molybdopterin guanine dinucleotide were found per mol enzyme. Selenium was absent (Meckenstock *et al.*, 1999). The isoelectric point is 4.2, the specific activity of the enzyme is highest between pH 6.0 and 7.0, and the temperature optimum is 50°C. Though the acetylene hydratase reaction (Eq. 3) is not a redox reaction, in the photometric assay a strong reductant like Ti(III)citrate or dithionite has to be used. Meckenstock *et al.* (1999) showed that acetylene hydratase contains one [4Fe-4S] cluster with a midpoint redox potential of –410 ± 20 mV (Figure 1.6 A). Enzyme activity also depends on the redox potential of the solution with 50% maximum activity at –340 ± 20 mV (Figure 1.6 B). Acetylene hydratase is slightly oxygen sensitive, the [4Fe-4S] cluster degrades to a [3Fe-4S] cluster when purified under air as shown by EPR-spectroscopy (Meckenstock *et al.*, 1999).

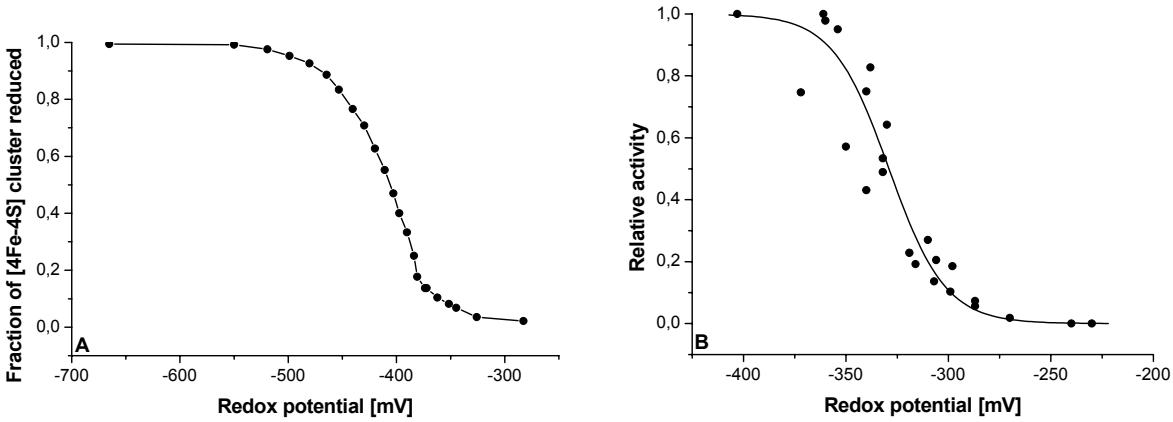

Figure 1.6 Redox properties of acetylene hydratase (Meckenstock *et al.*, 1999).
(A) Redox titration of the [4Fe-4S] center as determined by measuring A_{430}. The maximal A_{430} was taken as totally oxidized, the minimal as totally reduced which is equal to an absolute difference (ΔA_{430}) of 0.33. Enzyme prepared under N_2/H_2.
(B) Dependence of acetylene hydratase activity on the redox potential. Enzyme prepared under N_2/H_2.

1.6. *Pelobacter acidigallici* transhydroxylase

Pelobacter acidigallici strain MaGal2 (DSM 2377) is a strictly anaerobic, chemoorganothroph, and gram-negative bacterium that ferments gallic acid, pyrogallol, phloroglucinol, and 2,4,6,-trihydroxybenzoic acid to three molecules of acetate (plus CO_2; Schink and Pfennig, 1982; Hille *et al.*, 1999). It was isolated from black, anaerobic marine mud of Rio Marin, a channel about 2.5 m wide and 70 cm deep, located in the city of Venice, Italy. The cells are rod-shaped with 0.5 – 0.8 x 1.5 – 3.5 µm in size. The DNA base ratio is 51.8% ± 0.4 mol% G + C (Schink and Pfennig, 1982).

1.6.1. Metabolism of gallic acid by *Pelobacter acidigallici*

Aerobic degradation of aromatic compounds involves oxygenase reactions in the primary attack on the mesomeric ring structure. In the absence of dioxygen, the stability of the aromatic nucleus is often overcome by a reductive attack (Evans, 1977; Reichenbecher *et al.*, 1994).

Trihydroxybenzenes are common intermediates formed in the degradation of plant materials such as glycosides, flavonoids, tannins, and lignin (Brune *et al.*, 1992). In *P. acidigallici* gallic acid (3,4,5-trihydroxybenzoic acid) is decarboxylated to pyrogallol and subsequently transformed to phloroglucinol in a unique reaction through transhydroxylase (Figure 1.7). Although this hydroxyl transfer between two aromatic compounds is no net redox reaction, the substrate pyrogallol is oxidized in position 5 and the cosubstrate 1,2,3,5-tetrahydroxybenzene is reduced in position 2. Recently it was shown, by incubation with $^{18}OH_2$, that there is no oxygen transfer from water in the transhydroxylase reaction, and that the hydroxyl groups are transferred only between the phenolic substrates (Reichenbecher and Schink, 1999).

With this, transhydroxylase differs fundamentally from all known hydroxylating molybdenum enzymes, which derive their hydroxyl groups from water. Phloroglucinol, the product of the transhydroxylase reaction, undergoes reductive dearomatization (Schink and Pfennig, 1982; Brune and Schink, 1990) and subsequent hydrolytic cleavage to 3-hydroxy-5 oxohexanoate that is oxidized and thiolytically cleaved to three acetyl-CoA molecules (Brune and Schink, 1992).

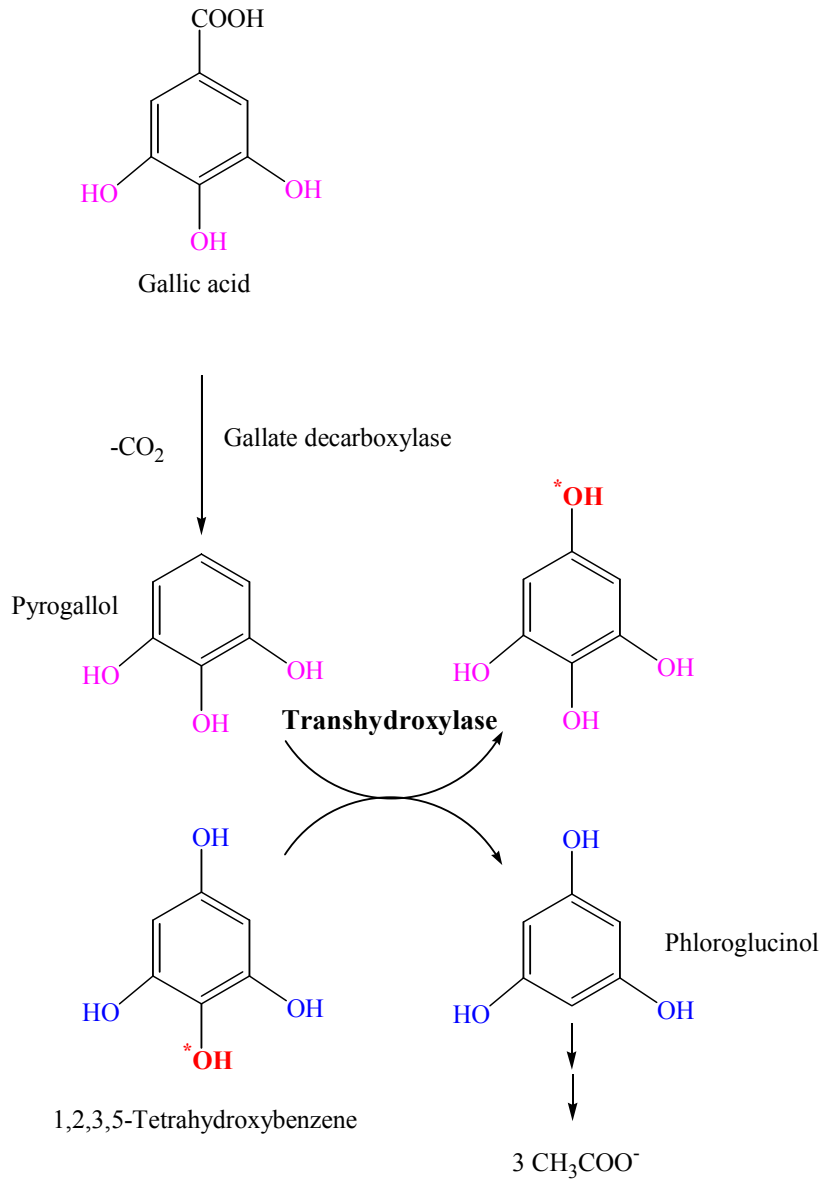

Figure 1.7 Transhydroxylase reaction in the pathway of gallic acid degradation in *Pelobacter acidigallici* (Brune and Schink, 1992).

1.6.2. Molecular properties of transhydroxylase

Transhydroxylase (pyrogallol:phloroglucinol hydroxyltransferase, E.C. 1.97.1.2) is a heterodimeric enzyme, with a molecular mass of 133.3 kDa, composed of a 100.4 kDa and a 31.3 kDa subunit. It contains 11.56 ± 1.72 Fe, 0.96 ± 0.21 Mo (atomic absorption spectroscopy), and 13.13 ± 1.68 acid labile sulfur per heterodimer. Furthermore, two molybdopterin guanine dinucleotide per heterodimer had been postulated (Reichenbecher *et al.*, 1994; Reichenbecher *et al.*, 1996; Baas and Rétey, 1999). The isoelectric point is 4.1, the specific activity of transhydroxylase is highest at pH 7.0, and the temperature optimum is between 53 and 58°C (Reichenbecher *et al.*, 1994).

Sequence analyses showed that transhydroxylase belongs to the family of the DMSO-reductases (Baas and Rétey, 1999). In all members of this family the coenzyme is a dimeric molybdopterin guanine dinucleotide (Kisker *et al.*, 1999). In contrast to most enzymes of the DMSO-reductase family, transhydroxylase has neither an α,β,γ structure nor a signal sequence and is not anchored in the cell membrane. While the large subunit has relatively few cysteines that are not clustered, the small subunit has 13 cysteines, some of which are clustered. This makes it likely that the Fe-S centers are located on the small subunit, while the entire MGD cofactor is associated with the large subunit. EPR studies showed that there must be at least two different types of [4Fe-4S] centers. Furthermore, the existence of [2Fe-2S] sites could not be excluded (Kisker *et al.*, 1999). Figure 1.8 shows experimental and simulated EPR spectra (9.5 GHz, 14 K, 0.6 mW) of the Fe-S centers in dithionite-reduced transhydroxylase.

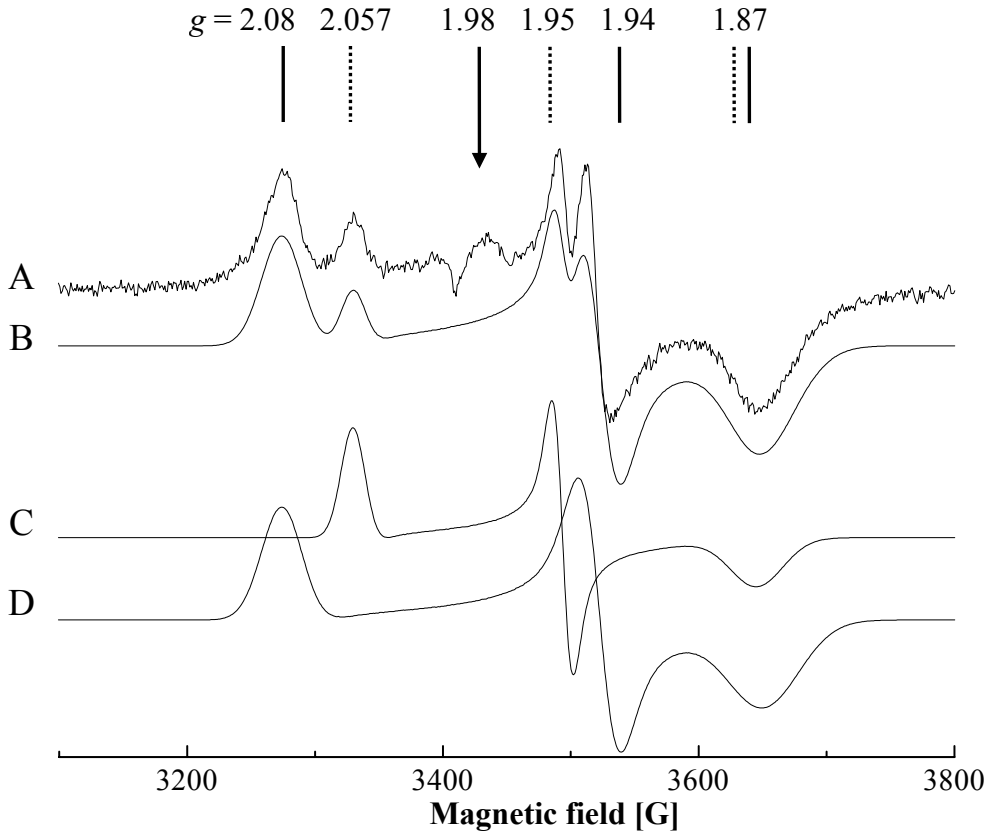

Figure 1.8 EPR spectra of dithionite-reduced transhydroxylase from *P. acidigallici*.
X-band, 14 K, 0.6 mW microwave power; (Kisker *et al.*, 1999)
(A) Enzyme as isolated under exclusion of air; 4.3 mg ml^{-1} in 40 mM TEA buffer, 300 mM NaCl pH 7.3, after addition of 3.5 equivalents sodium dithionite.
(B) Combined simulations, with signals C and D, weight 2:3.
(C) Simulated spectrum, with $g_x = 1.874$, $g_y = 1.953$, $g_z = 2.057$.
(D) Simulated spectrum, with $g_x = 1.869$, $g_y = 1.940$, $g_z = 2.080$.

1.7. Scope of the study

In the world of molybdenum and tungsten containing enzymes, *Pelobacter acetylenicus* W-acetylene hydratase and *Pelobacter acidigallici* Mo-transhydroxylase catalyze two unusual reactions. Both reactions represent no net redox chemistry although in the case of transhydroxylase the substrate is oxidized and the cosubstrate is reduced at the same time. To achieve a better understanding of the mechanisms of these reactions, and to get a deeper insight into the active sites of these novel molybdopterin enzymes, experiments have been performed aiming at the three-dimensional structure and a detailed biochemical and spectroscopic picture of the metal centers.

In the first place, this required the optimization of the growth conditions of the bacteria as well as the development of efficient purification protocols with high yields of the two metallo-enzymes.
In the case of acetylene hydratase, the replacement of tungsten by molybdenum and vanadium has been attempted which might help in unraveling the mechanism of the transformation of acetylene to acetaldehyde. This replacement might also help in solving the phase problem for the X-ray structure.
Another important point relates to evolutionary aspects of both enzymes, which appear to belong to the family of the dimethyl sulfoxide reductases.

2. Materials and Methods

2.1. Chemicals and biochemicals

If not specified elsewhere, chemicals were of p.a. quality and obtained from Merck (Darmstadt), Riedel-de Haën (Seelze), or Fluka (Buchs, CH). Other chemicals, at least in p.a. quality, were purchased from other manufacturers:

Buffers:

Roth, Karlsruhe: Tris (Tris-(hydroxymethyl)-aminomethane), HEPES (4-[2-Hydroxyethyl]-piperazine-1-[ethanesulfonic acid]). *Sigma, Deisenhofen:* MOPS 3-Morpholinopropanesulfonic acid, PIPES (1,4-Piperazinediethanesulfonic acid).

Chromatographic resins:

Whatman, Maidstone, UK: DE 52 (microgranular DEAE cellulose). *Pharmacia-Biotech, Freiburg*: HiLoad 16/60 Superdex 75 column, HiLoad 26/60 Superdex 200 column, Mono Q HR 16/10.

Dyes:

Serva, Heidelberg: Coomassie-brilliantblue G-250, bromphenolblue (sodium salt).

Enzymes:

Serva, Heidelberg: Bovine serum albumin (BSA). *Boehringer, Mannheim*: Yeast Alcohol dehydrogenase (400 U mg^{-1}).

Sulfolobus solfataricus alcohol dehydrogenase was a generous gift of C.A. Raia, Institute of Protein Biochemistry and Enzymology, National Council of Research, 80125 Naples, Italy.

Gas:

Messer Griesheim, Krefeld: Argon 5.0, Helium 4.6, Acetylene 2.6, Hydrogen 5.0. *Sauerstoff-werk Friedrichshafen*: Nitrogen 5.0, N_2/CO_2 (8:2, v/v), N_2/H_2 (94:6, v/v).

Liquid helium was delivered by the department of physics, Universität Konstanz.

Protein standards:

BioRad, München: Low molecular mass standards (PAGE). *Sigma, Deisenhofen*: Gel filtration molecular mass markers.

Reagents:

Sigma, Deisenhofen: BCA (bicinchoninic acid solution). *Boehringer, Mannheim*: NADH (nicotinamide adenine dinucleotide).

Non-commercial available compounds:

Titanium (III) citrate was synthesized according to Zehnder and Wurhmann (1976). The concentration was determined by titration against $K_3[Fe(CN)_6]$ using Beers Law and the molar extinction coefficient $\varepsilon_{420nm}(K_3[Fe(CN)_6]) = 1020\ M^{-1}\ cm^{-1}$ (Peck *et al.*, 1965).
1,2,3,5-tetrahydroxybenzene (TTHB) was synthesized according to Brune (1990), Baxter and Brown (1967), Baxter *et al.* (1949), and Baker *et al.* (1929). Purity was checked by NMR.

Media and buffers for molecular biology

Media and buffers used for molecular biology experiments were mixed as described by Hanahan (1983) or Maniatis *et al*. (1987).

Crystal screen solutions

Crystal screen solutions were obtained from Hampton Research (Laguna Hills, USA).

2.2. Organisms

2.2.1. *Pelobacter acetylenicus*

Pelobacter acetylenicus strain WoAcy 1 was provided by R.U. Meckenstock, Universität Konstanz. The strain is deposited in Deutsche Sammlung von Mikroorganismen und Zellkulturen GmbH (DSMZ), Braunschweig, under the number 3246.

2.2.2. *Pelobacter acidigallici*

Pelobacter acidigallici strain Ma Gal 2 was provided by W. Dilling, Universität Konstanz. The strain is deposited in the DSMZ, under the number 2377.

2.3. Cultivation of bacteria

2.3.1. *Pelobacter acetylenicus*

Batch cultures of *P. acetylenicus* (0.1, 1, 20 or 50 l) were grown in freshwater medium (Table 2.1) at 30°C. The medium was sterilized at 121°C, cooled under a N_2/CO_2 (8 : 2, v/v) atmosphere, buffered with 30 mM $NaHCO_3$, and reduced with Na_2S. After addition of trace element solutions (Table 2.2, 2.4) and vitamin solution (Table 2.3) the pH was adjusted to 7.0 – 7.4 with 1 M HCl. The redox potential of the medium was monitored by the indicator resazurin (≈ 1 µM). Cultures were inoculated with 10% (by vol.) of a stock culture. The substrate acetylene was continuously supplied with 5 – 10 kPa. Growth was monitored by measuring the optical density at 578 nm, and the pH of the medium was maintained at pH 7.0 with 2 M Na_2CO_3. Cells were harvested at the end of the exponential growth phase after one day (A_{578} = 0.6) with a Pellicon ultrafiltration unit (cutoff 100 kDa, Millipore Corporation, Eschborn). The concentrate was centrifuged at 10000 *g* (30 min, 4°C) and the resulting cell pellets were stored in liquid nitrogen prior to use. Figure 2.1 shows the 50 l batch culture system.

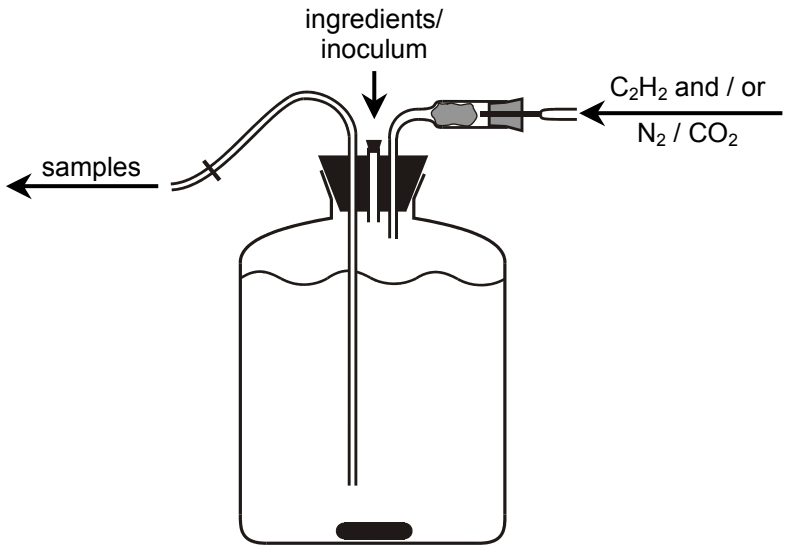

Figure 2.1 The 50 l batch culture system.

Compound	[mM]	[g l^{-1}]
NaCl	17.1	1.0
$MgCl_2 \cdot 6H_2O$	2.0	0.4
KH_2PO_4	1.5	0.2
NH_4Cl	4.7	0.25
KCl	6.7	0.5
$CaCl_2 \cdot 2H_2O$	1.0	0.15

Table 2.1 Freshwater medium (Schink, 1985).
The compounds were dissolved in water and sterilized at 121°C.

Compound	[mM]	[mg l^{-1}]
$FeCl_2 \cdot 4H_2O$	7.54	1500
$ZnCl_2$	0.51	70
$MnCl_2 \cdot 4H_2O$	0.79	100
$CoCl_2 \cdot 6H_2O$	0.80	190
$CuCl_2 \cdot 2H_2O$	0.01	2
$NiCl_2 \cdot 6H_2O$	0.10	24
H_3BO_3	0.10	6

Table 2.2 Modified trace element solution SL10 (Widdel and Pfennig, 1981).
The components were dissolved in 10 ml of 25% HCl, the volume adjusted to 1 l, and sterilized at 121°C.

Compound	[µM]	[mg l^{-1}]
4-Aminobenzoic acid (Vitamin H_1)	365	50
(+)-Biotin (Vitamin H)	41	10
D-Pantothenic acid Calcium salt	52	25
Cyanocobalamin (Vitamin B_{12})	37	50
Nicotinic acid (Vitamin B)	812	100
Pyridoxamine dihydrochloride	965	250
Thiamine hydrochloride (Vitamin B_1)	148	50

Table 2.3 Vitamin solution (Widdel and Pfennig, 1981).
Vitamins were dissolved in water and sterilized by filtration (0.2 µm).

Name	Compound	[µM]	[mg l^{-1}]
Na_2S solution	$Na_2S \cdot 9H_2O$	540000	120000
Vanadate solution	$NaVO_3 \cdot 4H_2O$	5000	975
	NaOH	125000	5000
Selenite solution	$Na_2SeO_3 \cdot 5H_2O$	11	3
	NaOH	12500	500
Molybdate solution	$Na_2MoO_4 \cdot 2H_2O$	1000	242
	NaOH	12500	500
Molybdate (^{95}Mo) solution	$^{95}MoO_3$	1000	143
Tungstate solution	$Na_2WO_4 \cdot 2H_2O$	400	132
	NaOH	12500	500
Tungstate (^{183}W) solution	$^{183}WO_3$	1000	231

Table 2.4 Special trace element solutions (Widdel, 1980; modified).
$^{183}WO_3$ and $^{95}MoO_3$ were diluted in hot, concentrated, NaOH giving $^{183}WO_4^{2-}$ and $^{95}MoO_4^{2-}$ (Greenwood and Earnshaw, 1990). Appropriate dilutions were done with water and were sterilized at 121°C.

(a) Tungstate cultivation

P. acetylenicus was cultivated in freshwater medium (Table 2.1) as described above. Additional ingredients were added according to table 2.5.

Compound	[ml l^{-1}]	concentration
$NaHCO_3$ (1 M)	30	30 mM
Trace element solution (Table 2.2)	1	
Selenite solution (11 µM, Table 2.4)	1	11 nM
Tungstate solution (400 µM, Table 2.4)	1	400 nM
Vitamin solution (Table 2.3)	0.5	
Na_2S solution (Table 2.4)	2	1 mM

Table 2.5 *P. acetylenicus* tungstate cultivation; additional ingredients.

(b) Molybdate cultivation (^{95}Mo)

P. acetylenicus was cultivated in freshwater medium (Table 2.1) as described above. Additional ingredients were added according to table 2.6. To replace tungsten by ^{95}Mo, the culture was transferred at least 6 times in medium containing 2 µM $^{95}MoO_4^{2-}$ and 2 nM $^{183}WO_4^{2-}$. Cells of a 50 l batch culture were harvested after 2 days (A_{578} = 0.2).

Compound	[ml l^{-1}]	concentration
$NaHCO_3$ (1 M)	30	30 mM
Trace element solution (Table 2.2)	2	
Selenite solution (11 µM, Table 2.4)	2	22 nM
Molybdate solution (^{95}Mo, 1 mM, Table 2.4)	2	2 µM
Tungstate solution (^{183}W, 1 µM, Table 2.4)	2	2 nM
Vitamin solution (Table 2.3)	1	
Na_2S solution (Table 2.4)	2	1 mM

Table 2.6 *P. acetylenicus* molybdate (^{95}Mo) cultivation; additional ingredients.

(c) Vanadate cultivation

P. acetylenicus was cultivated in freshwater medium (Table 2.1) as described above. Additional ingredients were added according to table 2.7. To replace tungsten by vanadium, the culture was transferred at least 6 times in medium containing 2 nM $^{95}MoO_4^{2-}$, 2 nM $^{183}WO_4^{2-}$, and 10 µM VO_3^-. Cells of a 50 l batch culture were harvested after 2 days (A_{578} = 0.2).

Compound	[ml l^{-1}]	concentration
$NaHCO_3$ (1 M)	30	30 mM
Trace element solution (Table 2.2)	2	
Vanadate solution (5 mM, Table 2.4)	2	10 µM
Selenite solution (11 µM, Table 2.4)	2	22 nM
Molybdate solution (^{95}Mo, 1 µM, Table 2.4)	2	2 nM
Tungstate solution (^{183}W, 1 µM, Table 2.4)	2	2 nM
Vitamin solution (Table 2.3)	1	
Na_2S solution (Table 2.4)	2	1 mM

Table 2.7 *P. acetylenicus* vanadate cultivation; additional ingredients.

2.3.2. *Pelobacter acidigallici*

Batch cultures of *P. acidigallici* (0.1, 1, 20 or 50 l) were grown at 30°C in bicarbonate-buffered, sulfide-reduced saltwater mineral medium (Table 2.8, 2.9) in an 80% N_2 – 20% CO_2 atmosphere (Brune and Schink, 1990). After addition of trace element solutions (Table 2.2, 2.4), and vitamin solution (Table 2.3) the pH was adjusted between 7.2 and 7.4 with 1 M HCl. The redox potential of the medium was monitored by the indicator resazurin (1 μM). Cultures were inoculated with 10% (v/v) of a stock culture. The substrate gallic acid was dissolved in water under exclusion of air, neutralized to pH 7.0 with concentrated NaOH, sterilized by filtration (0.2 μm), and fed at the start (7 mM) and twice (7 mM) during cultivation. Growth was monitored by measuring the optical density at 578 nm, and the pH of the medium was maintained at pH 7.2 with 2 M Na_2CO_3. Cells of a 50 l batch culture were harvested at the end of the exponential growth phase after one day (A_{578} = 0.8) with a Pellicon ultrafiltration unit (cutoff 100 kDa, Millipore Corporation, Eschborn). The concentrate was centrifuged at 10000 *g* (30 min, 4°C) and the resulting cell pellet was stored at –70°C prior to use. In Figure 2.1 the 50 l batch culture system is shown.

Compound	**[mM]**	**[g l^{-1}]**
NaCl	342	20.0
$MgCl_2 \cdot 6H_2O$	15	3.0
KH_2PO_4	1.5	0.2
NH_4Cl	4.7	0.2
KCl	6.7	0.5
$CaCl_2 \cdot 2H_2O$	1.0	0.15

Table 2.8 Saltwater medium (Brune and Schink, 1990).
The components were dissolved in water and sterilized at 121°C.

Compound	[ml l^{-1}]	concentration
$NaHCO_3$ (1 M)	30	30 mM
Trace element solution (Table 2.2)	1	
Selenite solution (11 µM, Table 2.4)	1	11 nM
Molybdate solution (100 µM, Table 2.4)	1.5	150 nM
Vitamin solution (Table 2.3)	0.5	
Na_2S solution (Table 2.4)	2	1 mM
Gallic acid solution pH 7 (500 mM)	14	7 mM

Table 2.9 *P. acidigallici* cultivation; additional ingredients.

2.4. Glycerol cryo-cultures

A microscopically pure overnight 1 l culture of *P. acetylenicus* or *P. acidigallici* was harvested by centrifugation at 10000 *g* (30 min, 4°C). Sterile glycerol solution (80% v/v, in water) was added to the cell pellet (1:1 w/w) and mixed to homogeneity. Aliquots of 500 µl were taken and slowly frozen at –20°C for 24 hours. Final storage was done at –70°C. The frozen cells were tested for growth after 2 weeks storage at –70°C by inoculating a 100 ml batch culture with one 500 µl aliquot.

2.5. Enzyme purification

All chromatographic steps were performed with a Pharmacia FPLC system (pump P-500, gradient controller GP-250, Pharmacia Biotech, Freiburg). Detection was carried out at 280 nm and 405 nm (Uvicord S II, Pharmacia Biotech, Freiburg).

Centrifugation was done in a RC 5C centrifuge (Sorvall Instruments, Du Pont de Nemours, Bad Homburg), or in a Optima^{TM} LE-80K ultracentrifuge (Beckman Instruments Inc., Palo Alto, USA) at 4°C.

2.5.1. Acetylene hydratase

Acetylene hydratase was purified at room temperature (Meckenstock *et al*., 1999) in an anaerobe chamber (Coy, Grasslake, Michigan, USA; 94% N_2, 6% H_2), equipped with a Palladium catalyst (Typ K-0242, 0.5% Pd on Al_2O_3, ChemPur, Karlsruhe) in order to remove traces of dioxygen, an automatic airlock (Coy), and an oxygen/hydrogen gas analyzer (Coy). The content of dioxygen in the anaerobe chamber was 0 – 10 ppm.
Dioxygen from buffers was removed by 8 to 10 cycles of vacuum and flushing with argon according to Beinert *et al*. (1978). Traces of dioxygen were removed from argon by a catalyst type R3-11 (BASF, Ludwigshafen). All glass and plasticware as well as buffers were stored in the anaerobe chamber for at least 24 hours prior to use in order to equilibrate with temperature and atmosphere.

(a) Acetylene hydratase - tungstate cultivation

The frozen cell suspension was thawed at 30°C in the anaerobe chamber, and the density was adjusted to $A_{578} = 135$ with 50 mM Tris/HCl pH 7.5. Cells were lysed with lysozyme (0.6 mg ml^{-1}, 2 mM EDTA) for 30 min at room temperature. DNA was digested with DNase I in the presence of 10 mM $MgCl_2$ for 30 min. The suspension was centrifuged at 10000 *g* for 30 min and the supernatant (crude extract) was subjected to $(NH_4)_2SO_4$ precipitation. In the first precipitation step, 4 M $(NH_4)_2SO_4$ in water was added slowly to a final concentration of 2.3 M. The solution was stirred on ice for 30 min. After centrifugation (30 min, 10000 *g*) acetylene hydratase was precipitated from the supernatant by a further 4 M $(NH_4)_2SO_4$ addition to a final concentration of 3.2 M and stirring on ice for 30 min. After another centrifugation step the pellet was dissolved in about 10 ml of 50 mM Tris/HCl pH 7.5 and dialyzed overnight against the same buffer supplemented with 1 mM dithiothreitol. The dialyzed solution was centrifuged at 10000 *g* for 5 min and was loaded on a Mono Q anion-exchange chromatography column (HR 10/16, Pharmacia Biotech, Freiburg) equilibrated with 50 mM Tris/HCl pH 7.5. The column was developed with a linear 0 – 0.5 M NaCl gradient. Active fractions were pooled and concentrated to 1.5 ml, using Centicon centrifugal filter devices (YM-30, Millipore, Eschborn). The concentrate was loaded on a HiLoad® 16/60 Superdex 75 column (1.6 cm x 60 cm, Pharmacia Biotech, Freiburg), equilibrated with 50 mM Tris/HCl 200 mM NaCl pH 7.5 and eluted with the same buffer. Active fractions were pooled and concentrated with Centricon centrifugal filter

devices. The pure acetylene hydratase was stored in liquid nitrogen or, under exclusion of dioxygen, in a gas-tight bottle at 4°C.

(b) Acetylene hydratase - molybdate (^{95}Mo) and vanadate cultivation

Because of the lower yield of cells, a modified purification procedure, leading to an enriched acetylene hydratase of about 90 – 95% purity, had to be applied.
Lyse of the cells and ammonium sulfate precipitation was done as described in chapter 2.5.1.a.
The pellet, obtained after the 3.2 M $(NH_4)_2SO_4$ precipitation step, was dissolved in 10 ml 50 mM Tris/HCl, pH 7.5, concentrated to 1.5 ml by ultrafiltration (30 kDa cutoff) in a stirring cell (Amicon, Beverly, MA, USA), and loaded on a HiLoad® 16/60 Superdex 75 column (1.6 cm x 60 cm, Pharmacia Biotech, Freiburg), equilibrated with 50 mM Tris/HCl 200 mM NaCl pH 7.5. Active fractions were pooled and concentrated with Centricon centrifugal filter devices (YM-30, Millipore, Eschborn). The purified acetylene hydratase was stored in liquid nitrogen or, under exclusion of air, in a gas-tight bottle at 4°C.

2.5.2. Transhydroxylase

Transhydroxylase was prepared at 5°C according to Sommer (1995) and Reichenbecher *et al*. (1994) with some modifications.
Frozen cells were thawed at 30°C in a water bath and suspended in 50 mM triethanolamine (TEA) pH 7.5. Some DNase I/$MgCl_2$ was added, and the cells were disrupted by 3 passages through a French Press (Aminco 1-FA-073, SLM Instruments, Urbana, Illinois, USA) at 137 MPa. The suspension obtained was centrifuged (13200 *g*, 30 min, 4°C) in order to remove rough material. The resulting supernatant was centrifuged at 100000 *g* (60 min, 4°C) to separate the membrane fraction (pellet) from the soluble fraction (supernatant = crude extract). The soluble fraction was kept on ice or frozen at –70°C prior to use.
The crude extract was passed through a 100 ml anion exchange column (DE 52, Whatman, UK) previously equilibrated with 50 mM TEA pH 7.5. After loading, the column was flushed with three bed volumes of buffer containing 175 mM NaCl. A five bed volume linear gradient of buffer with increasing NaCl concentration from 175 mM to 500 mM eluted transhydroxylase. Fractions showing transhydroxylase on a SDS-PAGE gel were pooled and concentrated to a final volume of 2 ml by ultrafiltration (30 kDa cutoff) in a stirring cell (Amicon), loaded on a HiLoad® 26/60 Superdex 200 column (2.6 cm x 60 cm, Pharmacia Biotech, Freiburg), and eluted

with 50 mM TEA 200 mM NaCl pH 7.5 at a flow rate of 1 ml min^{-1}. Active fractions were pooled, concentrated by ultrafiltration (30 kDa cutoff), and stored at –70°C.

2.6. Enzyme activity

2.6.1. Acetylene hydratase

(a) Assay of acetylene hydratase activity

Enzyme activity was measured photometrically in a coupled assay with alcohol dehydrogenase (Meckenstock *et al.*, 1999; Rosner and Schink, 1995). The reaction was performed in glass cuvettes sealed with rubber stoppers under N_2/H_2. In a typical assay, 10 µl acetylene hydratase solution were added to 960 µl of 1.5 mM titanium (III) citrate in 50 mM Tris/HCl pH 7.5 (Zehnder and Wuhrmann, 1976). After addition of 20 µl of 10 mM NADH and 10 µl of 2000 U ml^{-1} yeast alcohol dehydrogenase (Y-ADH), the reaction mixture was incubated for 10 min at 50°C. The reaction was started by addition of 1 ml acetylene to the gas phase. Depletion of NADH was followed at 365 nm. Activity was calculated using Beers Law and ε_{365} (NADH) = 3.4 mM^{-1} cm^{-1} (Ziegenhorn *et al.*, 1976). 1 µmol acetylene converted to acetaldehyde per min corresponds to 1 Unit (U).

(b) Assay with thermostable alcohol dehydrogenase

In experiments at higher temperatures Y-ADH was replaced, or completed, by the thermostable alcohol dehydrogenase of *Sulfolobus solfataricus* (S-ADH). In a typical assay, 10 µl acetylene hydratase solution were added to 940 µl of 1.5 mM titanium (III) citrate in 50 mM Tris/HCl pH 7.5 (Zehnder and Wuhrmann, 1976). After addition of 20 µl of 10 mM NADH, and 10 µl of 2000 U ml^{-1} Y-ADH, and 20 µl S-ADH (62 µg), the reaction mixture was incubated for 10 min at 50°C. The reaction was started by addition of 1 ml acetylene to the gas phase. Depletion of NADH was followed at 365 nm. Activity was calculated using Beers Law and ε_{365} (NADH) = 3.4 mM^{-1} cm^{-1} (Ziegenhorn *et al.*, 1976).

2.6.2. Transhydroxylase

(a) Assay of transhydroxylase activity

Enzyme activity was assayed at 25°C in the anaerobe chamber (Chapter 2.5.1.) equipped with a cooler (Coolmatic RA-40, Mobitronic Gleichrichter EPS-100W, Waeco, Emsdetten). A discontinuous test system (Reichenbecher *et al.*, 1994; Brune and Schink, 1990) was used.
The reaction was performed in Eppendorf reaction tubes. In a typical assay 775 µl of 100 mM potassium phosphate buffer (KPi), pH 7.0 were mixed with 100 µl pyrogallol (100 µM in KPi), 100 µl 1,2,3,5-tetrahydroxybenzene (100 µM in KPi), and incubated for one minute. The assay was started by addition of 25 µl transhydroxylase solution. Aliquots (100 µl) were taken after 3 and 5 min incubation and immediately added to 100 mM H_3PO_4 (400 µl). Samples were kept on ice and analyzed quantitatively for pyrogallol and phloroglucinol by Reverse Phase HPLC within 1 h.

(b) Substrate and product analysis

Samples were analyzed by High Pressure Liquid Chromatography (S100 Solvent Delivery System, S5110 Injector Value System, S8100 Low Pressure Gradient Mixer, S3300 UV Detector, S4010 Column Thermo Controller, Sykam, Gilching; Lambda 1000 UV Detector, Bischoff, Leonberg) equipped with a Reverse Phase C18 column (Gromsil GSOD50512S2504, Grom Analytik, Herrenberg) at 40°C, in a methanol/phosphate (12.5% methanol, by vol.; 100 mM KPi pH 2.6) solvent system. Samples (20 µl) were injected and eluted at a flow rate of 1.5 ml min^{-1}. Aromatic compounds were detected with a Sykam S 3300 UV detector (Sykam, Gilching) at 205 nm. Data were analyzed by computer programs (AXXI-Chrom 727, Version 3.8; AXXIOM Chromatography, Calabasas California, USA) and quantified by comparison with external and internal standards of known composition. Peak identification was performed by comparison of retention times and UV spectra with those of standard samples.

2.6.3. Alcohol dehydrogenase

Enzymatic activity was assayed photometrically by measuring the disappearance of NADH at 365 nm. The reaction was performed in glass cuvettes sealed with rubber stoppers under N_2/H_2.

(a) Yeast alcohol dehydrogenase (Y-ADH)

In a typical assay 915 µl of 1.5 mM titanium (III) citrate in 20 mM Tris/HCl pH 7.0 were added to 25 µl of 10 mM NADH and 10 µl of 40 U ml^{-1} Y-ADH. The reaction mixture was incubated at an appropriate temperature for 10 min. The reaction was started by addition of 50 µl of acetaldehyde. Disappearance of NADH was followed at 365 nm. Activity was calculated using Beers Law and ε_{365} (NADH) = 3.4 mM^{-1} cm^{-1} (Ziegenhorn *et al.*, 1976).

(b) *Sulfolobus* alcohol dehydrogenase (S-ADH)

In a typical assay 920 µl of 1.5 mM titanium (III) citrate in 20 mM Tris/HCl pH 7.0 were added to 25 µl of 10 mM NADH and 5 µl of S-ADH (15.5 µg), further manipulations see above.

2.7. UV/Vis spectroscopy

UV/Vis spectra were obtained on a Cary 50 spectrometer (Varian, Darmstadt), a Lambda 16 spectrometer (Perkin Elmer), a HP 8452A diode array spectrophotometer (Hewlett Packard, Stuttgart), or a Lamda 16 spectrometer (Perkin Elmer, Überlingen) at room temperature if not indicated otherwise. The Cary 50 spectrometer was equipped with a temperature control unit (80% glycerol/water, v/v), allowing temperatures up to 80°C.

2.8. EPR spectroscopy

EPR spectra were recorded with a Bruker ESP 300 spectrometer connected to an ER 041 MR microwave bridge, an ER 048 H microwave controller, and an ER 032 M field controller (Bruker, Analytische Meßtechnik, Karlsruhe). The cavity was cooled with a Helitran-system (model LTD-3-110 C; Air Products and Chemicals, Allentown, USA). The temperature was controlled by manually adjusting the flow from the liquid helium storage vessel that was operated at a pressure of ≈ 70 kPa. The microwave frequency was measured with an Autohet Counter Mode 350 D (microwave frequency; Dana Electronics, Darmstadt), the magnetic field with a NMR Gaussmeter ER 035 M (Bruker), and the temperature with an APD-T1 thermometer (Air Products and Chemicals). The modulation frequency was always 100 kHz and the modulation amplitude was typically 1 mT. Measurements were performed with a Bruker ER 4116 DM bimodal cavity. The resonance frequency for the perpendicular mode was ≈ 9.65 GHz. The sample tubes were Suprasil quartz tubes with a diameter of 3 – 4 mm and the sample volume was most 300 µl.

The *g*-values were calculated according to the resonance equation:

$$g = \frac{h \cdot \nu}{\beta \cdot H}$$

with $h = 6.6262 \cdot 10^{-34}$ J s (Planck constant)

$\beta = 9.274096 \cdot 10^{-24}$ J T^{-1} (Bohr Magneton)

$[\nu] = s^{-1}$ (Microwave frequency)

[H] = T (Magnetic field)

2.9. Crystallization

Crystals were grown by the method of vapor diffusion where the protein solution was mixed with a precipitant solution and equilibrated against a higher concentrated precipitant reservoir in a closed environment. Under regular conditions, using non-volatile precipitants such as polyethylene glycol or salts, equilibrium is reached by diffusion of water from the protein drop to the reservoir, thus slowly increasing the concentration of all components in the drop (McPherson, 1982).

Crystals of acetylene hydratase or transhydroxylase were grown by the sitting drop vapor diffusion method (Figure 2.2) using Cryschem plates (Charles Supper Company, Natick, USA) or CrystalClear Strips (Hampton Research, Laguna Hills, USA). Buffers of low ionic strength were used for crystallization experiments, most commonly 5 mM HEPES/NaOH pH 7.0. Buffer exchange was carried out on NAP 5 gravity flow columns (Pharmacia Biotech, Freiburg). Each drop was prepared by mixing 2 µl of the protein solution with the same amount of the crystallization solution in the well of the crystallization device and was equilibrated by vapor diffusion against 500 µl of the solution contained in the reservoir of Cryschem plates or 80 µl in the reservoir of CrystalClear Strips plates respectively. The reservoir and the protein solution in the well were sealed with transparent (crystal clear) tape. In order to screen large numbers of more complex precipitant solutions, the method of sparse matrix sampling was applied (Carter Jr. and Carter, 1979; Jancarik and Kim, 1991) to obtain promising starting conditions.
Crystallization experiments of acetylene hydratase and transhydroxylase were performed under a N_2/H_2 atmosphere (95 : 5, v/v) and the preparations were stored in a desiccator at 20°C.
Proteins were stored at concentrations as high as 25 mg ml^{-1} and were diluted to 5 – 15 mg ml^{-1} immediately prior to crystallization experiments. Higher protein concentrations were beneficial for crystal growth.

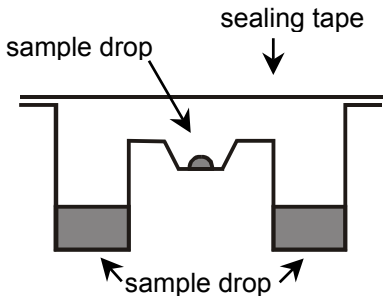

Figure 2.2 Schematic view of a sitting drop crystallization unit.

2.10. Sequencing of the acetylene hydratase gene

2.10.1. N-terminal amino acid sequencing

The N-terminal amino acid sequence was reported by Rosner (1994), containing 19 amino acids:

1	2	3	4	5	6	7	8	9	10	11	12	13	14	15	16	17	18	19
Ala	Ser	Lys	Lys	His	Val	Val	Cys	Gln	Cys	Cys	Asp	Ile	Asn	Cys	Val	Val	Glu	Ala
A	S	K	K	H	V	V	C	Q	C	C	D	I	N	C	V	V	E	A

2.10.2. Cyanogen bromide digestion

In order to obtain an internal fragment of the acetylene hydratase amino acid sequence, a cyanogen bromide digestion was carried out. 100 µg of acetylene hydratase and 20 µl of freshly prepared 0.5 M BrCN in 0.1 M HCl was filled up with 0.1 M HCl to 50 µl. The molar ratio BrCN : acetylene hydratase was 7500 : 1. The resulting solution was mixed, incubated at room temperature in the dark for 51 h, and stored at –20°C prior to use. The digestion products (10 µl) were separated on a 15% SDS-PAGE gel. Two sheets of PVDF-membrane (polyvinylidene diflouride, Bio Rad, München) and 10 sheets of blotting paper (Biometra, Göttingen) were prepared according to the gel size and incubated for 5 minutes in buffer according to Lämmli (1970). On the anode of the Biometra Fastblot system B32 (Biometra, Göttingen) 5 sheets of wet blotting paper, 2 sheets wet PVDF-membrane, the gel, and 5 sheets of wet blotting paper were applied in this order and air bubbles were removed by rolling out with a test tube. Transfer was done at 4°C with ≈ 2 mA cm^{-2} gel surface and about 100 mW electric power for 60 min. The PVDF membranes were stained with 0.025% (w/v) Coomassie Violet R150 (Merck, Darmstadt) in 40% methanol for 5 min. Excess dye was removed with 50% Methanol. The PVDF membranes were air-dried over night and stored at 4°C. The fragments of interest were excised and analyzed by automated Edman-degradation by L. Cobianci (Universität Konstanz) on an Applied Biosystems 477A-Protein sequencer.

2.10.3. DNA preparation

(a) Chromosomal DNA

Chromosomal DNA was prepared according to Maniatis *et al*. (1987) and H. Brinkmann (Universität Konstanz, personal communication). About 1.0 g of frozen *P. acetylenicus* cells were suspended in 10 ml of ATL-Lysis buffer (Qiagen, Hilden) and incubated for 30 min at 50°C in a water bath with gentle agitation. After addition of 0.6 mg ml^{-1} of lysozyme (Fluka) the mixture was incubated at 42°C for 30 min with periodic mixing. Proteins were digested during a 30 min incubation step at 45°C with 0.2 mg ml^{-1} proteinase K (Gibco BRL, Karlsruhe) and gentle inversion every 10 min. After addition of 0.2% SDS (w/v) and 60 min incubation at 45°C with gentle inversion, the solution was centrifuged at 10000 *g* (5 min, 4°C) to eliminate larger debris.

For removal of proteins the supernatant was subjected to a phenol extraction: half a volume of TE-buffer equilibrated phenol (Roth, Karlsruhe) was added to the supernatant and mixed for 10 min by gentle inversion. Another half a volume of a chloroform : isoamyl alcohol (24 : 1, Sigma) mixture was added, the mixture was gently inverted for 3 min, and centrifuged (12000 *g*, 10 min, 4°C). The upper (aqueous) phase was separated and subjected to another phenol precipitation. The resulting aqueous phase was washed with half a volume of chloroform : isoamyl alcohol (24 : 1) and centrifuged (12000 *g*, 10 min, 4°C).
DNA was purified by adding 2 volumes of pure ethanol to the aqueous phase and precipitated as white filaments. The solution was gently mixed by inversion. The DNA was recovered with a glass-rod, washed 3 times with 70% ethanol (in water) solution (v/v), excess liquid was eliminated with clean cellulose. The recovered DNA was dissolved in 500 µl of TE buffer.

(b) Plasmid DNA

Plasmid DNA was isolated from *Escherichia coli* using the QiaPlasmid Kits (Qiagen, Hilden).

2.10.3. Primers for polymerase chain reaction

Primers (M13/pUC Forward, M13/pUC Reverse) of the multiple cloning site of the pUC18 plasmid were synthesized according to the manufacturer (Boehringer, Mannheim).
Primers were ordered from MWG Biotech (Ebersberg, Germany).

2.10.4. PCR techniques

(a) Polymerase chain reaction

Polymerase Chain Reaction (Innis *et al*., 1988; Saiki *et al*., 1988) was carried out with REDTaq DNA Polymerase (Sigma, Deisenhofen) or with the Expand Long Template PCR System (Roche Diagnostics, Mannheim) containing Taq and Pwo DNA polymerase on a GeneAmp PCR System 9700 (PE applied biosciences, UK). In a typical assay 1 µl of forward (10 pmol μl^{-1}), 1 µl of reverse primer (10 pmol μl^{-1}), 1 µl of REDTaq (1 U μl^{-1}), 2.5 µl of dNTP's (10 µM), 2.5 µl of 10 x amplification buffer (Sigma), and 20 ng of DNA were filled up with water to 25 µl and

amplified (Table 2.10). PCR products were analyzed on a 1% agarose gel with ethidiumbromide staining and 1 kb ladder standard (Gibco BRL, Karlsruhe) and purified using the QIAquick PCR Purification Kit (Qiagen, Hilden) or by excision from a preparative agarose gel and further purification with the QIAquick Gel Extraction Kit (Qiagen, Hilden).

Denaturation step	94°C	3 min	
Melting step	94°C	1 min	
Annealing step	45 – 60°C	1 min	35 cycles
Elongation step	72°C	2 min	
Final elongation step	72°C	10 min	
Cooling/storing step	4°C	∞ min	

Table 2.10 Typical amplification protocol for Taq polymerase.

(b) Colony PCR

In order to avoid the expensive and time-consuming plasmid DNA preparations, colony PCR has been carried out. 1 µl of a transformed overnight *E. coli* liquid culture or the cells of a transformed overnight *E. coli* agar culture were mixed with PCR reagents (Chapter 2.10.4. a), appropriate primers (Chapter 2.10.3.), and amplified (Table 2.10).

(c) Inverse PCR

Inverse PCR was the first method used for sequencing of unknown regions of DNA flanking a known fragment. Genomic DNA was treated with a restriction endonuclease (Maniatis *et al*., 1987) which, after digestion, was inactivated by heat. The digest was then diluted and incubated with T4 DNA ligase (Promega, Mannheim). This led to a religation of the restriction fragments, while the dilution step increased the possibility of self-ligation. PCR on such a religated DNA ring with primers pointing out of the known region would then amplify the unknown region between the primers and the next restriction site of the enzyme chosen. Digests with different enzymes allowed for reliable genome walking with fragments averaging between 300 and 700 bp.

(d) Anchor-ligated Genome Walking

In order to overcome the practical size limitations for new fragments obtained through inverse PCR, an anchor-ligated PCR approach in combination with nested PCR was applied using the Universal Genome Walker Kit (Clontech, Heidelberg, Figure 2.3).

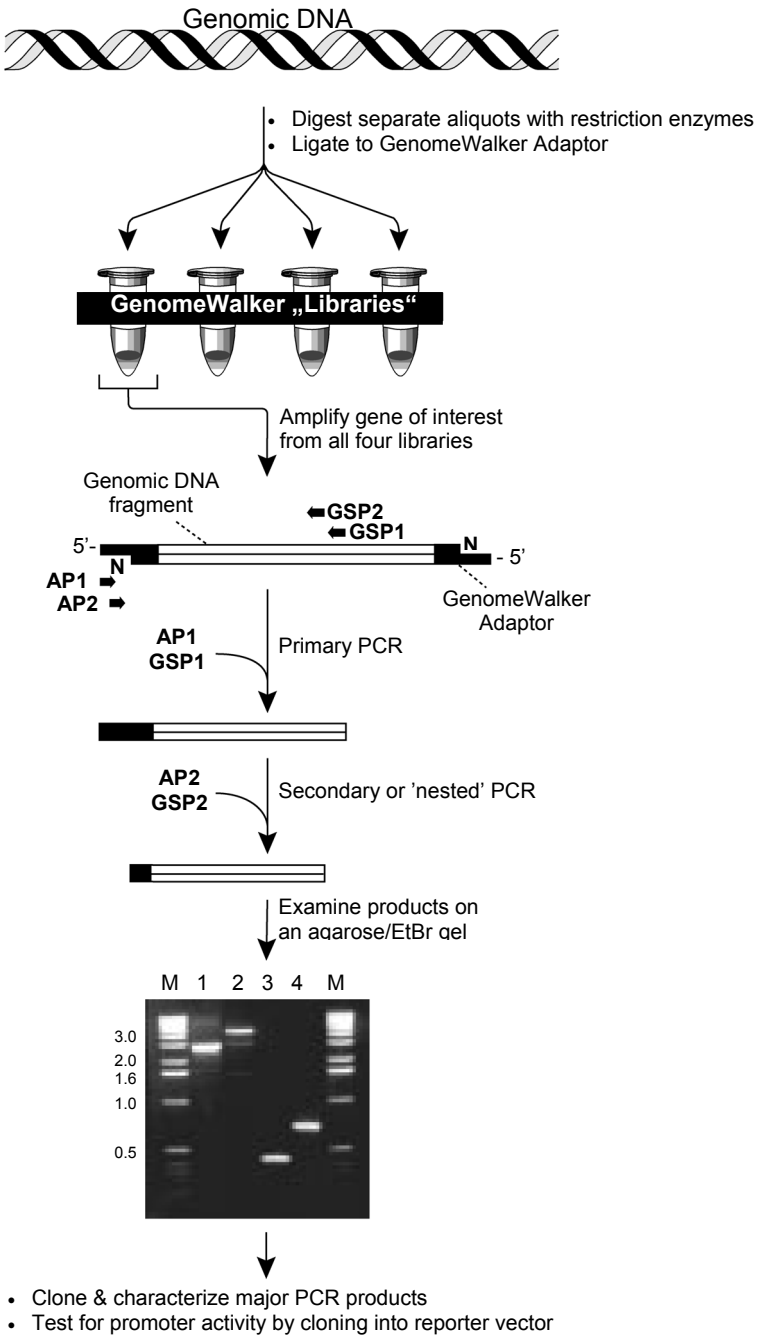

Figure 2.3 Flow chart of the GenomeWalker protocol.
The gel shows the products generated by walking with human GenomeWalker libraries and gene-specific primers derived from the human p53 cDNA sequence.
Lane 1: EcoR V Library. Lane 2: Dra I Library. Lane 3: Pvu II Library. Lane 4: Ssp I. AP1/AP2: Adaptor primers. GSP: Gene-specific primers. (Clontech, Heidelberg, Universal GenomeWalker Kit User Manual PT3042-1 (PRO3300), 21 March 2000).

2.10.5. Sequencing

PCR products were analyzed on a 3100 Capillary Array with 16 capillaries (Applied Biosystems, Langen). Data were collected and processed using the 3100 Data Collection Software Version 1.0 (Applied Biosystems).

PCR products were amplified according to Applied Biosystems protocols using fluorescence marked dideoxyribonucleotide triphosphates in the DNA Sequencing Kit (PE applied biosciences, UK). In a typical protocol 10 µg PCR product, 1 µl primer (10 pmol μl^{-1}) and 1.5 µl sequencing mix (PE applied biosciences) were filled up with water to 10 µl and incubated (Table 2.11). After a ethanol/sodium acetate precipitation (Table 2.12) the purified product was used for analysis in the 3100 Capillary Array system.

Sequence analysis was performed with the program Sequence Navigator (Applied Biosystems).

Melting step	94°C	10 sec	
Annealing step	45 – 60°C	5 sec	25 cycles
Elongation step	60°C	4 min	
Cooling/storing step	4°C	∞ min	

Table 2.11 Typical amplification protocol for Taq polymerase using the DNA sequencing kit of PE Applied Biosciences.

Step	Action
1	Mix 1 µl of 3 M sodium acetate (NaOAc) pH 4.6 and 25 µl of 95% ethanol in a 1.5 ml microcentrifuge tube.
2	Add 10 µl of the sequencing reaction.
3	Vortex and leave on ice for 15 min to 24 h.
4	Spin the tubes for 20 min at maximum speed.
5	Carefully aspirate the supernatant and discard.
6	Rinse the pellet with 500 µl of 70% ethanol.
7	Vortex briefly.
8	Spin for 5 min at maximum speed. Again carefully aspirate the supernatant and discard.
9	Dry the pellet in a vacuum for 5 min.
10	Dissolve the pellet in 10 µl water.

Table 2.12 Ethanol/sodium acetate precipitation and purification protocol for sequencing reaction products.

2.10.6. Cloning

Digested genomic *P. acetylenicus* DNA or blunt end PCR products were ligated in a pUC18 vector (Boehringer, Mannheim) and transfected by heat shock (Inoue *et al*., 1990) into competent *E. coli* K12 XL1blue cells (Bullock *et al.*, 1987). The relevant genotype is:

recA1 supE44 endAI hsdR17 gyrA96 relA1 thi-1 (lac-proAB)
[*F' proAB* lac_{Iq} *lacZ M15 Tn10 (Tet* $^{+}$ *)*]

Media (SOB, SOC, and LB) were prepared as described by Hanahan (1983). For selection of transformed *E. coli* LB plates, containing 100 µg Ampicillin ml^{-1}, were used. To make TB (10 mM Pipes, 55 mM $MnCl_2$, 15 mM $CaCl_2$, 250 mM KCl) all components except $MnCl_2$ were mixed and the pH was adjusted to 6.7 with 5 M KOH. Then, $MnCl_2$ was dissolved, the solution sterilized by filtration through a prerinsed 0.45 µm filter unit, and stored at 4°C. All salts were added as solids.

Frozen stock XL1blue cells were thawed, plated on a LB agar plate, and cultured overnight at 37°C. One colony was isolated with a platinum loop, inoculated to 5 ml of LB medium in a 15 ml polypropylene tube (Greiner, Frickenhausen), and grown over night at 37°C. A 2 liter flask with 200 ml of SOB medium was inoculated with this overnight culture and grown in 25 h at 18°C to $A_{600} = 0.6$. The flask was removed from the incubator and placed on ice for 10 min. The culture was spun at 2500 *g* (4°C, 10 min). The pellet was resuspended in 64 ml of ice cold TB, incubated on ice for 10 min, and spun at 2500 *g* (4°C, 10 min). The pellet was gently resuspended in 16 ml of ice cold TB, and DMSO was added to a final concentration of 7%. After incubating in an ice bath for 10 min the cell suspension was dispensed by 1 ml and immediately frozen in liquid nitrogen. The frozen cells can be stored in liquid nitrogen for at least one month without a detectable loss of competence (Inoue, 1990).

Ligation of DNA in a pUC18 Vector (Boehringer, Mannheim) was done with the Pharmacia SureClone Ligation Kit (Pharmacia, Freiburg) according to the manufacturers instructions.

The following standard protocol for plasmid transformation was taken from Inoue *et al.* (1990). 2 ml of competent *E. coli* were thawed at room temperature. Aliquots of 200 µl were filled into 15 ml polypropylene tubes (Greiner) and placed in an ice bath. 5 µl of the plasmid solution were added to each tube and the cells were placed in an ice bath for 30 min. Afterwards they were heat-pulsed without agitation at 42°C for 30 s, and transferred to an ice bath for 2 min. After addition of 0.8 ml of ice cold SOC, the tubes were incubated at 37°C for 1 h. A desired portion of the mixture (200 µl or 20 µl + 180 µl SOC-medium) was plated out on LB plates containing 100 µg Ampicillin ml^{-1}. Colonies were used for colony PCR after overnight incubation at 37°C.

2.10.7. Computer programs and Internet websites

Protein Database searches

- National Center For Biotechnology Information (NCBI), BLASTP searches
  http://www.ncbi.nlm.nih.gov:80/BLAST/
- National Center For Biotechnology Information (NCBI), Conserved Domain Database
  http://www.ncbi.nlm.nih.gov/Structure/cdd/cdd.shtml
- European Bioinformatics Institute (EBI)
  http://www.ebi.ac.uk/fasta3/
- The Institute For Genomic Research (TIGR)
  http://www.tigr.org/
- The rRNA WWW server
  http://rrna.uia.ac.be/
- Swiss Institute of Bioinformatics, ExPASy Molecular Biology Server (Appel *et al.*, 1994)
  http://www.expasy.ch
- ExPASy ProtParam tool
  http://www.expasy.ch/tools/protparam.html

Computer Programs for phylogenetic analyses

- ClustalX (Thompson *et al*., 1997)
  http://www-igbmc.u-strasbg.fr/BioInfo/ClustalX/Top.html
- Treecon (Van de Peer and De Wachter, 1993, 1994, 1997)
  http://www.evolutionsbiologie.uni-konstanz.de/peer-lab/peer.htm
- Puzzle5.0 (Strimmer and von Haeseler, 1996, 1997)
  http://www.tree-puzzle.de
- Mega2 (Kumar *et al.*, 1994)
  http://www.megasoftware.net/
- MUST (Philippe, 1993)
  http://bufo.bc4.u-psud.fr/must.html
- MOLPHY version 2.3 (Adachi and Hasegawa, 1996)
- PAUP* version 4 (Swofford, 1999)

2.10.8. Sequence handling and phylogenetic analysis

Based on BLASTP searches with sequences of acetylene hydratase and transhydroxylase the obtained sequences were extracted from GenBank and a first alignment was produced by ClustalX (Thompson *et al.*, 1997). This alignment was manually refined using the program ED of the MUST package (Philippe, 1993). Regions of uncertain similarity were omitted from the analysis. The tree topology was inferred using protein maximum-likelihood (Prot-ML) as implemented in the MOLPHY package (version 2.3; Adachi and Hasegawa, 1996). Using the JTT-F model and the NJDIST option a NJ-tree was constructed and further optimized using the local rearrangement option. Distance analyses were performed with the Mega2 package (Kumar *et al.*, 1994) using amino acid gamma-corrected values and the NJ method (Saitou and Nei, 1987). Parsimony analysis was performed using PAUP* (Swofford, 1999) with 1000 bootstrap replicates and 10 times random addition. Gamma parameters and ML-bootstrap parameters were obtained using Puzzle 5.0 (Strimmer and von Haeseler, 1996, 1997). The significance of different ML topologies was tested with the Kishino-Hasegawa function as implemented in Puzzle 5.0. Accession numbers the proteins and the corresponding amino acid sequences were taken from the NCBI. Additional sequences were taken from "The TIGR Microbial Database" (http://www.tigr.org).

2.11. Analytical methods

2.11.1. ICP-MS

Inductively coupled plasma mass spectrometry (ICP-MS) was performed by Spurenanalytisches Laboratorium Dr. Baumann (Maxhütte-Haidhof). The concentrations of vanadium, iron, zinc, molybdenum, and tungsten were determined by ICP-MS in 4 different samples containing acetylenehydratase (100 µl, ≈ 2 mg ml^{-1}). A buffer sample served as a control.

2.11.2. Protein

Protein was determined using bicinchoninic acid (BCA) (Smith *et al.*, 1985). This method is based on the Biuret reaction (Goa, 1953). Bovine serum albumin was used as a standard. The concentration of BSA standard stock solutions was photometrically determined with $\varepsilon_{279nm} = 0.667$ (mg ml^{-1})$^{-1}$ cm^{-1} (Foster and Sterman, 1956). 100 µl of unknown or standard proteins (5 – 20 µg) were mixed with 1 ml of a solution containing 50 : 1 (v/v) BCA and $CuSO_4 \cdot 5H_2O$ (4%, w/v). The reaction mixture was incubated for 20 min at 60°C. The calibration curve was recorded on a Hewlett Packard diode array spectrophotometer (Hewlett Packard, Waldbronn) and the absorbance was monitored at 562 nm.

2.11.3. Polyacrylamide gel electrophoresis

SDS-PAGE was carried out with the Mighty Small System (SE 250, 100 x 80 x 0.75 mm, Hoefer Scientific Instruments, San Francisco, USA) according to Lämmli (1970). 10 – 15% acrylamide gels were used.
The molecular mass of the subunits was estimated using low molecular mass markers (BioRad Laboratories, München). Gels were stained with coomassie (Zehr *et al.*, 1989) or silver (Rabilloud, 1990; Heukeshoven and Dernick, 1985).

2.11.4. Agarose gels

In order to separate DNA 1% agarose (Boehringer Ingelheim, Heidelberg) gels with ethidium-bromide staining and TAE buffer were performed using an EC105 System (EC Apparatous Corporation).

3. Results

3.1. Acetylene hydratase of *Pelobacter acetylenicus*

3.1.1. Growth of *Pelobacter acetylenicus* under various conditions

In order to obtain large quantities of acetylene hydratase it was necessary to produce high amounts of *P. acetylenicus* cells. R.U. Meckenstock (Universität Konstanz, personal communication; Meckenstock *et al*., 1999) described that the expression of the enzyme is increased 10-fold if a 50 l batch culture is fed continuously with 5 – 10 kPa of acetylene and the pH is adjusted between 6.8 and 7.0. The solubility of acetylene in water is 1185 mg ml^{-1} or 45.5 mM (20°C, 100 kPa; material safety data sheet acetylene, Messer, Griesheim).

(a) Tungstate cultivation

A 50 l batch culture of *P. acetylenicus* on 400 nM tungstate led to 37 g wet cell mass. The cells grew within 23 hours to an optical density of 0.6 at 578 nm (Figure 3.1) and were harvested at the end of the exponential growth phase.

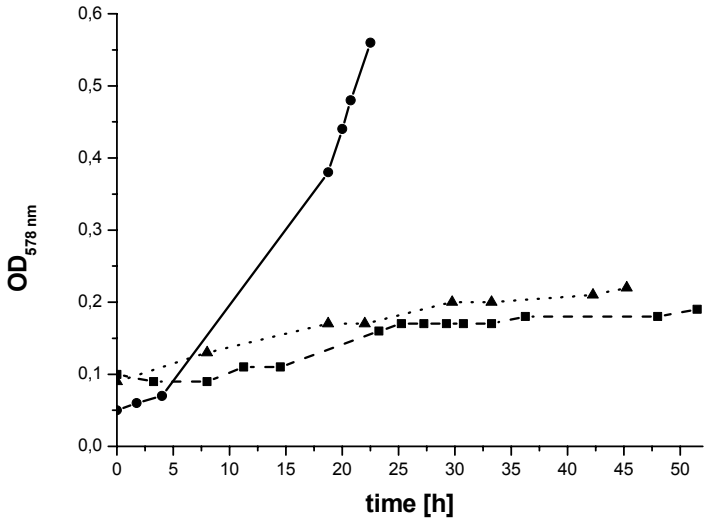

Figure 3.1 Growth of *P. acetylenicus*.
50 l batch culture, 10 kPa C_2H_2 as energy and carbon source, freshwater medium.
- ● 400 nM tungstate
- ■ 2 µM molybdate (^{95}Mo) and 2 nM tungstate (^{183}W)
- ▲ 10 µM vanadate, 2 nM molybdate (^{95}Mo), and 2 nM tungstate (^{183}W)

(b) Molybdate cultivation (^{95}Mo)

A 50 l batch culture of *P. acetylenicus* on 2 µM molybdate (^{95}Mo) and 2 nM tungstate (^{183}W) led to 4 g wet cell mass. The cells grew within 52 hours to an optical density of 0.2 at 578 nm (Figure 3.1).

(c) Vanadate cultivation

A 50 l batch culture of *P. acetylenicus* on 10 µM vanadate, 2 nM molybdate (^{95}Mo), and 2 nM tungstate (^{183}W) led to 8 g wet cell mass. The cells grew within 46 hours to an optical density of 0.2 at 578 nm (Figure 3.1).

3.1.2. Purification of acetylene hydratase

Figure 3.2 (A) shows a flow chart of the enzyme purification that had been carried out for acetylene hydratase from the tungstate cultivation (Meckenstock *et al*., 1999). In order to avoid degradation of iron-sulfur clusters by dioxygen, all purification steps were done in an anaerobe chamber. In figure 3.2 (B) the flow chart for the enzyme purification of the molybdate and vanadate cultivation is shown.

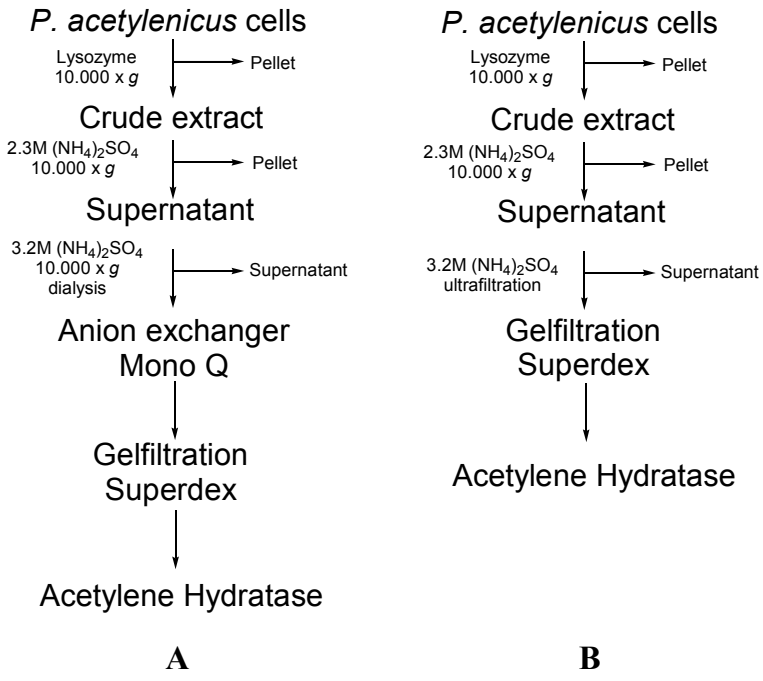

Figure 3.2 Purification scheme of *P. acetylenicus* acetylene hydratase.
(A) Tungstate cultivation.
(B) Molybdate and vanadate cultivation.

(a) Tungstate cultivation

Ammonium sulfate precipitation:

The crude extract was subjected to a 2.3 M ammonium sulfate precipitation. After centrifugation, the whole acetylene hydratase activity was found in the supernatant. About 80% of the contaminating enzymes were removed in this step. The supernatant was subjected to a 3.2 M ammonium sulfate precipitation and the acetylene hydratase activity was found in the pellet. After the first (2.3 M) step about 70% of the initial activity was recovered, after the second step about 50% (Table 3.1).

Anion exchange chromatography:

After dialysis of the resuspended pellet, the protein was loaded onto a Mono Q anion exchange column, equilibrated with 50 mM Tris/HCl pH 7.5. With a salt gradient from 0 to 500 mM NaCl, flow rate of 1 ml min^{-1}, acetylene hydratase eluted with 300 mM NaCl. During the elution the absorption of the eluted proteins was measured at 280 nm and 405 nm. About 63% of the initial activity was recovered (Table 3.1).

Gel filtration:

The fractions of the Mono Q purification step, showing acetylene hydratase activity, were pooled, concentrated to 1.5 ml, and loaded onto a Superdex 75 gel filtration column, equilibrated with 50 mM Tris/HCl 200 mM NaCl pH 7.5. Acetylene hydratase eluted, at a flow rate of 1 ml min^{-1}, after 62 min. About 50% of the initial activity was recovered after the final gel filtration step. According to the specific activity acetylene hydratase was enriched 32 fold with a high specific activity of 42 U mg^{-1} (Table 3.1). 25 g of wet cell mass led to 39 mg of pure acetylene hydratase.

	Protein [mg]	**Activity [U]**	**Specific activity [U mg^{-1}]**	**Yield (Protein) [%]**	**Yield (activity) [%]**	**Enrichment factor**
Crude extract	2533	3311	1.31	100	100	1
3.2M AS	364	1701	4.68	14	51	3.6
Mono Q	104	2071	19.83	4	63	15.1
Superdex	39	1662	42.25	1.5	50	32.3

Table 3.1 Purification of acetylene hydratase from tungstate grown *P. acetylenicus*.
25 g of wet cells were used; activity was measured at 50°C.
1 U = 1 µmol acetylene min^{-1}; AS = ammonium sulfate.

Figure 3.3 shows a SDS-PAGE of a typical acetylene hydratase purification. After coomassie staining the gel was silver-stained and digitized. The enrichment of the acetylene hydratase band (73 kDa) during the purification procedure is clearly shown on the gel.

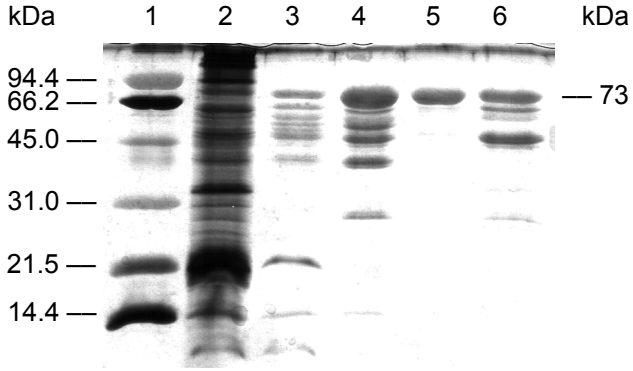

Figure 3.3 SDS-PAGE (12%) of acetylene hydratase purification from tungstate grown *P. acetylenicus*.
Lane 1: Molecular weight markers; Lane 2: Crude extract (9 µg); Lane 3: Protein after 3.2 M $(NH_4)_2SO_4$ precipitation (5.6 µg); Lane 4: Protein after anion exchanger Mono Q (4.4 µg); Lane 5: Pure acetylene hydratase after gel filtration (2.3 µg); Lane 6: Protein of gel filtration border fractions (5.4 µg).

(b) Molybdate (^{95}Mo) and vanadate cultivation

Cultivation of *P. acetylenicus* on molybdate (^{95}Mo) and vanadate led to 4 g and 8 g cell mass, respectively. In view of the small amount of cell material, the purification procedure was modified (Figure 3.2 B), leading to a 90 – 95% enriched acetylene hydratase.
Ammonium sulfate precipitation and gel filtration were done as described above, with the omission of the anion exchanger Mono Q.

About 5 mg of acetylene hydratase was obtained from the molybdate (^{95}Mo) cultivation. The protein was enriched 105 fold and the specific activity was 17 U mg^{-1}, which is less than half of the specific activity of acetylene hydratase from tungstate cultivation (42.25 U mg^{-1}; Tables 3.1, 3.2).

	Protein [mg]	Activity [U]	Specific activity [U mg^{-1}]	Yield (Protein) [%]	Enrichment factor
Crude extract	134	22	0.16	100	1
3.2M AS	16	128	8.11	12	51
Superdex	5.5	92	16.74	4	105

Table 3.2 Purification of acetylene hydratase from molybdate (^{95}Mo) grown *P. acetylenicus*. 4 g of wet cells were used; activity was measured at 50°C. 1 U = 1 µmol acetylene min^{-1}; AS = ammonium sulfate.

Purification of acetylene hydratase from vanadate cultivation led to 28 mg of acetylene hydratase with a very low specific activity of 2.6 U mg^{-1} corresponding to only 6% of the specific activity of acetylene hydratase from tungstate cultivation. The protein was enriched 12 fold during purification (Table 3.3).

	Protein [mg]	Activity [U]	Specific activity [U mg^{-1}]	Yield (Protein) [%]	Enrichment factor
Crude extract	270	57	0.21	100	1
3.2M AS	74	75	1.01	27	4.8
Superdex	28	73	2.59	10	12.3

Table 3.3 Purification of acetylene hydratase from vanadate grown *P. acetylenicus*. 8 g of wet cells were used; activity was measured at 50°C. 1 U = 1 µmol acetylene min^{-1}; AS = ammonium sulfate.

Figure 3.4 shows a SDS-PAGE of the acetylene hydratase purification from the molybdate (^{95}Mo) and the vanadate cultivation. After coomassie staining the gel was silver-stained and digitized.

Acetylene hydratase from the molybdate (^{95}Mo) cultivation shows a major band at about 73 kDa, the corresponding acetylene hydratase from the vanadate cultivation is moving slower on a SDS-PAGE and shows a dominant band at about 80 kDa as well as a band at about 40 kDa (Figure 3.4).

Because of the modified purification procedure, both acetylene hydratases contained other proteins. Rosner (1994) showed that some of these minor bands were decomposition products of the 73 kDa band as a consequence of the denaturing steps of the SDS-PAGE procedure. However, the purified acetylene hydratase was enriched by a factor of 105 ($^{95}MoO_4^{2-}$) and 12.3 (vanadate) with respect to the specific activity.

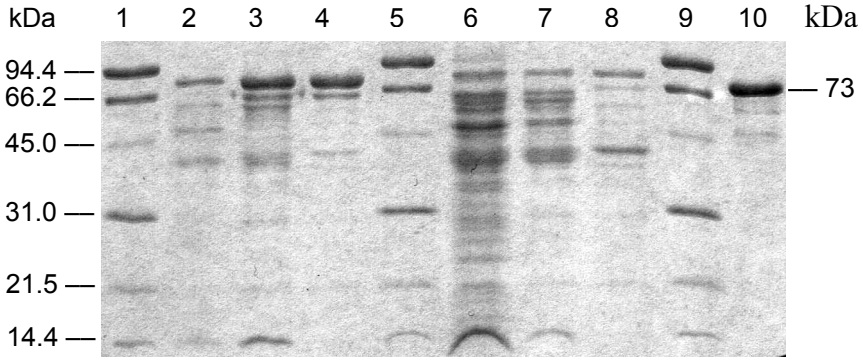

Figure 3.4 SDS-PAGE (12%) of acetylene hydratase purification from molybdate ($^{95}MoO_4^{2-}$) and vanadate (VO_3^-) grown *P. acetylenicus*.
Lane 1, 5, 9: Molecular weight markers; Lane 2: Crude extract ($^{95}MoO_4^{2-}$, 6.5 µg); Lane 3: Protein after 3.2 M $(NH_4)_2SO_4$ precipitation ($^{95}MoO_4^{2-}$, 5 µg); Lane 4: Acetylene hydratase after gel filtration ($^{95}MoO_4^{2-}$, 2.5 µg); Lane 6: Crude extract (VO_3^-, 6.4 µg); Lane 7: Protein after 3.2 M $(NH_4)_2SO_4$ precipitation (VO_3^-, 5 µg); Lane 8: Acetylene hydratase after gel filtration (VO_3^-, 2.8 µg); Lane 10: Acetylene hydratase from tungstate cultivation (2.5 µg).

3.1.3. Thermostability of acetylene hydratase, Y-ADH, and S-ADH

Rosner (1994) reported that acetylene hydratase is rather thermostable with a temperature optimum at 50°C. In the test system for acetylene hydratase (Chapter 2.6.1.) Yeast alcohol dehydrogenase (Y-ADH) was used. This enzyme shows a temperature optimum at 35°C and a strong decrease of activity at higher temperatures (Figure 3.5 A).

In contrast, the thermostable alcohol dehydrogenase from *S. solfataricus* (S-ADH) shows an increase in activity at higher temperatures (Figure 3.5 B). Enzyme activity of S-ADH was easily detectable between 50°C and 65°C but it is significantly lower compared to Y-ADH. Activity is increasing rapidly at higher temperatures. The highest activity was observed at 80°C. This is also the highest possible temperature of our instrument.

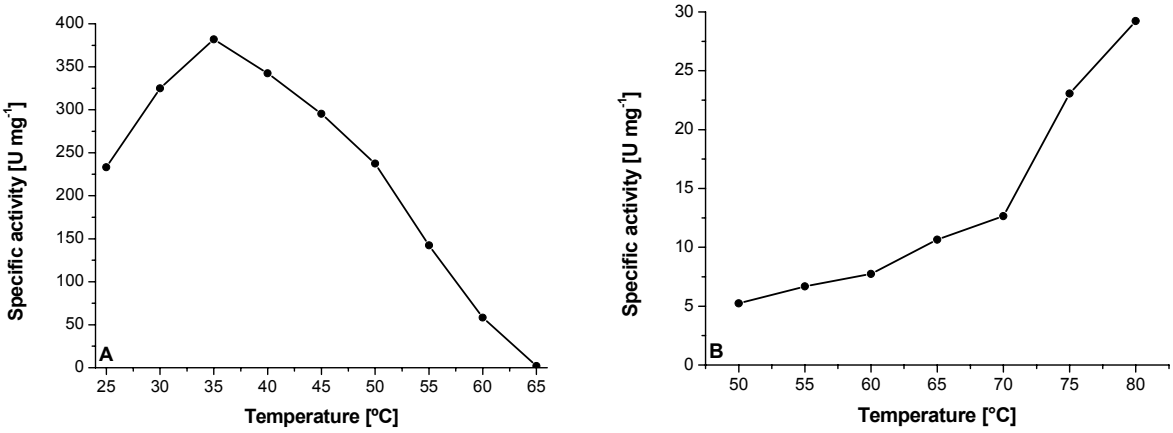

Figure 3.5 Temperature dependence of the specific activity of two alcohol dehydrogenases.
(A) Yeast.
(B) *S. solfataricus*.

Figure 3.6 shows the temperature dependence of the specific activity of acetylene hydratase from two different preparations. In both samples the highest activity was measured between 45°C and 55°C with a temperature optimum at 50°C. The low activity of the thermostable S-ADH around 50°C is a problem of the test system. To compensate for this fact higher amounts of S-ADH were used. However, the provided quantity was limited because S-ADH is not commercially available and was a generous gift of C.A. Raia, Naples, Italy. Perhaps the temperature optimum of acetylene hydratase is not 50°C, but it is in the range between 50°C and 55°C. However, using the commercially available Y-ADH the best temperature for the standard assay is 50°C.

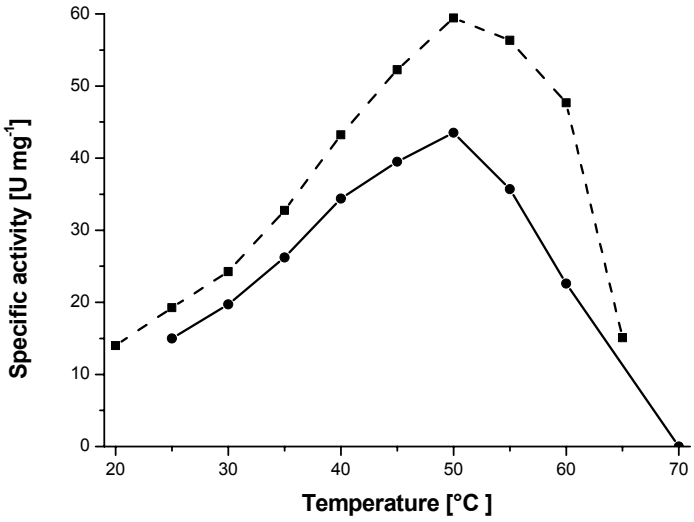

Figure 3.6 Temperature dependence of the specific activity of *P. acetylenicus* acetylene hydratase.
- ● Only Y-ADH was used.
- ■ Y-ADH was used between 20°C and 50°C, a mixture of Y-ADH and S-ADH was used between 50°C and 60°C, only S-ADH was used at 65°C.

3.1.4. Long-term study on acetylene hydratase activity

Acetylene hydratase is a very stable enzyme when stored under exclusion of dioxygen in a nitrogen/hydrogen atmosphere at 6°C. Within 3 months there was no detectable loss in acetylene hydratase activity from tungstate-grown *P. acetylenicus* (Figure 3.7). Activity was measured sporadically within 3 months at 30°C and 50°C. The average specific activity is 22 U mg^{-1} and 47 U mg^{-1} at 30°C and 50°C, respectively.

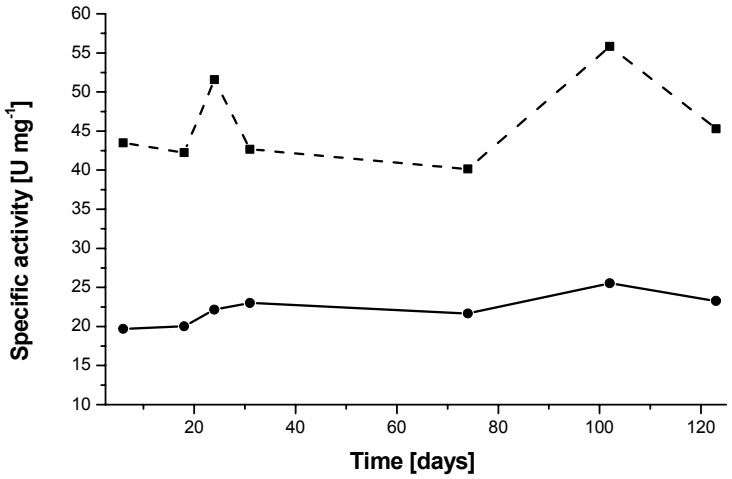

Figure 3.7 Long-term study on *P. acetylenicus* acetylene hydratase specific activity. Protein was stored between 2°C and 6°C in a fridge under a N_2/H_2 atmosphere. Activity was measured at ● 30°C and ■ 50°C in 100 mM Tris/HCl pH 7.0.

3.1.5. Metal content of acetylene hydratase

UV/Vis and EPR data indicated that iron, tungsten, and/or molybdenum are implemented in acetylene hydratase (Meckenstock *et al.*, 1999; Kisker *et al.*, 1999; Rosner, 1994). Earlier studies showed that preparations of acetylene hydratase from tungstate-cultivated cells also contained zinc (Krieger, 1997). Thus, the different preparations of acetylene hydratase were investigated by ICP-MS to determine the content of various metals (Table 3.4).

The highly active acetylene hydratase from tungstate-cultivated *P. acetylenicus* (22 U mg^{-1}, 30°C) contained about four mol iron and one mol tungsten per mol enzyme with a Fe/W ratio of 3.1. Molybdenum was absent in this sample. The zinc contents of acetylene hydratase from tungstate, molybdate (^{95}Mo), and vanadate cultivations were lower than 0.2 mol zinc per mol

enzyme and therefore significantly lower than the previously reported 0.65 (Table 3.4; Krieger, 1997).

Cultivation of *P. acetylenicus* on molybdate (^{95}Mo) led to a Mo-enriched acetylene hydratase that practically contained no tungsten. About 0.5 mol molybdenum and 3.1 mol iron per mol acetylene hydratase gave a Fe/Mo ratio of 6.1.

Acetylene hydratase from vanadate cultivation contained almost no tungsten, molybdenum, and vanadium as demonstrated by the Fe/V ratio of 241 (Fe/W = 48, Fe/Mo = 60). The iron content was significantly lower than in acetylene hydratase from tungstate or molybdate cultivation.

Krieger (1997) purified an acetylene hydratase with a specific activity of 12.56 U mg^{-1} (30°C) that contained 3.61 mol iron, 0.38 mol tungsten, and no molybdenum. The Fe/W ratio was 9.5. Selenium was not detected in this sample.

AH-Sample	V	Fe	Zn	Mo	W	Fe/M
^{95}Mo	0.00	3.11	0.18	0.51	0.01	6.1
V	0.01	2.41	0.12	0.04	0.05	241
W	0.00	3.52	0.18	0.00	1.13	3.1
Krieger (1997)	n.d.	3.61	0.65	0.00	0.38	9.5

Table 3.4 ICP-MS analysis of acetylene hydratase from different cultivations.
^{95}Mo: AH from molybdate ($^{95}MoO_4^{2-}$) cultivation; V: AH from vanadate cultivation; W: AH from tungstate cultivation. Acetylene hydratase, analyzed by Krieger (1997), was from a tungstate cultivation.
Enzyme concentration: about 2.0 mg ml^{-1}
A molecular mass of 84 kDa (81.85 kDa (amino acid chain) + 352 Da (1 x [4Fe-4S] cluster) + 1.7 kDa (W-bisMGD)) was used for calculations.
n.d.: not determined. M = Mo, W, V.

3.1.6. UV/Vis spectra of acetylene hydratase

Purified acetylene hydratase shows a green-yellow color that appears brown at higher concentrations. The absorption peak at 280 nm results from the absorption of aromatic amino acids. The absorption shoulder at 375 nm of “as isolated“ and dithionite-reduced acetylene hydratase is typical for iron-sulfur clusters. Two other shoulders at 320 nm and 590 nm were also present. Figure 3.7 A, B, and D shows the UV/Vis spectra of acetylene hydratase from tungstate, molybdate (^{95}Mo), and vanadate cultivation between 250 and 1100 nm. In figure 3.7 C the UV/Vis spectra of “as isolated“ and dithionite-reduced acetylene hydratase from tungsten cultivation are compared.

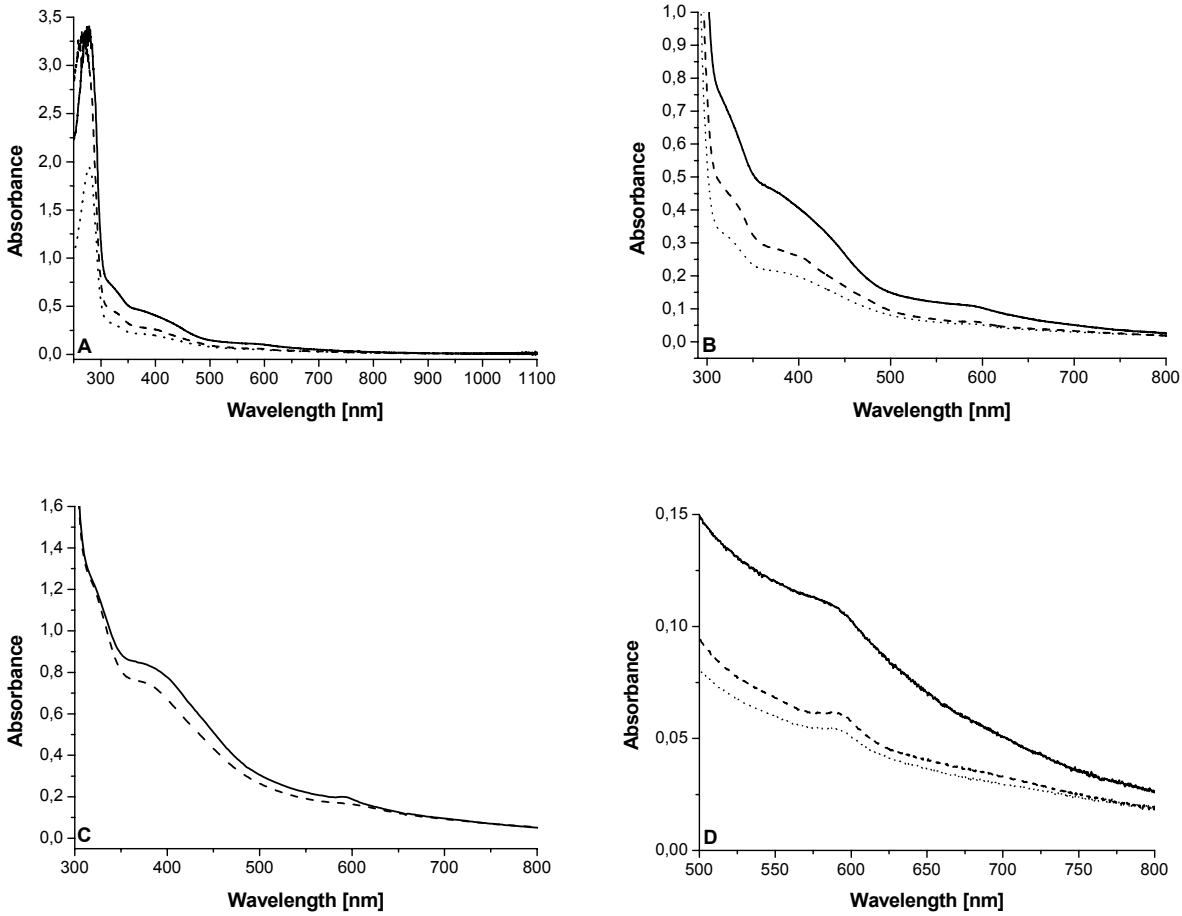

Figure 3.8 UV/Vis spectra of *P. acetylenicus* acetylene hydratase.
Solid line: AH from tungstate cultivation; Dashed line: AH from molybdate (^{95}Mo) cultivation; Dotted line: AH from vanadate cultivation. Enzyme: 2.25 mg ml^{-1} in 20 mM Tris/HCl pH 7.0.
A: 250 – 1100 nm; B: 290 – 800 nm (enlarged); D: 500 – 800 nm (enlarged)
C: AH from tungstate cultivation, 5 mg ml^{-1} in 5 mM HEPES pH 7.5. Solid line: "as isolated" AH; Dashed line: dithionite-reduced AH.

3.1.7. EPR spectra of acetylene hydratase

(a) Acetylene hydratase - tungsten cultivation

"As isolated" acetylene hydratase from tungsten grown *P. acetylenicus* showed a weak signal of a most likely truncated [3Fe-4S] cluster with a g_{av} = 2.02 (Figure 3.9 A).

Upon reduction with dithionite, an intense rhombic signal appeared with *g* values at 2.048, 1.934, and 1.920 (g_{av} = 1.97; Figure 3.9 B). The line shape and *g* values indicate that this EPR signal results from a low potential ferredoxin type [4Fe-4S] cluster (Cammack *et al*., 1985).
When the enzyme was oxidized with $[Fe^{III}(CN)_6]^{3-}$, a new EPR signal was observed with resonances at *g* = 2.048, 2.015, and 2.005 (g_{av} = 2.022; Figure 3.9 B) that was tentatively assigned to a W(V) center (Meckenstock *et al.*, 1999).

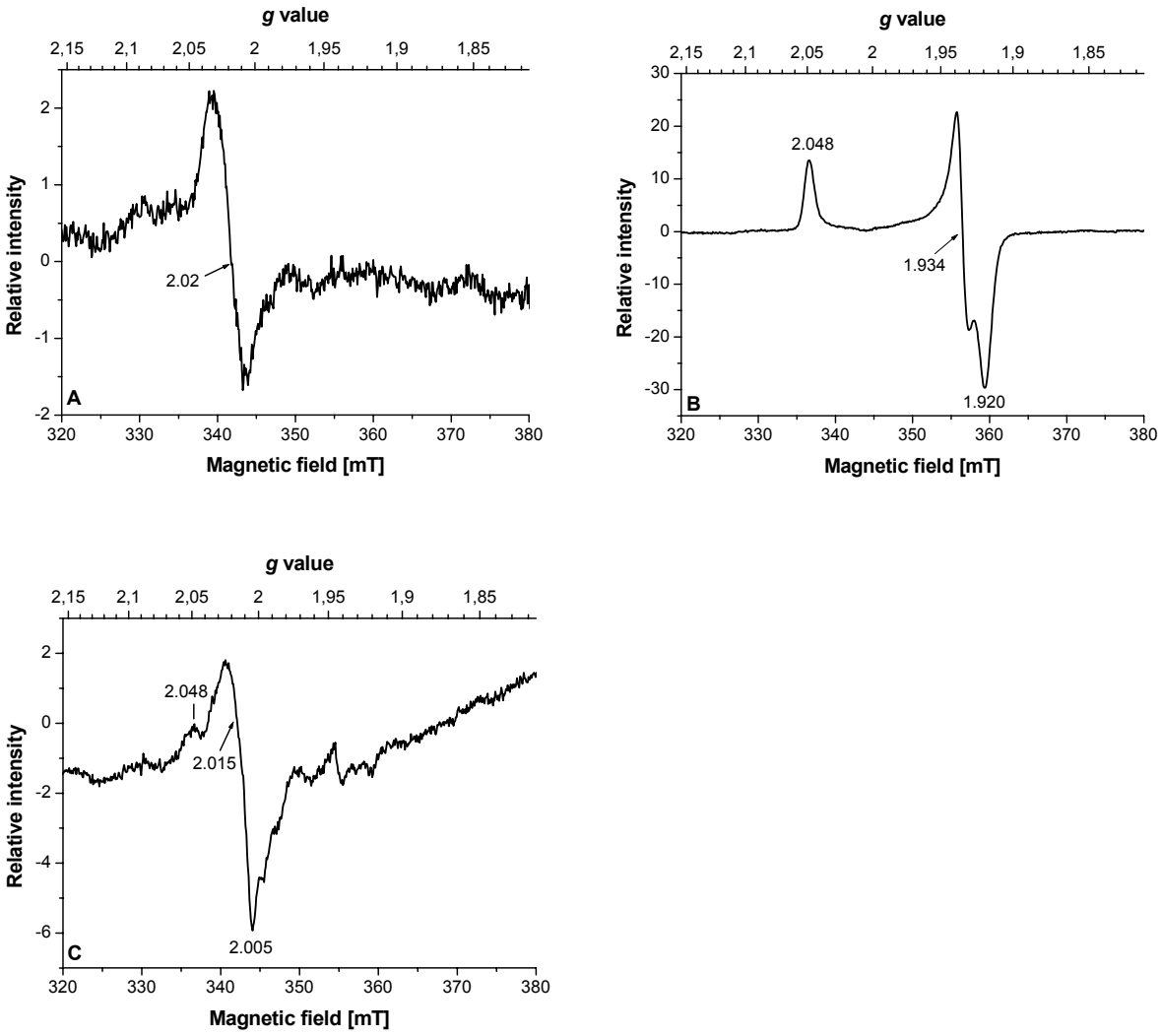

Figure 3.9 Acetylene hydratase X-band EPR spectra from *P. acetylenicus*, cultivated on tungstate.
Protein: 4 mg ml^{-1} in 50 mM Tris/HCl 200 mM NaCl pH 7.5; microwave frequency 9.665 GHz; microwave power: 2 mW; modulation amplitude: 1 mT; temperature: 16 K; scans: 16.
A: AH, "as isolated"; B: AH, reduced with 49 µM sodium dithionite; C: AH, oxidized with 2.8 mM $[Fe^{III}(CN)_6]^{3-}$.

(b) Acetylene hydratase - molybdate (^{95}Mo) cultivation

"As isolated", acetylene hydratase from molybdate (^{95}Mo) cultivation showed a weak axial signal of a most likely truncated [3Fe-4S] cluster with a g_{av} = 2.01 (Figure 3.10 A). In addition, the rhombic signal of a ferredoxin type [4Fe-4S] cluster with *g* values at 2.048, 1.934, and 1.920 (g_{av} = 1.97) could be seen. Upon reduction, the intensity of the rhombic signal was increased by a factor of ≈ 10 (Figure 3.10 B). When the enzyme was oxidized with $[Fe^{III}(CN)_6]^{3-}$ a new signal appeared that was tentatively assigned to ^{95}Mo(V) with I = 5/2 (Figure 3.10. C).

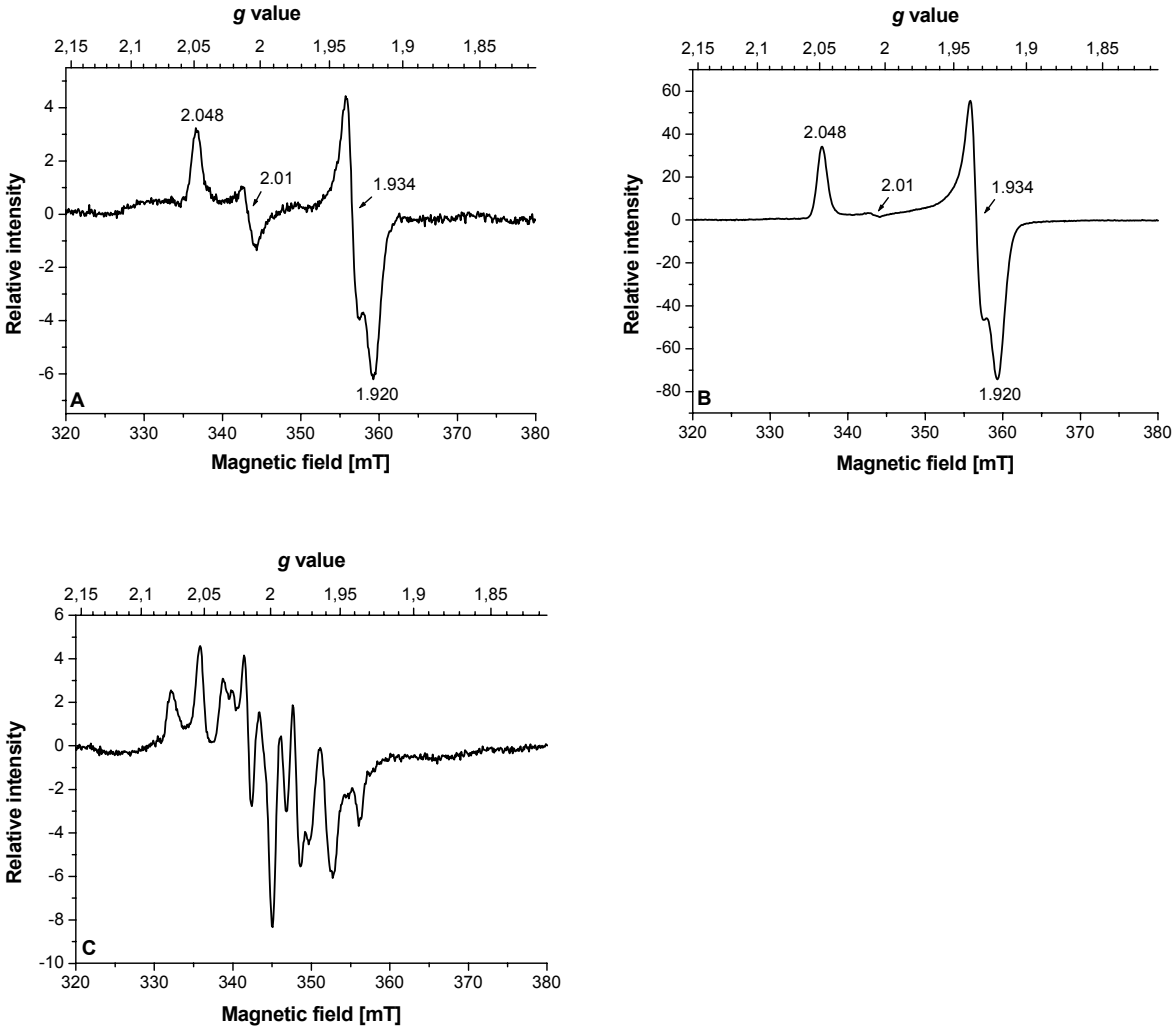

Figure 3.10 Acetylene hydratase X-band EPR spectra from *P. acetylenicus*, cultivated on molybdate (^{95}Mo).
Protein: 4 mg ml^{-1} in 50 mM Tris/HCl 200 mM NaCl pH 7.5; microwave frequency 9.665 GHz; microwave power: 2 mW; modulation amplitude: 1 mT; temperature: 16 K; scans: 16.
A: AH, "as isolated"; B: AH, reduced with 49 µM sodium dithionite; C: AH, oxidized with 2.8 mM $[Fe^{III}(CN)_6]^{3-}$.

(c) Acetylene hydratase - vanadate cultivation

"As isolated" acetylene hydratase from vanadate cultivation showed a weak signal of a most likely truncated [3Fe-4S] cluster with a $g_{av} = 2.01$ (Figure 3.11 A). Further, the weak rhombic signal of a ferredoxin type [4Fe-4S] cluster with g values at 2.048, 1.935, and 1.920 ($g_{av} = 1.97$) could be seen. After reduction with dithionite, the observed rhombic signal was stronger than in the "as isolated" state (Figure 3.11 B). When the enzyme was oxidized with $[Fe^{III}(CN)_6]^{3-}$ an EPR signal with resonances at $g = 2.058$, 2.018, and 2.005 ($g_{av} = 2.027$, Figure 3.11 C) appeared.

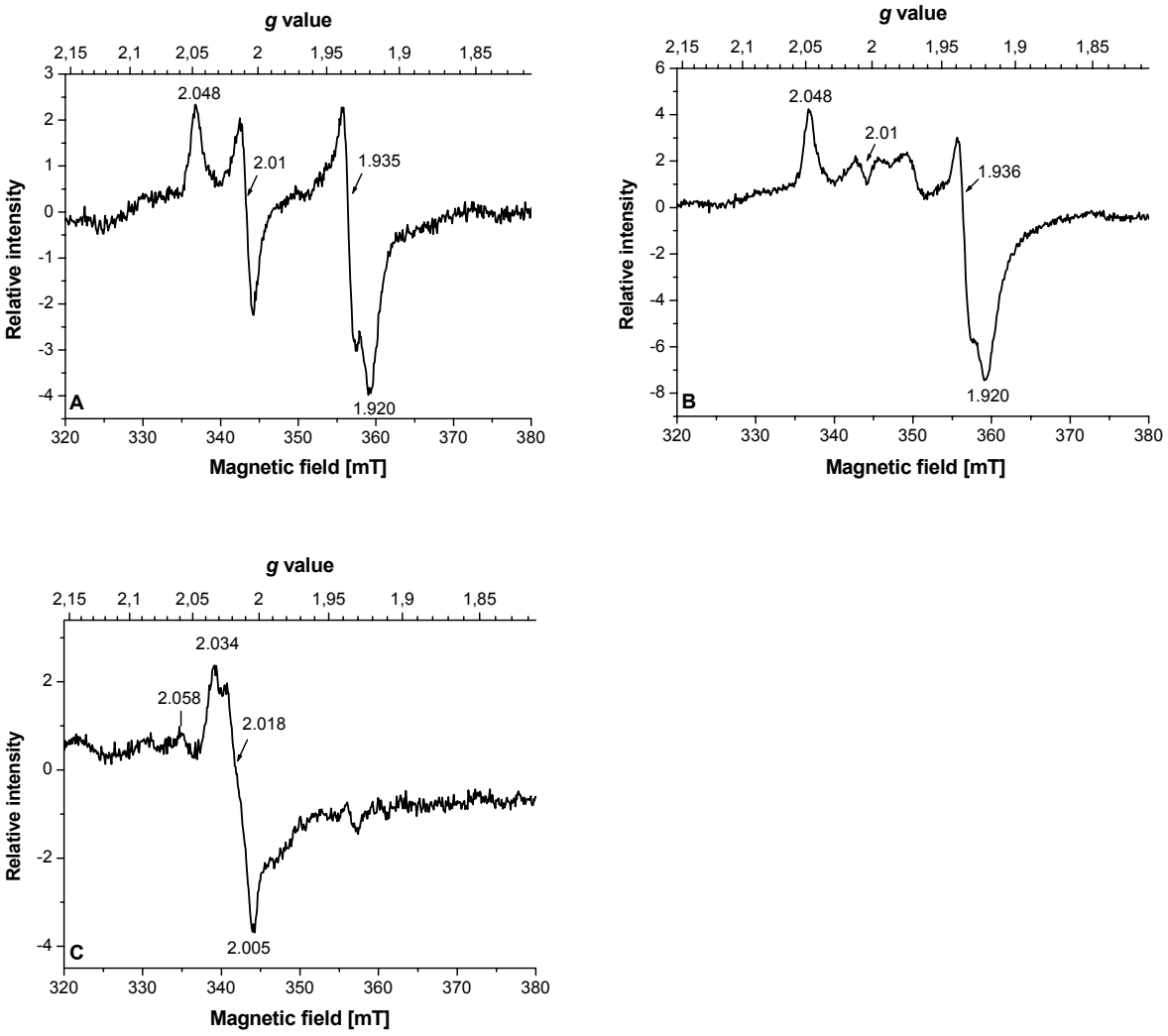

Figure 3.11 Acetylene hydratase X-band EPR spectra from *P. acetylenicus*, cultivated on vanadate.
Protein: 4 mg ml^{-1} in 50 mM Tris/HCl 200 mM NaCl pH 7.5; microwave frequency 9.665 GHz; microwave power: 2 mW; modulation amplitude: 1 mT; temperature: 16 K; scans: 16.
A: AH, "as isolated"; B: AH, reduced with 49 µM sodium dithionite; C: AH, oxidized with 2.8 mM $[Fe^{III}(CN)_6]^{3-}$.

3.1.8. Identification, amplification, and sequencing of the acetylene hydratase gene structure via PCR based techniques

The most difficult problem to overcome in the course of the DNA sequence determination was to get the first positive amplification product. After this the determination of the complete sequence was relatively simple since techniques like “Anchor ligated Genome Walking” or “Inverse PCR” were developed in the last few years and are routinely used in laboratories. The Internet provides many tools for analysis and comparison of the obtained sequences.

(a) Primer design

Primers for PCR were designed using the program OLIGO 4.04 (National Biosciences Inc., Plymouth, MA, USA). The first set of PCR primers (Table 3.5) was derived from the N-terminal amino acid sequence (+ strand, forward primer, 1 – 3) and the N-terminal sequence of the cyanogen bromide digestion (– strand, reverse primer, 4 – 6).

		1	2	3	4	5	6	7	8	9	10	11	12	13	14	15	16	17	18	19	
		Ala	Ser	Lys	Lys	His	Val	Val	Cys	Gln	Cys	Cys	Asp	Ile	Asn	Cys	Val	Val	Glu	Ala	3′
+ strand	5′	GCN	wsn	AAR	AAR	CAY	GTN	GTN	TGY	CAR	TGY	TGY	GAY	ATH	AAY	TGY	GTN	GTN	GAR	GCN	3′
Primer 1	5′			AAR	AAR	CAY	GTN	GTI	TGY	CA											3′
Primer 2	5′								TGY	CAR	TGY	TGY	GAY	ATH	AA						3′
Primer 3	5′												GAY	ATH	AAY	TGY	GTN	GTI	GA		3′

		10	9	8	7	6	5	4	3	2	
		Thr	Arg	Ile	Gln	Asp	Ala	Asn	Val	Ser	
- strand	5′	NGT	nck	DAT	YTG	RTC	NGC	RTT	NAC	nsw	3′
Primer 4	5′		CK	IAT	YTG	RTC	IGC	RTT	NAC		3′
Primer 5	5′	GT	NCG	IAT	YTG	RTC	NGC	RTT			3′
Primer 6	5′	GT	YCT	IAT	YTG	RTC	NGC	RTT			3′

Table 3.5 Primers used for AH gene identification.
Forward primer 1 – 3, derived from the N-terminal amino acid sequence (Rosner, 1994). Reverse primer 4 – 6, derived from the N-terminal sequence of the cyanogen bromide digestion. Abbreviations are illustrated in the appendix.

(b) Amplification of the first fragment using degenerated primer

With the degenerate primer 1 – 3 (forward) and 4 – 6 (reverse), a total of 9 different reactions was carried out. These reactions led to PCR-products from 50 – 2000 bp length. Direct sequencing of the longer fragments did not lead to interpretable sequences.
Cloning of a small PCR-product obtained from a PCR-reaction with forward primer 1 and reverse primer 4, amplification with the M13/pUC Forward and M13/pUC Reverse primer, and sequencing of the amplification product, led to a DNA fragment of 137 bp in length. This fragment included the codons of 10 of the 19 amino acids of the known N-terminus of AH and the codons of 7 amino acids of the internal fragment of the cyanogen bromide digestion.

(c) Extension of the first fragment

After the first fragment had been identified successfully, the “Anchor ligated Genome Walking” was started. The sequence was checked at least 2 times on the forward and on the reverse strand in order to minimize sequencing errors. The sequenced 6030 bp of the acetylene hydratase region are shown in figure 3.12.

```
     1          11         21         31         41         51
     |          |          |          |          |          |
     ATCAGGGCCT TCTTTGACAC CATTGACCAT GAACTGATGA TGCGTGCGGT AGAAAAGCAC    60
  61 GTACCGGAGA AATGGATCCA ACTCTACATC CAACGCTGGT TGGAGAGTGA AGTTGAGCTG   120
 121 GCAGATGGAA CGATAGGAAC ACGGAACTGC GGAACTCCGC AGGGTGGTGT CATCAGCCCA   180
 181 CTGCTGGCGA ATCTCTACCT GCACTATGCC TTTGATCACT GGATGCAGCG GAATCATCCG   240
 241 GCCATACCGT TTGAGCGGTA CGCGGATGAT GTGCTCTGCC ACTGTCGAAG TCAGAAGGAG   300
 301 GCTGAGGCGC TCTTAGAAGC GCTACGAGAA AGACTGTCCG ATTGCAGGCT GGAGCTACAC   360
 361 CCGGCAAAGA CGAAACTGGT CTACTGCAAG GATGGGAAGC GAAGGGCAAA GTATGCCCAT   420
 421 ACCCGCTTTG ATTTCCTCGG ATTCAGCTTT CATGGACGAA CCGTACAGGA CAGGCGCGGG   480
 481 AACCTTTTTA CGGGTTTCAA TCCAGCAGTG AGCCGAAAGG CACTGAAACG GATGAACCAA   540
 541 GCAGTCCGAG ACCTCAAAAT CCACCGTAGA ACGAGCTTAA CTCTTCAAGA GTTGGCTGCC   600
 601 CTCCTCAATC CAATGGTACG AGGATGGGTG GGATACTATG GAACCTTCTA CCCAGAACCG   660
 661 CTGCGACGGT TTCTGGTTAG ACTGGATCTG AGACTAGGAC GCTGGGCAAG GAAGAAGTAC   720
 721 AAGACCTTGC GAAGGAGAAA GCAGCGCTCA TGGGCATGGC TCAAGCGCTG CAGAAAGTCT   780
 781 TCCCCGCGGT TGTTTGTACA TTGGGAATAT TTGTTCTCA**T** **AA**GGCGATGG ATAAGAAGAG   840
 841 CCGGATGAAG CGAGAGTTTC ACGTCCGGTT CTGTGAGGGC CTGAGGGGGA GGTTCCTTCG   900
 901 GGCTACTCGA CCTCCTGTTG ATTACGCAGT CTTATTGCAA AGGTCGCCTT CGGGTGGCCT   960
 961 TTTTGGTTAA GGGGGTAACC GTACAGTTCC GATTGTTCCC CAGTTGCGAG TTTGACAGGG  1020
1021 CCAGCTACCA GAGTTCCTTT GCGGGGCTAA CTTGTAAAGT TCTTGGCGTT TGTTCAGCCT  1080
1081 ACCTTTTCCC TAACCAGCGG TCGGGGTGCT GGTGGTCGGC TTGAACAGGA AGTGGGAGGC  1140
1141 CGGGGTCAGA GAACACCGTT TGAAGATACG CTCTTTAACT ATTAGCACCT TGCTCACCAC  1200
1201 CGTTTTTAGT TTGTCCTAGG CCCTCTTGCA GCAAGCCCTT CTGTAGAACG AGAAAGCCTG  1260
1261 AACGTGGGCA TCTAGAACCA TCCCCAATCT CTCACACAAA TAAGCTAGGC AAAAAACTTG  1320
1321 CGACTATGAC AACAGCGGAA CTGGCGACCT TGATCTGGAC CTTTCCACCT CTCAGCTCGA  1380
1381 CCGGTTCATA GCTCCAGTCG AATTGAAACC CCTCTTCCGG CGCAAAATCC AAGGGAACGA  1440
1441 ACGCCATGCT CGCCCCATTG ATCTGCTGTC GCCATTTTTT GTCCCATAAG GTCTCACGTC  1500
1501 AAACAGTGTT GCAGATAAAG GTTGACACGG AAAAGTAACA CCTGATAGTT TGTTAGTTAT  1560
1561 CCAACCAAAG TTGGTTATCC AACCAAACGG TTGGCCAGCT AAGCCTAGAG GTTGTGTCCC  1620
1621 GATAAATAAC AAGAAAGCGC GCCTGCTGAA AGCGGGCAAT TTTGTGGGTT TGGCTGGTTC  1680
1681 GCGGCGGATG CGGAAGGAAG GAGGTGGCGG CGAGAAGATA AAGGGATGGC AGAACTGGTT  1740
1741 GTCGCTGACA GGCTGCCGGA GGGTTTCTGG AGTGCTTAGA AGGATATGAA ACTTTCTTGT  1800
1801 TTGTCTGGTT GGTAATTGAT GGAAGGTCAA TTCAAGAAAT GGAGTGGGTT ATCAA**ATG**GC  1860
1861 TGTGAAAACT TTGAAAAGCT TTCTGTTTGT AGTAGTGGCG CTGTGCGGTC TAAGTCTTGT  1920
1921 CGGTAATGTG GACACTGCTC GTGCTGGACT GATTCCCTAT AGTTTCATTC AACCTCACGA  1980
1981 TTTTCAGCTT CCGATAGGGA AGGAAGTTCC GGCTGGTGGC CTCGATTTGT ATGTTTCCTA  2040
2041 TAACACCTAT AGGGAAGAGG GAAAAGCTTG GGATGGTGAC AGTGGTACTC GGAGCGTGTT  2100
2101 TCTAAACCTT AACCGCTACA TACACGTATG GACGGTCGAA GGATTGGATA ACTGGAGCTT  2160
2161 TCTTACCGAG GGTGTAGTTG GTCTCGGAAG GGTGCTGACT AAAGACGATA ATAGCGAAAC  2220
2221 TGGGCTGCTG GATACAATGG TCGGTGGTGC CGCTGCGTAT AGAACGGGTA ACTGGACAAG  2280
2281 CGTCCTTGAA TACTTTCTGT TCATGCCTAC CGGTAGCGAT GAGCTGTCTT CGAATTCCTG  2340
2341 GAACCACAGC CTTACCTATC TGACAAACTA CCACGTAGGT GCTTTCACTT TTGACGGTTC  2400
2401 CGTAGGTTAC CAGCTTAAGG GGGACAGCAA GGTAGGCGGT ACTCACATTG AGCAAGGAGA  2460
2461 CACCTTTTAC GTTAATACTG TTTTTGCTTA CAAGTTTCAG GACCTCATAG AGCCTTACAT  2520
2521 TAAGGTTGAT TACCAGACAA CCGAGTCTGG AAAGAATAAG AATACCGGCG ATTCTATTTC  2580
2581 CAGCCAGGAT GAGCTTGCTG TGGGGATTGG TAACCACTTC ACGTTAAGCG ACAGACTGAC  2640
2641 TCTTGCGCTG TCGTATGAAA AAGGCGTTTC GGGAAGAAAT ACGACTAAAA CAAATGCCGG  2700
2701 TTGGGCTCGC TTTATCTGGG TTTTC**TAA**CG TTTGTTTAGG CAGCGTAACG TTGAGTCCGG  2760
2761 GCGGGAGTCT GCTGTCGTTA GACTGTCGTT CTTGGGCTCT TGGGAAGAGA AGTCAATTAT  2820
2821 TTTTTTAACT CAACAAAAAG GTACTTGGGT CGGAGGGTAG TCCTGTTGAC CCGCTAAGCA  2880
2881 CTAGGAGGTA CAAA**ATG**GCT AGCAAGAAGC ACGTTGTCTG TCAGTCCTGC GACATTAATT  2940
2941 GTGTTGTAGA GGCTGAAGTG AAGGCTGACG GTAAGATCCA AACAAAGAGT ATCTCAGAGC  3000
3001 CTCACCCGAC AACTCCCCCC AATAGTATTT GTATGAAGTC GGTGAATGCG GACACGATCA  3060
3061 GGACTCATAA GGATCGTGTG CTCTATCCTC TGAAAAACGT GGGTAGTAAG AGGGGAGAGC  3120
3121 AAAGGTGGGA GCGAATCAGT TGGGACCAGG CATTGGATGA AATTGCCGAA AAGTTGAAAA  3180
3181 AGATTATAGC GAAATACGGT CCGGAGTCCC TTGGTGTAAG CCAGACTGAG ATTAATCAGC  3240
3241 AAAGCGAATA TGGAACGCTC CGGAGATTCA TGAATCTCTT GGGTAGCCCG AACTGGACTT  3300
3301 CCGCCATGTA TATGTGTATC GGGAATACAG CCGGAGTTCA TAGAGTAACT CATGGAAGTT  3360
3361 ACTCTTTTGC GAGTTTTGCC GACTCTAATT GCCTTTTGTT CATTGGTAAA AATCTCAGTA  3420
3421 ATCATAATTG GGTCTCCCAG TTCAATGACC TTAAGGCTGC TTTAAAAAGA GGCTGCAAGC  3480
3481 TTATTGTGCT TGATCCGCGC AGAACCAAGG TCGCAGAGAT GGCGGATATT TGGCTTCCTC  3540
3541 TTCGGTATGG AACAGATGCA GCTCTATTTC TCGGGATGAT TAACGTTATC ATCAATGAAC  3600
3601 AGTTGTACGA CAAAGAGTTT GTTGAAAACT GGTGTGTTGG GTTTGAAGAG CTTAAAGAAC  3660
```

```
3661 GGGTTCAGGA ATATCCTTTA GACAAAGTTG CGGAAATAAC CGGATGCGAT GCTGGAGAAA  3720
3721 TCAGGAAAGC GGCTGTTATG TTCGCAACTG AGAGTCCCGC ATCCATACCT TGGGCTGTTT  3780
3781 CAACTGATAT GCAGAAAAAT AGTTGTTCGG CGATCCGCGC CCAATGTATT TTAAGGGCAA  3840
3841 TTGTCGGCAG CTTTGTGAAT GGAGCGGAGA TTTTGGGGGC CCCTCATTCG GATCTGGTGC  3900
3901 CCATTTCCAA AATTCAGATG CACGAAGCAC TGCCTGAAGA AAAGAAAAAA CTTCAGCTCG  3960
3961 GTACAGAGAC GTACCCGTTC CTTACATACA CGGGGATGAG CGCGTTGGAA GAGCCGTCAG  4020
4021 AAAGAGTGTA TGGGGTGAAA TATTTCCATA ATATGGGCGC GTTTATGGCC AACCCGACTG  4080
4081 CTCTTTTTAC GGCTATGGCT ACCGAAAAAC CGTATCCTGT AAAGGCCTTT TTTGCGCTCG  4140
4141 CCAGCAATGC GCTGATGGGC TATGCAAATC AGCAAAACGC ACTTAAGGGC CTCATGAATC  4200
4201 AGGATTTGGT TGTTTGTTAT GATCAGTTCA TGACGCCTAC AGCGCAGCTT GCCGATTATG  4260
4261 TTCTCCCTGG TGACCACTGG CTGGAGAGGC CTGTTGTCCA GCCGAATTGG GAGGGCATTC  4320
4321 CTTTCGGCAA TACTTCCCAG CAAGTTGTCG AACCGGCTGG CGAAGCCAAG GATGAGTATT  4380
4381 ACTTCATCCG AGAGCTGGCC GTCAGGATGG GCCTTGAAGA GCATTTCCCA TGGAAGGACC  4440
4441 GGCTTGAATT GATCAACTAT AGGATAAGCC CGACTGGTAT GGAGTGGGAA GAGTACCAGA  4500
4501 AACAATACAC CTATATGTCT AAGCTGCCTG ATTACTTTGG ACCGGAGGGG GTAGGCGTAG  4560
4561 CGACTCCATC AGGAAAAGTT GAGCTGTATT CAAGTGTATT TGAAAAGCTT GGTTATGATC  4620
4621 CATTGCCGTA CTACCATGAG CCGCTGCAGA CTGAAATAAG TGATCCGGAA CTTGCGAAGG  4680
4681 AATATCCTTT AATCCTTTTT GCTGGTCTGC GTGAAGATTC AAACTTTCAA TCGTGTTATC  4740
4741 ACCAGCCTGG GATACTTAGA GACGCAGAGC CCGATCCTGT TGCCTTGCTT CATCCAAAAA  4800
4801 CTGCGCAGTC CCTTGGACTT CCCTCCGGCG AATGGATCTG GGTTGAGACA ACTCATGGGA  4860
4861 GGTTGAAGTT GCTCCTCAAG CATGATGGTG CGCAGCCGGA AGGTACGATA AGAATACCCC  4920
4921 ATGGACGGTG GTGCCCTGAA CAGGAAGGGG GGCCTGAGAC TGGATTTAGT GGAGCCATGC  4980
4981 TGCATAATGA TGCCATGGTA TTAAGTGATG ATGACTGGAA TCTCGATCCG GAGCAGGGTT  5040
5041 TGCCAAATCT TAGAGGCGGT ATTCTTGCGA AGGCATATAA ATGCTGAAAA AGGCTTGTGG  5100
5101 ATAGGTAGGT GGGGTATTGC AGCAGGCTGC CAGTCGATCG ATTTTACGTG CCGAGCGTTT  5160
5161 GATGAGTGAG GCGGATTGTG CAGATTTTCT GCCGGAGGTA GACCGCCGGC TTGCAGGATT  5220
5221 GGTTCTCATT CTTTGAGTTA CAGGATGTTC TGGTAAATCG GATTTCTTGG AAACCACCCC  5280
5281 ACTTCGGTGG CCATGCCTTC TCCTTCAGAA AGGATACTTT GTGTTTGGGG GAGGCATGGT  5340
5341 CACTACCCTT ACTTTGTTGA GGCAGATGAG TGATCACCCT ATTGGCAAAA TTAGTGCTTA  5400
5401 CGTGTCAGGT CCCGCATGAT TCCTGACCTG TTTATGGAAA AGTTCCATTT TCTTTTTTTG  5460
5461 CCAATCTTTT CGACAGTAAA CAACGCATAG ATTTCTAACG TCCCGTAGGG TTTCATGTTT  5520
5521 GGGAGGATGC TGCGATAAAA GGGAATTCGT CATTAATAAC CGGCATTATC CTCGTTGGCG  5580
5581 GATAGAACCG TCGTATGGGA ACCGATAGGG CATTCCTAAA AATCGAAGGC ATTTCCCTTT  5640
5641 TTAAACGGGT CCTCCAAGTT ATGGAGTGAC CTGCCCCACC TGATAGGTCT ACTTCGAATG  5700
5701 TTAGTGTAGC GCAACCCTGT CGGTTTCCAA TGCCGCTGCT TGAATAGGCA GCGGCATTAT  5760
5761 TGTTTCGGGT ACTGGTGGAC GGTAGCCGAG CGAACTGTGT GGACGGATTG TGTTGTAATG  5820
5821 TCATCGCCAC TGTTCAATCA GAATCTTGTC CTCCTTGAGG GTATAGAAAA TCTCCCCATT  5880
5881 GAGCAACTCA TCCCTCAGTT TACCGTTGAA GGATTCATTG TAACCGTTCT CCCAAGGGCT  5940
5941 GCCTGGCTCA ATGAATAACG TCTTGGCCCC GAGACGCTCC AACCAGCCCC TGACCAGCTT  6000
6001 TGCCGTAAAT TCTGCGCCAT TACCAGGCCC                                   6030
```

Figure 3.12 Nucleotide sequence of the 6030 sequenced bases of the acetylene hydratase region of *P. acetylenicus* DNA (forward strand).
The start codon ATG is shown in bold face, the sequence of the open reading frames is highlighted in grey, and the stop codon TAA/TGA in bold face. A putative –35/–10 promotor-region and a Shine Dalgarno Sequence upstream of the third orf (acetylene hydratase) is enframed.

(d) Open reading frames

On the forward strand three open reading frames (orf) were detected (Figure 3.12, Figure 3.13 Frame 1 – 3). The first orf is in frame 1 and is incomplete. It starts at nucleotide 1 and ends at position 819.

The second orf is in frame 2, starting at position 1856 and ending at 2725.

The third orf, the acetylene hydratase sequence, is on frame 3, starting at position 2895 and ending at 5084.

On the opposite strand no significant orf was detected in any of the three possible frames (Figure 3.13 Frame 4 – 6).

An *E. coli* like –35 promotor-region with the sequence 5'-TTGGGA-3' (consensus sequence 5'-TTGACA-3') is located 84 bases upstream of the initiating ATG of the acetylene hydratase gene. The respective TATA-box (consensus sequence 5'-TATAAT-3' = Pribnow box = –10 region) with the sequence 5'-TATTTT-3' is located 12 bases downstream of the –35 region. Therefore, the putative starting point of the transcription is 6 or 7 bases downstream. In the 5'-noncoding region a 5'-AGGAGG-3' Shine Dalgarno Sequence (consensus sequence 5'-AGGAGG-3') is located 6 bases upstream of the initiator ATG indicating that the translation of the corresponding mRNA starts at the marked ATG.

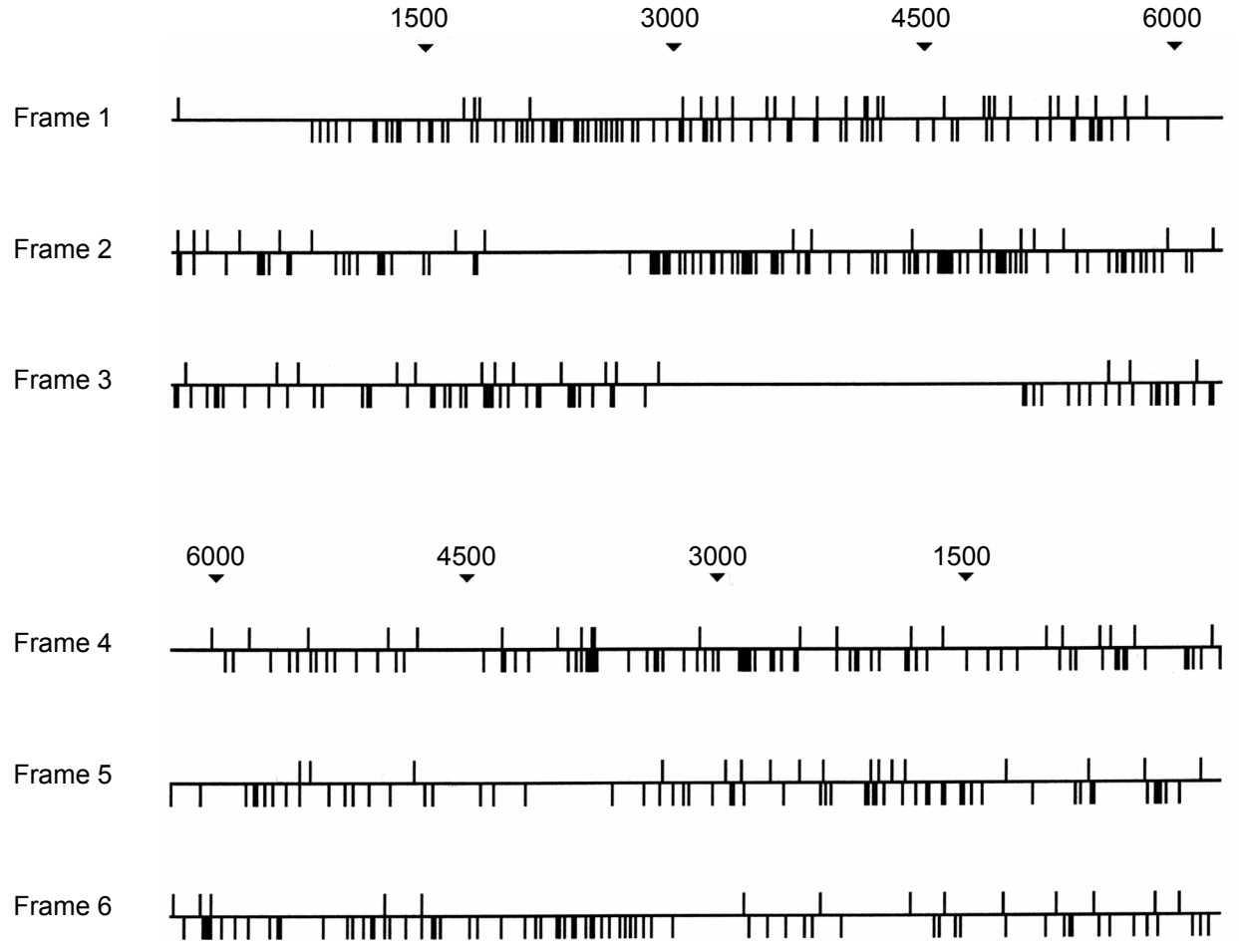

Figure 3.13 Overview of the open reading frames of the acetylene hydratase region.
An upturning line indicates a start codon, a downward line a stop codon. Frames 1 – 3 are the forward strand, frames 4 – 6 the reverse strand.

(e) Gene product (Orf1) of the first open reading frame (orf*1*)

The derived amino acid sequence of orf*1* is depicted in figure 3.14. The putative protein is 273 amino acids long and has a molecular mass of 32.6 kDa. BLASTP searches show that this protein is highly homologous to reverse transkriptase/maturase like proteins from *Escherichia coli* (CAA54637), *Bradyrhizobium japonicum* (AAG61023), *Sinorhizobium meliloti* (CAA72334), *or Shigella flexneri* (NP_085197). These proteins are about 420 amino acids long, so the Orf1 lacks about the first 150 amino acids. The sequenced DNA fragment was not long enough to give the complete amino acid sequence of Orf1.

```
     1          11         21         31         41         51
     |          |          |          |          |          |
   1 IRAFFDTIDH ELMMRAVEKH VPEKWIQLYI QRWLESEVEL ADGTIGTRNC GTPQGGVISP    60
  61 LLANLYLHYA FDHWMQRNHP AIPFERYADD VLCHCRSQKE AEALLEALRE RLSDCRLELH   120
 121 PAKTKLVYCK DGKRRAKYAH TRFDFLGFSF HGRTVQDRRG NLFTGFNPAV SRKALKRMNQ   180
 181 AVRDLKIHRR TSLTLQELAA LLNPMVRGWV GYYGTFYPEP LRRFLVRLDL RLGRWARKKY   240
 241 KTLRRRKQRS WAWLKRCRKS SPRLFVHWEY LFS
```

Figure 3.14 Deduced amino acid sequence of the first open reading frame.

(f) Gene product (Orf2) of the second open reading frame (orf*2*)

In figure 3.15 the amino acid sequence of Orf2 is shown. The putative protein is 290 amino acids long, it has a molecular mass of 32.0 kDa, and a theoretical pI of 5.1 (ProtParam tool, Chapter 2.10.7). With standard BLASTP searches no homologous proteins are detected.

```
     1          11         21         31         41         51
     |          |          |          |          |          |
   1 MAVKTLKSFL FVVVALCGLS LVGNVDTARA GLIPYSFIQP HDFQLPIGKE VPAGGLDLYV    60
  61 SYNTYREEGK AWDGDSGTRS VFLNLNRYIH VWTVEGLDNW SFLTEGVVGL GRVLTKDDNS   120
 121 ETGLLDTMVG GAAAYRTGNW TSVLEYFLFM PTGSDELSSN SWNHSLTYLT NYHVGAFTFD   180
 181 GSVGYQLKGD SKVGGTHIEQ GDTFYVNTVF AYKFQDLIEP YIKVDYQTTE SGKNKNTGDS   240
 241 ISSQDELAVG IGNHFTLSDR LTLALSYEKG VSGRNTTKTN AGWARFIWVF
```

Figure 3.15 Deduced amino acid sequence of the second open reading frame.

(g) Gene product (acetylene hydratase) of the third open reading frame (orf*3*)

The third detected open reading frame codes for the acetylene hydratase amino acid sequence. A –35/–10 promotor-region as well as a Shine Dalgarno Sequence are located upstream of the acetylene hydratase gene (Figure 3.12). The amino acid sequence is shown in figure 3.16. The protein is 730 amino acids long, the molecular mass of the amino acid chain is 81.85 kDa, and the theoretical pI is 5.4 (ProtParam tool, chapter 2.10.7). The experimental pI is 4.2 (Rosner, 1994). The N-terminal amino acid sequence, reported by Rosner (1994), had to be corrected at position 11. The reported cysteine is, according to the nucleotide sequence, a serine.

```
     1          11         21         31         41         51
     |          |          |          |          |          |
   1 MASKKHVVCQ SCDINCVVEA EVKADGKIQT KSISEPHPTT PPNSICMKSV NADTIRTHKD    60
  61 RVLYPLKNVG SKRGEQRWER ISWDQALDEI AEKLKKIIAK YGPESLGVSQ TEINQQSEYG   120
 121 TLRRFMNLLG SPNWTSAMYM CIGNTAGVHR VTHGSYSFAS FADSNCLLFI GKNLSNHNWV   180
 181 SQFNDLKAAL KRGCKLIVLD PRRTKVAEMA DIWLPLRYGT DAALFLGMIN VIINEQLYDK   240
 241 EFVENWCVGF EELKERVQEY PLDKVAEITG CDAGEIRKAA VMFATESPAS IPWAVSTDMQ   300
 301 KNSCSAIRAQ CILRAIVGSF VNGAEILGAP HSDLVPISKI QMHEALPEEK KKLQLGTETY   360
 361 PFLTYTGMSA LEEPSERVYG VKYFHNMGAF MANPTALFTA MATEKPYPVK AFFALASNAL   420
 421 MGYANQQNAL KGLMNQDLVV CYDQFMTPTA QLADYVLPGD HWLERPVVQP NWEGIPFGNT   480
 481 SQQVVEPAGE AKDEYYFIRE LAVRMGLEEH FPWKDRLELI NYRISPTGME WEEYQKQYTY   540
 541 MSKLPDYFGP EGVGVATPSG KVELYSSVFE KLGYDPLPYY HEPLQTEISD PELAKEYPLI   600
 601 LFAGLREDSN FQSCYHQPGI LRDAEPDPVA LLHPKTAQSL GLPSGEWIWV ETTHGRLKLL   660
 661 LKHDGAQPEG TIRIPHGRWC PEQEGGPETG FSGAMLHNDA MVLSDDDWNL DPEQGLPNLR   720
 721 GGILAKAYKC
```

Figure 3.16 Deduced amino acid sequence of acetylene hydratase.
The 15 cysteines are highlighted.

BLASTP searches showed that acetylene hydratase isolated from *P. acetylenicus* has the highest similarity to a putative molybdopterin oxidoreductase of the hyperthermophilic archaeon *Archaeoglobus fulgidus*. The sequence identity is about 35%. In figure 3.17 the five best matches of a BLASTP search are compared. These five proteins are representatives of three of the seven subfamilies of the DMSO-reductase family (Figure 3.25, Chapter 3.3.). This is a first indication of the unique status of acetylene hydratase within this family.

Five of the 15 cysteines of acetylene hydratase are highly conserved and four of them show a sequence motif (C-x-x-C-x-x-x-C-$(x)_n$-C), which could represent a motif for a [4Fe-4S] site. The enframed residues are putative prokaryotic molybdopterin/molybdopterin dinucleotide binding sites obtained from a Conserved Domain Database search at the NCBI.

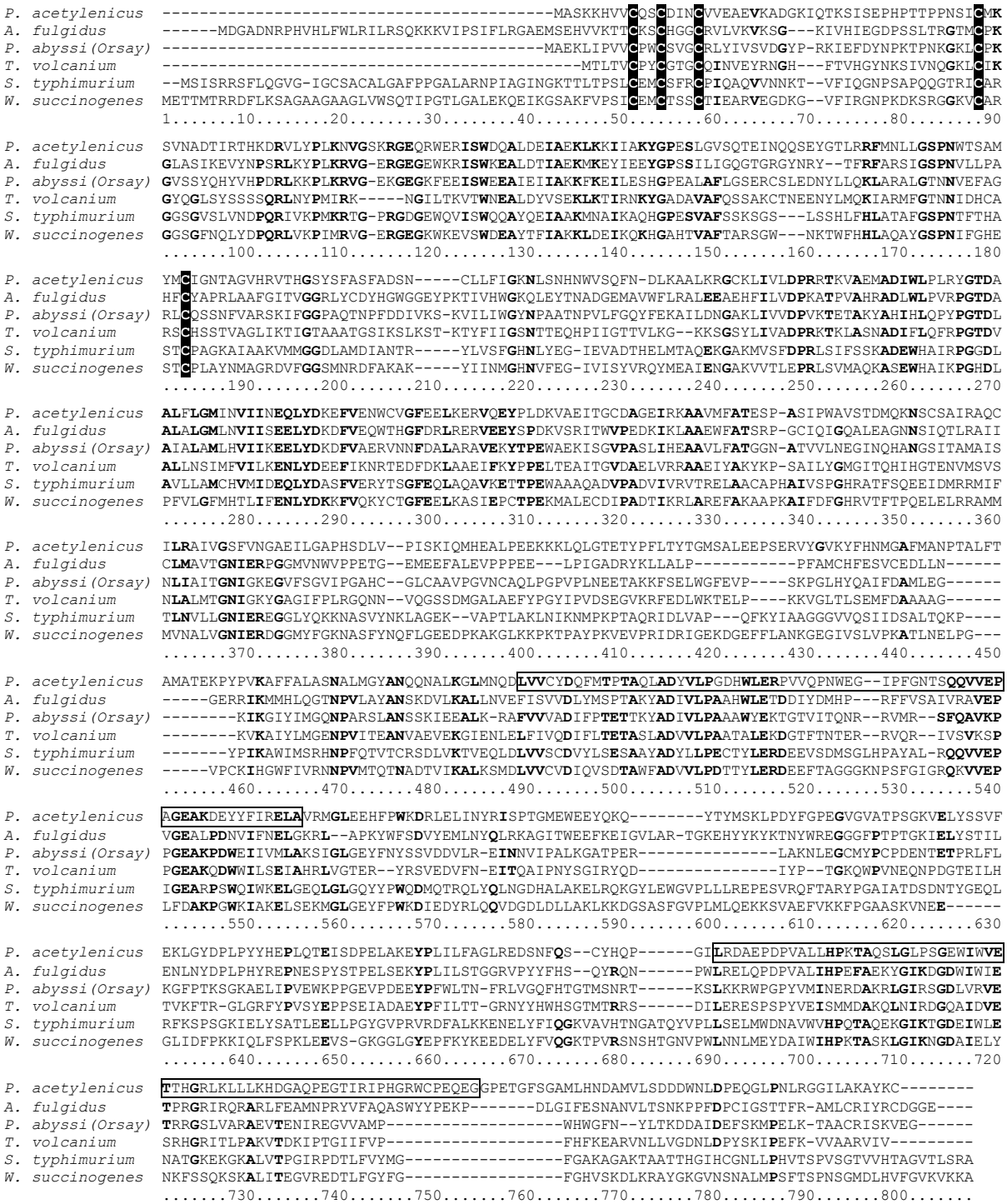

Figure 3.17 Alignment of amino acid sequences from *P. acetylenicus* acetylene hydratase and the five best matches from a BLASTP search.

Conserved regions are highlighted; conserved cysteines are highlighted in black. Putative prokaryotic molybdopterin/molybdopterin dinucleotide binding sites are enframed.

Archaeoglobus fulgidus: hypothetical molybdopterin oxidoreductase (Protein-accession number: NP_070031); *Pyrococcus abyssi* strain Orsay: alpha chain of formate dehydrogenease (B75061); *Thermoplasma volcanium*: Formate dehydrogenase, alpha subunit (NP_110521); *Salmonella typhimurium*: Thiosulfate reductase precursor (P37600); *Wolinella succinogenes*: Polysulfide reductase chain A (P31075).

3.1.9. Crystallization and three-dimensional structure of acetylene hydratase

Crystallization of acetylene hydratase was performed under N_2/H_2 atmosphere; the preparations were stored in a desiccator at 20°C. Crystals grew within one month from 5 mg ml^{-1} protein, reduced with 2.5 equivalents Na-dithionite, from 0.1 M Na-citrate pH 6.1, 0.1 M $(NH_4)_2SO_4$, 30% PEG 8000, and 0.02% NaN_3, or from 0.1 M MES pH 6.5, 0.2 M K/Na-tartrate, 30% PEG 8000, and 0.02% NaN_3. Crystals were also obtained with the second condition, using acetylene hydratase "as isolated" (5 mg ml^{-1}) and no reductant present.

Crystals from the reduced protein diffracted to resolutions better than 2.5 Å and belonged to space group C2, with unit cell dimensions of a = 120.7 Å, b = 70.5 Å, and c = 106.7 Å and angles of $\alpha = 90°$, $\beta = 123.8°$, and $\gamma = 90°$ (H. Nießen, Universität Konstanz, personal communication).

Refinement of the crystallization conditions and solution of the crystal structure are in progress, a preliminary picture has been obtained using the structures of nitrate reductase and formate dehydrogenase H for molecular replacement (Figure 3.18).

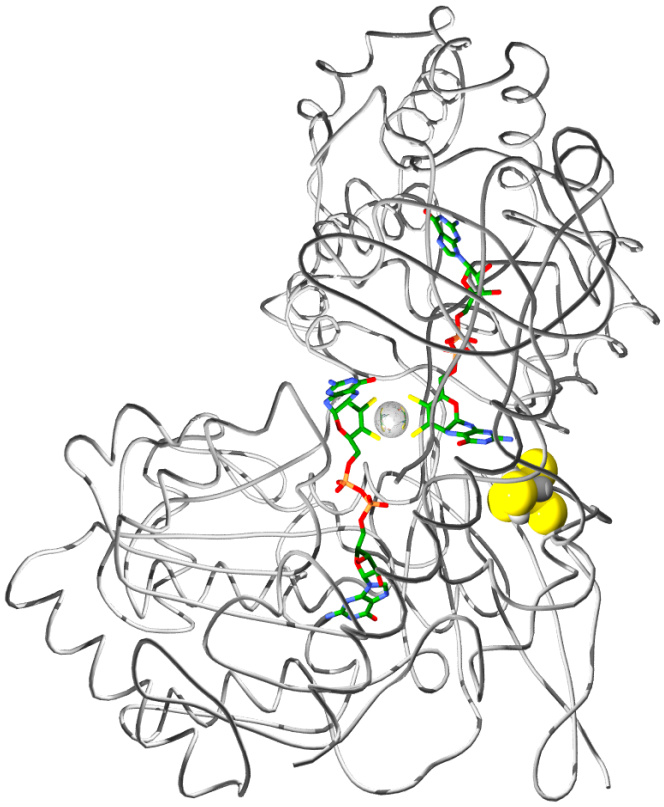

Figure 3.18 Preliminary three-dimensional structure of acetylene hydratase.
The W-bisMGD catalytic site is located in the center of the protein. The [4Fe-4S] center is printed in yellow and gray.

3.1.10. Acetylene hydratase activity in *Archaeoglobus fulgidus*

Because BLASTP searches showed a high similarity between acetylene hydratase and an unknown molybdopterin oxidoreductase from *A. fulgidus*, the archaebacterium was tested for acetylene hydratase activity. *S. solfataricus* alcohol dehydrogenase and sulfate-grown *A. fulgidus* were used in the test system at 80°C.

Neither in the crude extract nor in partially purified fractions acetylene hydratase activity was higher than the background level without protein.

3.2. Transhydroxylase of *Pelobacter acidigallici*

3.2.1. Growth of *Pelobacter acidigallici*

Cultivation of *P. acidigallici* in a 50 l batch culture led to 34 g of wet cell mass. The substrate gallic acid was fed 7 mM initially, and added twice during cultivation. The cells grew within 16 hours to an optical density at 578 nm of 0.8 (Figure 3.19).

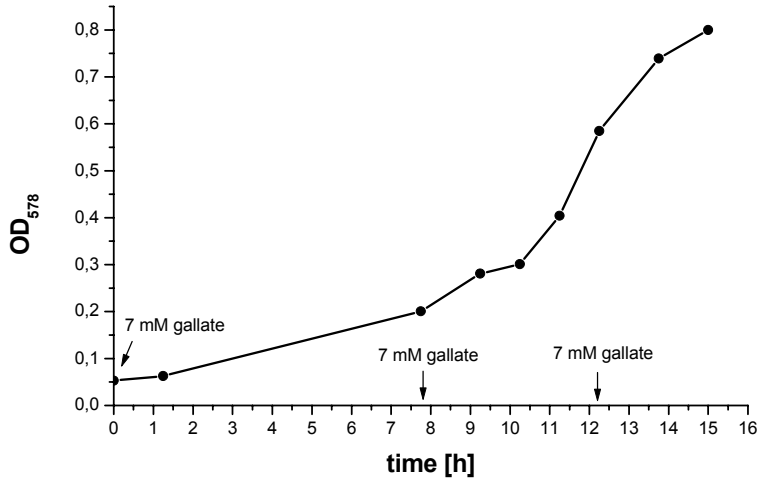

Figure 3.19 Growth of *P. acidigallici* in a 50 l batch culture with gallic acid as energy and carbon source in saltwater medium.

3.2.2. Purification of transhydroxylase

Figure 3.20 A shows a flow chart of the enzyme purification that was originally developed by Reichenbecher (1995) and modified by Sommer (1995). During chromatofocussing the protein is moving to its isoelectric point (pI), which is 4.1 in case of the transhydroxylase (Reichenbecher, 1995). Many iron-sulfur centers are known to be sensitive to acid pH and oxygen. The iron-sulfur centers of transhydroxylase appeared to degrade during the chromatofocussing step (Sommer, 1995). Thus, a modified protocol was developed (Figure 3.20 B) where the chromatofocussing step was omitted. This led to a highly active and electrophoretically pure enzyme.

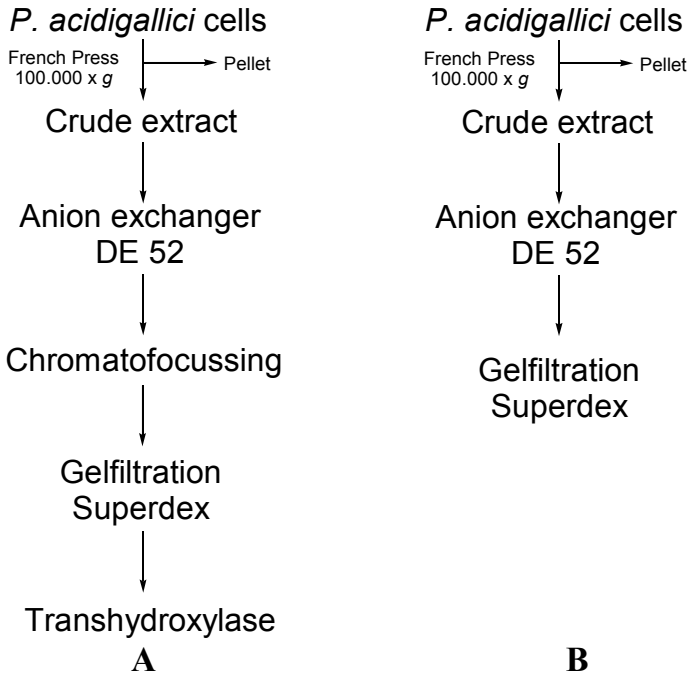

Figure 3.20 Purification scheme of *P. acidigallici* transhydroxylase.
(A) Purification scheme reported by Reichenbecher (1995) and Sommer (1995).
(B) Modified purification scheme.

Anion exchange chromatography:

The crude extract was passed through a 100 ml DE-52 anion exchanger column, equilibrated with 50 mM TEA pH 7.5. At these conditions, transhydroxylase did bind on this weak anion exchanger and was eluted by increasing the NaCl concentration of the buffer. About 62% of the initial activity was recovered (Table 3.6).

Gel filtration:

The fractions of the DE-52 purification step showing transhydroxylase bands on SDS-PAGE were loaded on a Superdex 200 gel filtration column. Transhydroxylase eluted, at a flow rate of 1 ml min^{-1}, as a single peak after 150 min. About 31% of the initial activity was recovered after the final gel filtration step. According to SDS-PAGE (Figure 3.21), transhydroxylase was purified to homogeneity and the specific activity was enriched 5.8 fold (Table 3.6). The two subunits of transhydroxylase are at 86 kDa and 38 kDa, respectively.

	Protein [mg]	Activity [U]	Specific activity [U mg^{-1}]	Yield (Protein) [%]	Yield (activity) [%]	Enrichment factor
Crude extract	3018	2417	0.80 (0.39)	100	100	1
DE-52	784	1501	1.92 (0.76)	26	62	2.4
Superdex	161	743	4.60 (3.10)	5	31	5.8

Table 3.6 Purification of *P. acidigallici* transhydroxylase.
34 g of wet cells were used, 1 U = 1 µmol phloroglucinol min^{-1}. Specific activity in brackets is from Reichenbecher *et al.* (1994).

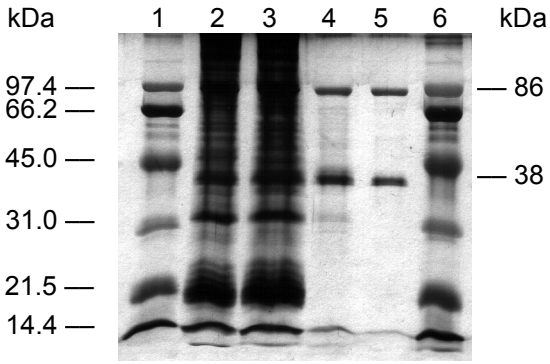

Figure 3.21 SDS-PAGE (12%) of the purification of *P. acidigallici* transhydroxylase.
Lane 1 and 6: Molecular weight markers; Lane 2: Crude extract before ultrafiltration (6.2 µg); Lane 3: Crude extract after ultrafiltration (5.8 µg); Lane 4: Transhydroxylase after anion exchanger DE-52 (2.9 µg); Lane 5: Transhydroxylase after gel filtration (2.1 µg).

3.2.3. UV/Vis spectra of transhydroxylase

Pure transhydroxylase shows a green-yellow color that turns into brown at higher concentrations. The optical spectrum of the reduced form is identical to the spectrum of the oxidized enzyme (Figure 3.22). The absorption peak at 280 nm results from the absorption of aromatic amino acids, the absorption shoulder at 384 nm is typical for iron-sulfur centers. The molar extinction coefficient ε_{384} is 29000 M^{-1} cm^{-1}. Another absorption shoulder between 660 and 670 nm probably results from sulfur-to-molybdenum charge-transfer-transitions of the molybdenum co-factor (Johnson and Rajagopalan. 2001). The molar extinction coefficient ε_{680} is 4700 M^{-1} cm^{-1}. The molar extinction coefficient at 384 nm is significantly higher than that previously reported (Sommer, 1995: ε_{384} = 9330 M^{-1} cm^{-1}, ε_{680} = 5330 M^{-1} cm^{-1}).

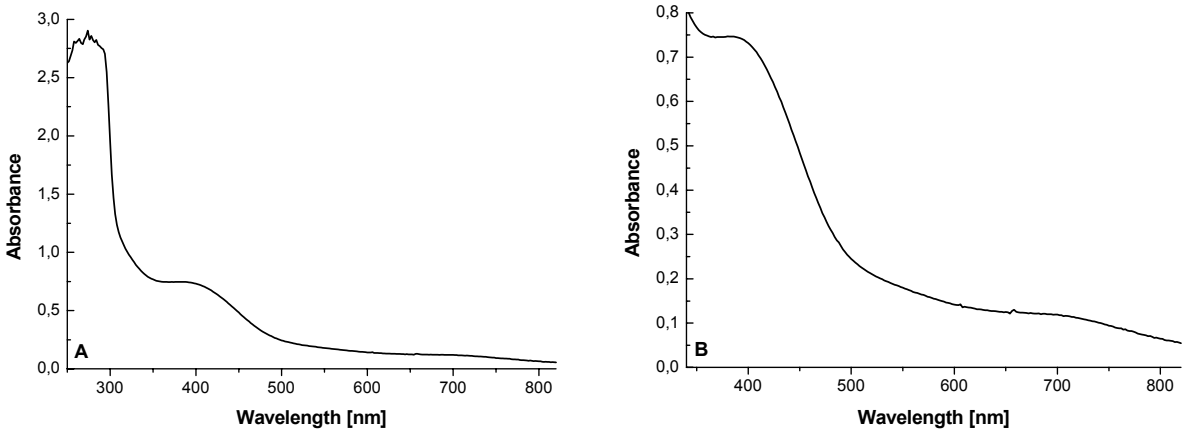

Figure 3.22 UV/Vis spectra of *P. acidigallici* transhydroxylase.
Enzyme: 3.4 mg ml^{-1} in 50 mM TEA 200 mM NaCl pH 7.5.

3.2.4. EPR spectra of transhydroxylase

Figure 3.23 A shows the EPR spectrum of transhydroxylase ("as isolated" in the presence of air, 50 mM TEA 200 mM NaCl pH 7.5). At 10 K the signal of [3Fe-4S] cluster with $g_{av} = 2.01$ and a Mo(V) 'resting' signal at $g_{av} \approx 1.98$ can be seen. Above 16 K, the [3Fe-4S] signal disappears because of relaxation broadening and a pure Mo(V) signal with hyperfine coupling from ^{95,97}Mo remains (Figure 3.23 A, dashed line).

Storage of transhydroxylase for 17 h in an anaerobe chamber led to a partially reduced enzyme (Figure 3.23 B, dashed line). The fully reduced transhydroxylase (5 equivalents of dithionite added) exhibited two intense new signals with $g_z = 2.08$, $g_y = 1.94$, and $g_x = 1.87$ and $g_z = 2.05$, $g_y = 1.96$, and $g_x = 1.87$, which are characteristic for iron-sulfur centers (Kisker *et al.*, 1999).

Oxidation of transhydroxylase, which had been stored for 17 h in an anaerobe chamber, by two equivalents of $[Fe^{III}(CN)_6]^{3-}$ led to an increase of the signal (Figure 3.23 C).

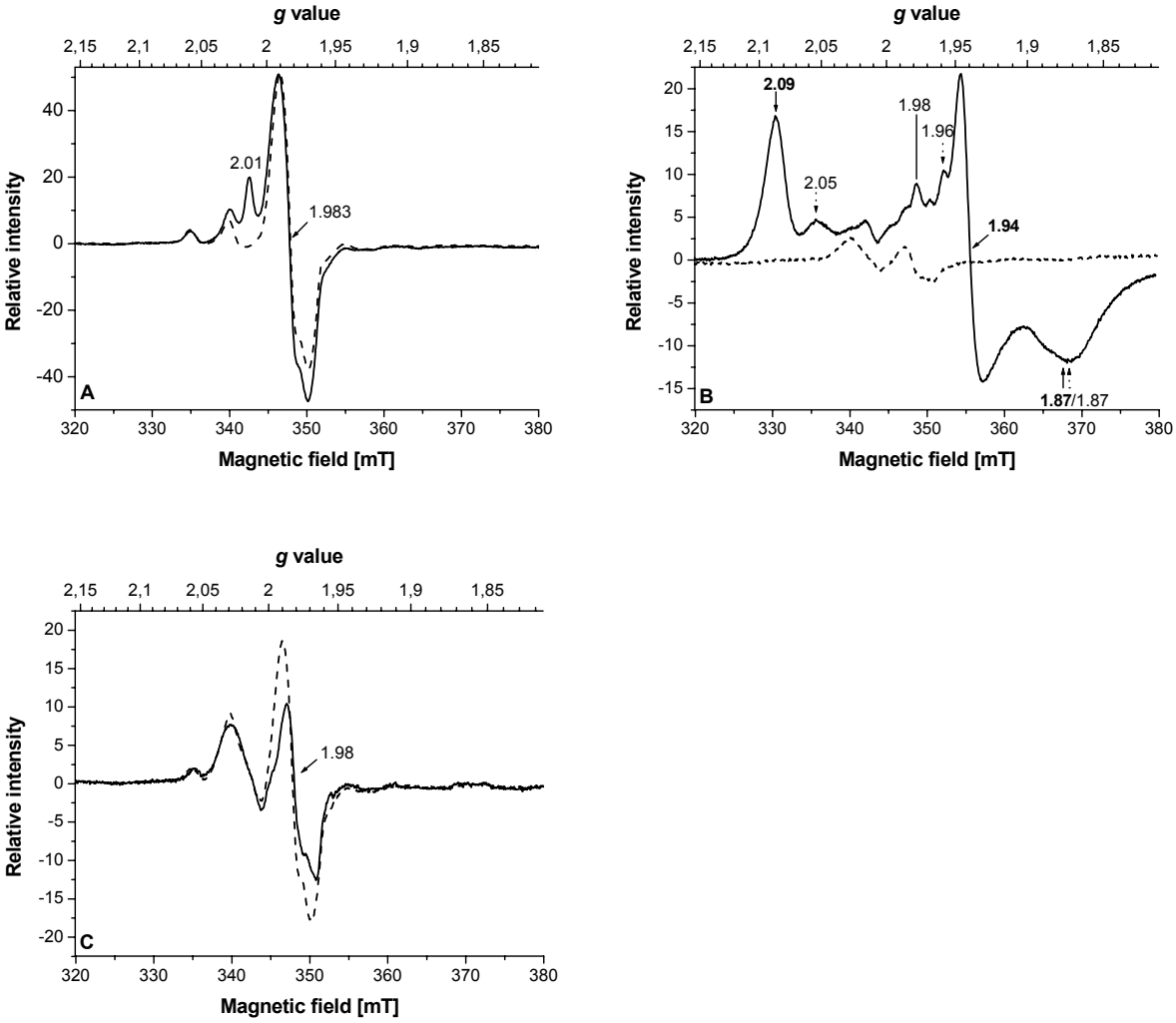

Figure 3.23 EPR spectra of transhydroxylase

A: Transhydroxylase, isolated under air, 12.1 mg ml^{-1} in 50 mM TEA 200 mM NaCl pH 7.5; microwave frequency 9.665 GHz; microwave power: 2 mW; modulation amplitude: 1 mT; scans: 16; temperature: solid line 12 K, dashed line 16 K.

B: Transhydroxylase, isolated under air and stored 17 h in an anaerobe chamber, 7 mg ml^{-1}, in 5 mM HEPES pH 7.8; microwave frequency 9.65 GHz; microwave power: 2 mW; modulation amplitude: 1 mT; scans: 16; temperature: 12 K; dashed line: enzyme stored in an anaerobe chamber for 17 h; solid line: enzyme reduced with 5 equivalents dithionite.

C: Transhydroxylase, isolated under air and stored 17 h in an anaerobe chamber, 7 mg ml^{-1}; microwave frequency 9.65 GHz; microwave power: 2 mW; modulation amplitude: 1 mT; scans: 16; temperature: 12 K; solid line: enzyme in 5 mM HEPES pH 7.8, stored in an anaerobe chamber for 17 h, and oxidized with two equivalents $[Fe^{III}(CN)_6]^{3-}$; dashed line: enzyme in 50 mM TEA 200 mM NaCl pH 7.5 stored under air.

3.2.5. Crystallization and three dimensional structure of transhydroxylase

Transhydroxylase was crystallized both in the “as isolated“ state and after addition of dithionite in the absence of dioxygen. Only the reduced enzyme led to suitable crystals (Figure 3.24). The crystals grew in a N_2/H_2 atmosphere within three days from 12 mg ml^{-1} protein, reduced with 12 equivalents Na-dithionite, from 0.05 M KPi pH 7.5, 20% PEG 8000. A 10% (v/v) additive of Crystal Screen I Factorial #7 (Hampton; 0.1 M sodium cacodylate pH 6.5, 1.4 M sodium acetate trihydrate) was beneficial for crystal growth.

The crystals looked like triangular prisms and diffracted to resolutions better than 3 Å. They belonged to space group P1, with unit cell dimensions of a = 175 Å, b = 180 Å, and c = 182 Å and angles of $\alpha = 63.3°$, $\beta = 63.3°$, and $\gamma = 64.1°$. Improvement of the crystallization conditions and solution of the crystal structure are in progress.

New crystals, obtained in collaboration with Dipl. Biol. Holger Nießen (Universität Konstanz) and Dr. Oliver Einsle (Max-Planck Institut für Biochemie, Martinsried), diffracted at the Deutsche Elektronen Synchrotron (DESY) in Hamburg to resolutions higher than 2.5 A.

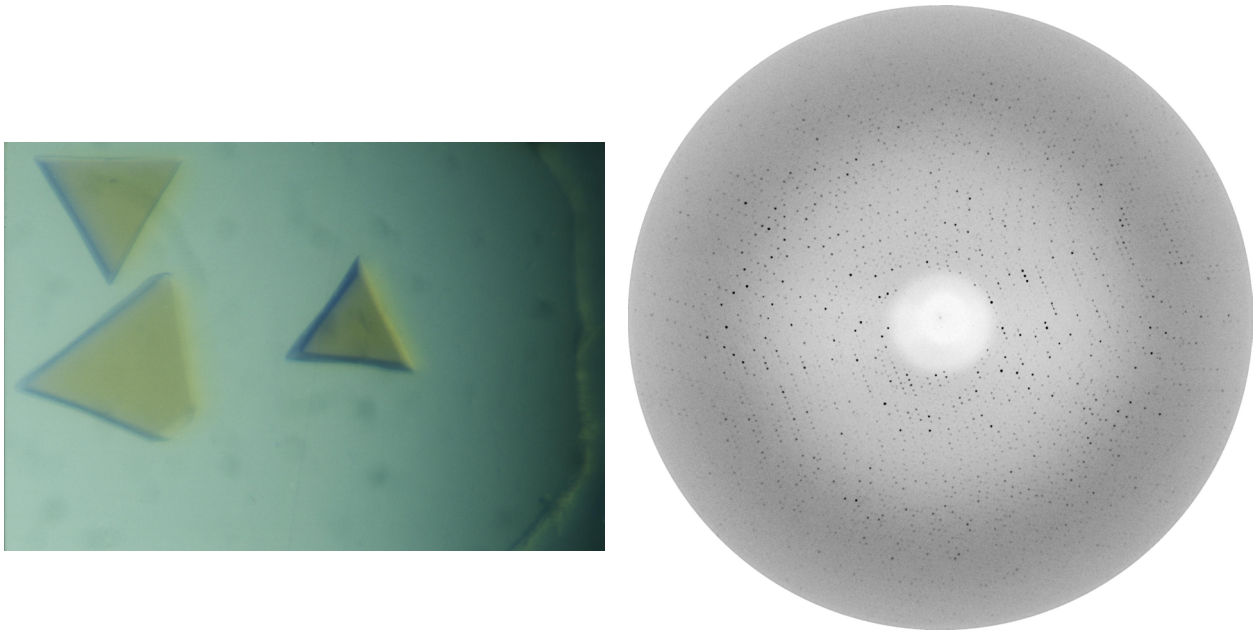

Figure 3.24 Crystals of transhydroxylase and corresponding diffraction image.

3.3. Phylogenetic analysis of acetylene hydratase and transhydroxylase

The molybdenum cofactor containing enzymes are divided into four different families, based on homologies at the amino acid level. These are the DMSO-reductase, the xanthine-oxidase, the sulfite-oxidase, and the aldehyde ferredoxin oxidoreductase (AOR) families (Kisker *et al.*, 1997). Acetylene hydratase and transhydroxylase belong to the DMSO-reductase family (Figure 3.25).

3.3.1. The DMSO-reductase family

BLASTP searches with acetylene hydratase from *P. acetylenicus* and transhydroxylase from *P. acidigallici* as query sequences did not show significant similarity to any eukaryotic enzymes. A phylogenetic analysis of the highest scoring sequences of bacterial and archaeal origin was done using 52 different complete protein sequences. Phylogenetic trees were reconstructed based on 452 unambiguously aligned amino acid positions by maximum-likelihood, neighbor-joining, and maximum-parsimony methods. In order to estimate the robustness of internal branches, bootstrap proportions were calculated and are indicated at the corresponding nodes.
The resulting tree (Figure 3.25) shows seven major groups of enzymes, the names of the groups were given according to enzymes with known function in each of the groups.

Legend to figures 3.25 and 3.26:
Symbols in brackets: α, γ, δ, ε: Proteobacteria; A: Archaebacteria (Euryarchaeota); Ca: Archaebacteria (Crenarchaeota); C: Cyanobacteria; *: Proteins with unknown function; +: Gram-positive bacteria with high/low GC; Thermus: Thermus/Deinococcus group.
The number after the @ sign is the protein accession number from NCBI. TIGR indicates sequences that were obtained from the unfinished microbial database at "The Institute for Genomic Research" (http://www.tigr.org). AH indicates the sequence of acetylene hydratase.
ML: Maximum likelihood analysis; NJ: Neighbor joining analysis; MP: Maximum parsimony analysis.
0.1: substitutions per site.
Numbers are representing the bootstrap support of the corresponding node. A node that was not recovered by ML, NJ, or MP analysis or has a support < 30 is indicated by a '–' sign.
Putative gene-duplications are indicated by a ♦.
The colors indicate a subfamily and the left border shows the earliest possible origin of this group of enzymes.

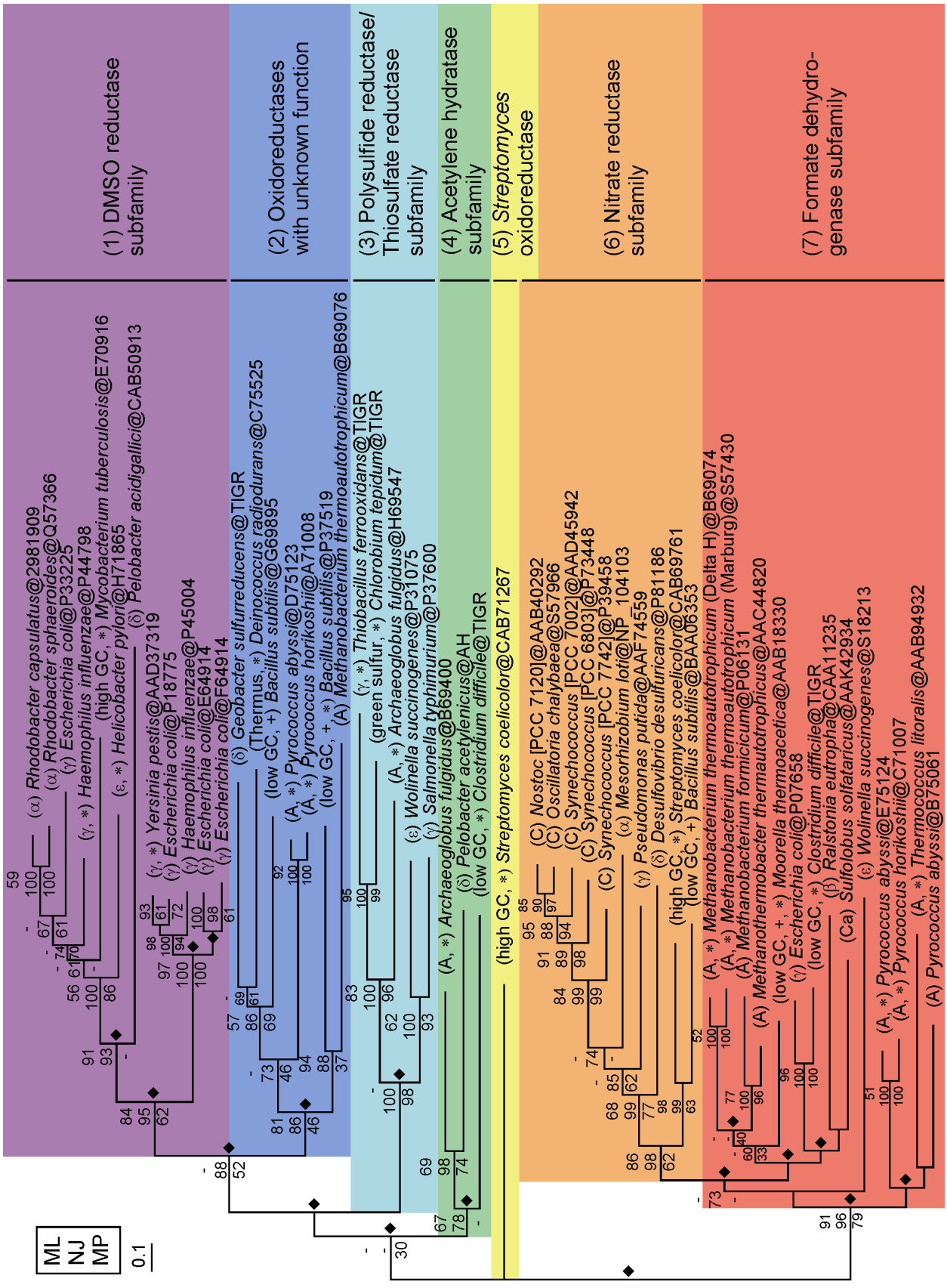

Figure 3.25 The DMSO reductase family.
Symbols are explained on the previous page.

The DMSOR family is deeply split into two major evolutionary groups. Both groups contain sequences from Archaea and Bacteria. The upper half consists of the DMSOR subfamily (Figure 3.25 A), the oxidoreductases with unknown function subfamily (B), the polysulfide/thiosulfate-reductase subfamily (C), the acetylene hydratase subfamily (D), and the *Streptomyces* oxidoreductase subfamily (E). The nitrate-reductases (F) and the formate-dehydrogenases (G) form a second monophyletic group. All subfamilies, except the formate-dehydrogenases, form monophyletic groups that are mainly supported by high bootstrap values.

The DMSOR subfamily (A) is deeply split into two monophyletic groups. With the exception of *M. tuberculosis*, only sequences of proteobacterial origin belong to these groups. The transhydroxylase is part of this subfamily. A more detailed analysis of this subfamily will be described in the next chapter and in figure 3.26.

The group of oxidoreductases with unknown activity (B) is a monophyletic group and contains enzymes of both, archaeal and bacterial origin. It is deeply split into two subgroups that both contain archaeal and bacterial enzymes. The upper subgroup consists of bacterial enzymes from γ-proteobacteria and gram-positive bacteria (*G. sulfurreducens*, *D. radiodurans*, *B. subtilis*) and two archaeal enzymes from *P. abyssi* and *P. horikoshii*. The lower subgroup contains only one enzyme from a gram-positive bacterium (*B. subtilis*) and one enzyme from an archaeon (*M. thermoautotrophicum*). The branches are supported by high bootstrap values. The deep phylogenetic split of this subgroup must be the result of an ancient gene duplication. Under the reasonable assumption that the observed topology is not the result of a lateral gene transfer between the studied organisms, we must therefore assume that the original gene duplication occurred in the last common ancestor of Bacteria and Archaea (Prokaryotes). The topology, with an ancient gene-duplication leading to two branches that both contain sequences from Bacteria and Archaea, seems to be characteristic for several other groups of enzymes (e.g. for the polysulfide/thiosulfate-reductases (C), acetylene hydratases (D), and perhaps also for the formate-dehydrogenases (G)). The fact that all these groups are homologous is leading to the conclusion that there must have been several more ancient gene duplications in a common prokaryotic ancestor, leading to the presently observed diversity of enzymes. The observed absence of eukaryotic sequences may be explained in two different ways: (i) independent loss of these enzymes in eukaryotic organisms or (ii) a large expansion of this gene family in the last common ancestor of Archaea and Bacteria.

The monophyletic polysulfide/thiosulfate-reductase subfamily (C) is also deeply divided into two parts essentially showing the same topology as discussed above, with the exception that the lower part is only formed by bacterial sequences. The upper part contains proteobacterial, green-sulfur bacterial, and one archaeal sequence from *A. fulgidus*. All enzymes of the upper part have unknown activities. The lower part consists of two enzymes from proteobacteria (*W. succinogenes*, *S. typhimurium*), known as thiosulfate-reductase and polysulfide-reductase. All branches are highly supported by bootstrap values.

Within the acetylene hydratase subfamily (D) the enzyme acetylene hydratase from the γ-proteobacterium *P. acetylenicus* is most closely related to an enzyme from the archaebacterium *A. fulgidus* and to an enzyme from *C. difficile*. The topology is identical to the one observed for the polysulfide/thiosulfate-reductases. The three proteins form a monophyletic group that has a rather slow evolutionary rate. It is unknown if the latter two enzymes have acetylene hydratase activity.

The nitrate-reductase subfamily (F) is a monophyletic group supported by high bootstrap values. Together with the DMSOR subfamily it is the only group that contains exclusively bacterial sequences from cyano-, proteo-, and gram-positive bacterial origin. The enzymes of the cyanobacteria form a very distinct group with branches supported by high bootstrap values. The nitrate-reductases of the proteobacteria (*M. loti*, *P. putida*, *D. desulfuricans*) represent a sister-group to the cyanobacterial nitrate-reductases, whereas the nitrate-reductases from *S. coelicolor* and *B. subtilis* form the most basal branch. The branches are mostly supported by high bootstrap values.

The formate-dehydrogenase subfamily (G) is a very heterogeneous group containing enzymes from both Bacteria and Archaea. The formate-dehydrogenase from *S. solfataricus* is the only crenarchaeotic enzyme that was found to be part of the DMSOR family. The upper distinct group also contains enzymes from both bacterial and archaeal origin. The topology is quite similar to the one discussed above but the bootstrap support is not very high. The upper part consists of enzymes from *M. thermoautotrophicum* (strains Delta H and Marburg), *M. formicium*, *M. thermoautotrophicus*, and *M. thermoacetica*; the lower part consists of enzymes from *E. coli*, *C. difficile*, *R. eutropha*, and *S. solfataricus*. The detailed phylogenetic relationship within these groups as well as the exact position of the formate-dehydrogenase from *W. succinogenes* remains unclear. A second group of euryarchaeal formate dehydrogenases consists of enzymes from

P. abyssi, *P. horikoshii*, and *T. litoralis*. Also in this group a basal gene duplication can be observed.

A more detailed analysis of the formate-dehydrogenase/nitrate-reductase group may lead to a better understanding of the relationships within the formate-dehydrogenase/nitrate-reductase subfamily.

3.3.2. The DMSO-reductase subfamily

A detailed analysis of the DMSOR subfamily was done with 30 sequences obtained from BLASTP-searches using the big subunit of transhydroxylase as the query sequence. The phylogenetic trees were reconstructed based on 393 unambiguously aligned amino acid positions by maximum-likelihood, neighbor-joining, and maximum-parsimony methods. In order to estimate the robustness of internal branches, bootstrap proportions were calculated and are indicated at the corresponding nodes. Except for *M. tuberculosis* only proteobacteria belong to this subfamily and sequences from γ-proteobacteria dominate. A lateral gene-transfer from a proteobacterium to *M. tuberculosis* can therefore not be completely excluded but there are no data in favor of this assumption.

The resulting tree (Figure 3.26) is deeply split into two parts and shows at least five major groups of enzymes with similar activity. The names of the groups were given according to enzymes with known activity in each of them.

The DMSOR subfamily is deeply separated into two monophyletic groups that are highly supported by bootstrap values. This separation represents the result of an ancient gene duplication in at least the common ancestor of all Proteobacteria/Bacteria. The gene duplication, which is at the basis of the separation of the two subgroups, is equivalent to the most basal duplication event in the subfamily of the oxidoreductases with unknown activity (Figure 3.25 B), but without sequences from Archaea, homologous to the DMSOR subfamily, this hypothesis cannot be confirmed.

The upper group consists of the *Rhodobacter* DMSO-reductases (Figure 3.26 a), the TMAO-reductases (b), and the BSO-reductases (c). The DMSO-reductases of the γ-proteobacteria (d), *M. tuberculosis*, and the transhydroxylase (e) form the lower group. Each of the new enzyme functions originated from at least one gene duplication.

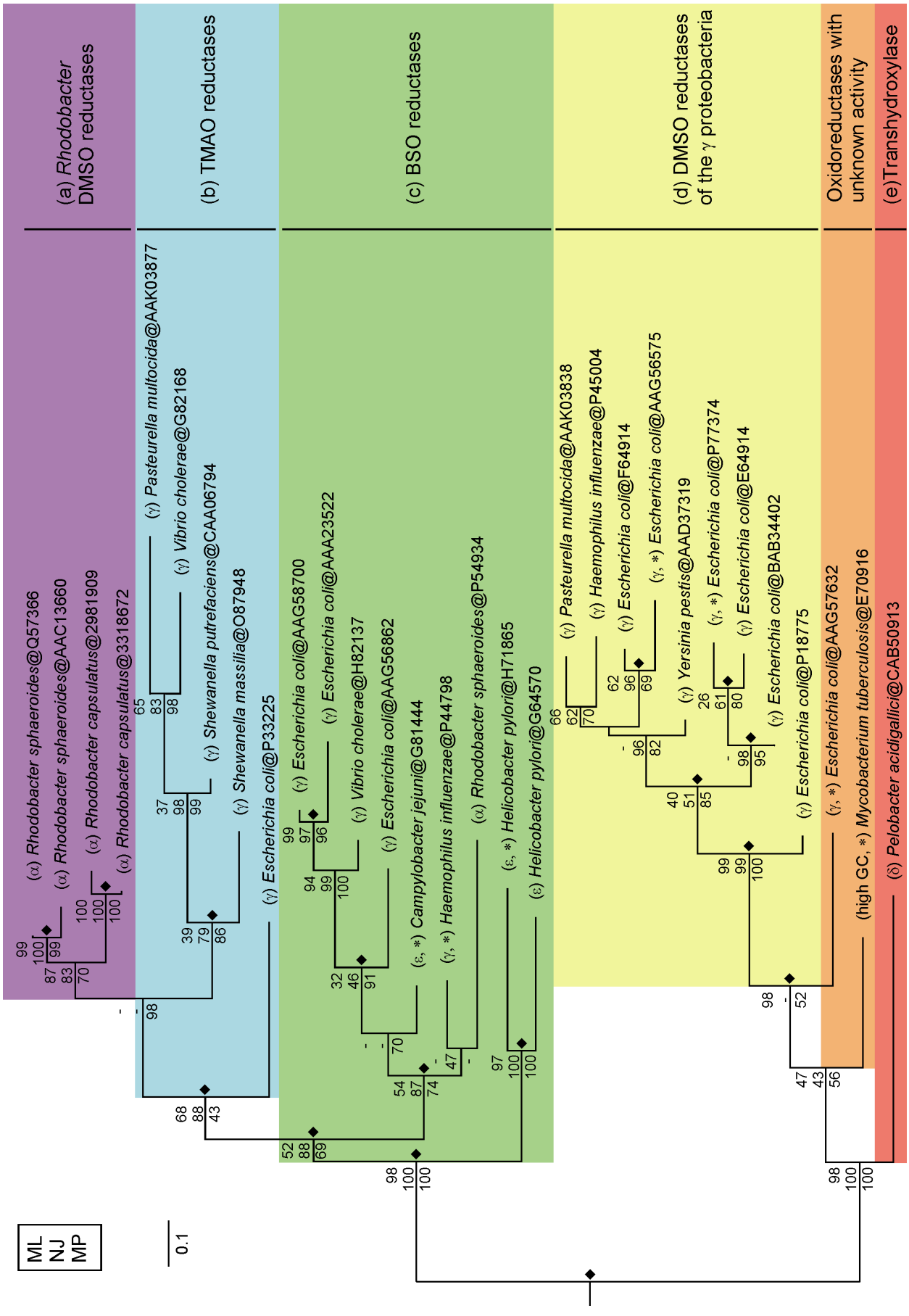

Figure 3.26 The DMSO reductase subfamily.
Symbols are explained in figure 3.25.

The *Rhodobacter* DMSO-reductases (Figure 3.26 a) are a monophyletic group that only contains enzymes from α-proteobacteria of the genus *Rhodobacter*. The branches are highly supported by bootstrap values. Clearly, they are phylogenetically closer related to the TMAO/BSO-reductases (b + c) than to the DMSO-reductases of the γ-proteobacteria (4).

The group of the TMAO-reductases (b) consists only of enzymes from the γ-proteobacteria. The enzymes from *P. multocida*, *V. cholerae*, *S. putrefaciens*, and *S. massilia* belong to a fast evolving monophyletic subgroup of the TMAO-reductases. The *E. coli* enzyme has an unusual basal position to this clade. It is separated from a common ancestor of the *Rhodobacter* DMSO-reductases (a) and the other TMAO-reductases. The branches are supported by high bootstrap values.

The BSOR-reductases (c) are deeply divided into two groups. The upper monophyletic group is deeply divided into two parts by a basal gene duplication. It consists of the enzymes from *E. coli*, *V. cholerae*, *C. jejunii*, *H. influenzae*, and *R. sphaeroides*. They are phylogenetically related to the TMAOR/*Rhodobacter* DMSOR (b + a) group. The most basal second group consists of only two *H. pylori* BSO-reductases. They separated from a common ancestor of the TMAOR/*Rhodobacter* DMSOR group. Most branches are highly supported by bootstrap values.

All the enzymes that belong to the second clade of the DMSOR subfamily form a monophyletic group and originated as a result of an ancient gene duplication. Transhydroxylase (*P. acidigallici*) separated first from the other DMSO-reductases of the γ-proteobacteria. The next branches are the enzymes from *M. tuberculosis* and *E. coli*. It seems possible to put these enzymes into an independent group. Unfortunately nothing is known about the function of these enzymes. The branches are supported by high bootstrap values.

The DMSO-reductases of the γ-proteobacteria (d) consists of seven enzymes from *E. coli* and one each from *H. influenzae* and *Y. pestis*. At least six gene-duplications are needed to explain these seven different *E. coli* DMSO-reductases. It is unclear why *E. coli* needs at least one TMAOR, three different BSO-reductases, and seven different DMSO-reductases.

4. Discussion

This study presents data on two novel, molybdopterin containing, enzymes: (i) the tungsten/iron-sulfur containing acetylene hydratase from *Pelobacter acetylenicus* and (ii) the molybdenum/iron-sulfur containing transhydroxylase from *Pelobacter acidigallici*. Although the overall reaction of both enzymes does not contain a net redox chemistry they contain a set of complex redox cofactors at the active site. Both enzymes were purified to homogeneity and characterized with biochemical and spectroscopic methods. Crystallization of both proteins led to crystals suitable for X-ray analysis. The solution of the three-dimensional structures was started and is still in progress. Sequence determination of the acetylene hydratase sequence was carried out and the amino acid sequences of acetylene hydratase and transhydroxylase were subjected to a phylogenetic analysis.

4.1. Molybdenum *versus* tungsten in enzymes

There are now a number of well established tungsten enzymes (Table 1.3). These enzymes are mostly from thermophilic or hyperthermophilic bacteria found, for example, at deep-sea hydrothermal vents (Johnson *et al.*, 1996; Kletzin and Adams, 1996). Tungsten containing acetylene hydratase is from a mesophilic bacterium that was isolated from a freshwater creek sediment near Konstanz (Schink, 1984). Tungsten enzymes catalyze reactions that are related to those catalyzed by the molybdenum enzymes (Stiefel, 1997). Moreover, the tungsten active sites contain the same type of pterin–ene-dithiolate ligand (moco, Figure 1.2 A) that the molybdenum enzymes employ (Johnson *et al.*, 1993; Chan *et al.*, 1995; Johnson *et al.*, 1996; Kletzin and Adams, 1996). In some cases molybdenum could replace tungsten forming an active enzyme (*E. coli* TMAO-reductase, Buc *et al.*, 1999; *R. capsulatus* DMSO-reductase, Stewart *et al.*, 2000; *P. acetylenicus* acetylene hydratase, this work). One of the remaining questions is: Why do both, molybdenum and tungsten, enzymes exist?

One reason why tungsten has been favored may be related to the chemical differences between molybdenum and tungsten that are selected by the special conditions under which the tungsten enzymes function. For example, tungsten is more difficult to reduce than molybdenum (Stiefel, 1997). The redox potentials of W-complexes are much lower than the potentials of Mo-complexes, typically 300 – 400 mV more negative (Johnson *et al.*, 1996). Therefore, if an enzyme is required to work at low redox potentials then tungsten can be evolutionarily favored

instead of the more common molybdenum systems. The greater inertness of tungsten towards substitution reactions can be an advantage in hyperthermophilic environments (≈ 100°C) where hydrolytic reactions can compromise the integrity of the active site (Stiefel, 1997). Therefore, the fitness of tungsten over molybdenum in certain cases may involve tungsten's ability of better functioning in the chemical or physical environment, which is characteristic of the organism in which the enzyme is found.

Another reason is that the chemical differences of molybdenum and tungsten do not manifest in the different reactivity but in the geochemical environment, the organisms live. Molybdenum deposits are mostly found in nature in the form of MoS_2, while the more oxophilic tungsten is found as $CaWO_4$ and $Fe/MnWO_4$ (Chapter 1.1.). The chemical difference of the two elements is sufficient to effect geochemical differentiation of these elements. In chemistry it is much more difficult to convert tungstate to tungsten sulfide compounds than it is to convert molybdate to molybdenum sulfide compounds (Greenwood and Earnshaw, 1990; Stiefel, 1997). Therefore, in sulfur-rich hydrothermal environments, in which many of the organisms have been found that contain tungsten enzymes, it is possible that molybdenum is not available, because it precipitated with the massive sulfide deposits of these habitats. The organisms therefore just can use tungsten. Further studies on the enzymes, the organisms, the biogeochemistry of the habitats, and the coevolution of these enzymes should help sort out the teleology of the molybdenum *versus* tungsten (Stiefel, 1997).

4.2. Cultivation of the bacteria and enzyme purification

Chemical properties as well as atomic and ionic radii of tungsten and molybdenum are very similar (Table 1.1). Over the last decade, some striking parallels between the nature and function of molybdenum and tungsten centers in enzymes have emerged (Johnson *et al.*, 1996; Hagen and Arendson, 1998). Bertram *et al.* (1994) showed that tungsten can substitute for molybenum and sustain the growth of *Methanobacterium thermoautotrophicum*. These authors identified and characterized a tungsten isoenzyme of formylmethanofuran dehydrogenase. In 1999, Buc *et al.* successfully substituted tungsten for molybdenum in *E. coli* TMAOR and obtained an active enzyme. Stewart *et al.* (2000) published the crystal structure of a highly active, tungsten substituted, DMSOR from *Rhodobacter capsulatus*.

In the latter publication, it was shown that *R. capsulatus* only can grow on tungstate in the presence of a low concentration (6 nM) of molybdate. The reason for the requirement of a small trace of molybdate is not clear. The authors presume that molybdate (i) is required for the

biosynthesis of some other molybdoenzymes, such as nitrate reductase or xanthine dehydrogenase, (ii) that it is needed as an activator for the biosynthesis of the molybdopterin cofactor, or (iii) that molybdate prevents the uptake of tungstate by the cell to a toxic level (Imperial *et al.*, 1998; Grunden *et al.*, 1999; Stewart *et al.*, 2000). The *Rhodobacter* cells grew well at a concentration of 3 µM tungstate (plus 6 nM molybdate). Significant inhibition of cell growth was obtained at tungstate concentrations higher than 100 µM, 60 mM tungstate in the medium inhibited cell growth completely.

It is known that *Azotobacter vinelandii* and *Azotobacter chroococcum* have an alternative nitrogen fixing system with a V-Fe nitrogenase instead of the Mo-Fe nitrogenase (Eady, 1996). In *A. vinelandii* this nitrogenase functions under conditions of Mo-deficiency (Robson *et al.*, 1986).

Vanadate ions (VO_3^-) inhibit purified nitrate reductase of *Chlorella vulgaris* but growth of the cells was not (Ramadoss, 1979).

4.2.1. *Pelobacter acetylenicus*

(a) Tungstate cultivation

P. acetylenicus grew well in medium containing tungstate. The specific activity of the purified enzyme was 42.25 U mg^{-1} at 50°C or 14.9 U mg^{-1} at 30°C. It was significantly lower than the previously reported 26.5 U mg^{-1} (30°C; Meckenstock *et al.*, 1999). Note that the specific activity of acetylene hydratase depended very much on the individual batch.

(b) Molybdate cultivation

Kisker *et al.* (1999) reported the existence of a molybdenum containing acetylene hydratase from *P. acetylenicus*. In order to obtain this Mo-acetylene hydratase *P. acetylenicus* was cultivated on molybdate ($^{95}MoO_4^{2-}$) in the presence of a small amount of tungstate (2 nM). In the 100 ml and 1 l batch culture bottles the cells grew well within 2 days, but in the 50 l batch culture they only grew within 2 days to an optical density of 0.2 at 578 nm (Figure 3.1). By ICP-MS methods it was shown that acetylene hydratase from molybdate cultivation contained 0.5 mol molybdenum but almost no tungsten (Table 3.4). The EPR spectra (Figure 3.10) also clearly demonstrated the substitution of tungsten by molybdenum. The specific activity of the enzyme was about 60% lower than the specific activity of the tungsten enzyme (Tables 3.1, 3.2). It appears to be

reasonable that the redox potential of the synthesized Mo-bisMGD cofactor is too high in order to ensure an effective specific activity (Chapter 4.3.2.). For future cultivation experiments on molybdate the minimal tungsten concentration should be employed for growth of *P. acetylenicus* in the presence of high amounts of molybdate. It should be checked if an increase of trace elements would have an effect on bacteria growth, on acetylene hydratase yield, and on specific activity.

(c) Vanadate cultivation

To check if *P. acetylenicus* is able to incorporate vanadium instead of tungsten into acetylene hydratase the cells were grown on vanadate. The 100 ml and 1 l batch cultures seemed to grow well on the selected medium, but in the 50 l batch culture the cells grew within 2 days to an optical density of 0.2 at 578 nm (Figure 3.1). The purified enzyme from this cultivation showed no incorporated vanadium and the tungsten or molybdenum content was almost zero (Table 3.4). It seems that an enzyme with an almost metal-free bisMGD cofactor was purified. The specific, acetylene hydrating, activity of the enzyme was detectable but it was very low (Table 3.3). This may be one reason why the bacteria did not grow as well as in the tungstate-containing medium. Another reason might be related to the vanadate concentration of 10 µM that might have been toxic.

4.2.2. *Pelobacter acidigallici*

P. acidigallici grew well in medium containing molybdate. Cultivation conditions with 10 µM molybdate and 10 nM tungstate as well as a three-fold increase of trace element solution lead to a remarkable increase in cell yield by more than 100% (H. Nießen, Universität Konstanz, personal communication). The enzyme obtained with the new purification procedure developed in this work was highly active (4.6 U mg^{-1}) compared to the previously reported 3.1 U mg^{-1} of Reichenbecher *et al.* (1994). About 250 mg of pure transhydroxylase out of 30 g wet cell mass were obtained by the new purification procedure (Chapter 3.2.2.).

A tungsten containing transhydroxylase will be extremely helpful in the solving of the crystal structure because of the strong anomalous scattering contribution at the tungsten L-edge. To obtain a tungsten containing transhydroxylase, cultivation on 10 µM tungstate and 50 nM molybdate was carried out. The cells grew well on this medium with a yield comparable to the

cultivation on molybdate (H. Nießen, Universität Konstanz, personal communication). Currently the purification of a tungsten-enriched transhydroxylase is in progress.

4.3. Spectroscopic properties of acetylene hydratase and transhydroxylase

4.3.1. UV/Vis spectroscopy

Iron-sulfur centers in proteins exhibit broad electronic absorptions between 350 and 800 nm, in many cases a shoulder between 380 and 420 nm is the only feature. Because the absorption bands of iron-sulfur centers are broad and featureless, the presence of the centers may go unnoticed in the UV/Vis spectra in the presence of other chromophores such as heme or flavin (Cammack, 1992). Nevertheless they can be useful e.g. in a redox titration experiment to calculate the midpoint redox potential of [4Fe-4S] clusters (Meckenstock *et al.*, 1999; Figure 1.6). On the other hand transitions from molybdenum sites can be buried under the absorptions from iron-sulfur centers (Johnson and Rajagopalan, 2001).

In the dithionite reduced state the *Rhodobacter* DMSO-reductases, the *E. coli* TMAOR, and the *R. sphaeroides* BSOR show Mo(IV) spectra with a broad absorption band between 600 and 700 nm and a low molar extinction coefficient (Temple *et al.*, 2000; Johnson and Rajagopalan, 2001). The same enzymes in the oxidized, Mo(VI), state exhibit complex UV/Vis absorption spectra between 350 and 800 nm (Johnson and Rajagopalan, 2001).

Stewart *et al.* (2000) showed that *R. capsulatus* DMSO-reductase is able to incorporate molybdenum as well as tungsten into the active site. The UV/Vis spectrum of "as isolated" Mo-DMSOR shows an absorption pattern typical for a Mo(VI) species. The "as isolated" W-DMSOR exhibits a similar absorption pattern with blue-shifted λ_{max}-values by ca. 150 nm (i.e. 3000 – 5000 cm^{-1}). These absorptions are considered to arise from ligand-to-metal charge-transfer transitions, from sulfur-based orbitals to a d^0 metal center. Consistent with this view, the blue-shift observed is similar to that (ca. 4350 cm^{-1} from Mo to W) for the two lowest energy transitions of the $[MS_4]^{2-}$ (M = Mo, W) anions (Diemann and Müller, 1973; Stewart *et al.*, 2000).

Acetylene hydratase and transhydroxylase in the “as isolated” as well as in the dithionite reduced state exhibit a UV/Vis spectrum that is dominated by the absorptions of iron sulfur centers between 350 and 800 nm (Figures 3.8, 3.22), with the typical shoulder between 360 and 400 nm. “As isolated” acetylene hydratase exhibited an iron-sulfur absorption band with a maximum at about 590 nm (Figure 3.8 D) that may result from sulfur-to metal charge-transfer-transitions of a, compared with Mo(VI), blue-shifted band from a W(VI) center. The acetylene hydratases from molybdate (^{95}Mo) and vanadate cultivation also had this band but with lower molar extinction coefficients. Acetylene hydratase from vanadate cultivation contained low amounts of tungsten and molybdenum (Table 3.4). The optical spectrum of dithionite reduced W-acetylene hydratase is also dominated by the absorptions of the [4Fe-4S] cluster. The molar extinction coefficient of the absorption band at 590 nm decreases and the absorption band is overshadowed by the iron-sulfur absorptions.

In contrast to acetylene hydratase transhydroxylase contains at least two [4Fe-4S] clusters and perhaps another [4Fe-4S] cluster or [2Fe-2S] clusters. Therefore, the UV/Vis spectra of transhydroxylase are more overshadowed by the absorptions of iron-sulfur clusters than the spectra of acetylene hydratase. “As isolated” and dithionite reduced transhydroxylase gave similar spectra with a broad absorption between 650 and 750 nm. This may be a result of the absorptions of Mo(VI) and Mo(IV) species within the bisMGD cofactor. The absorption pattern for Mo(IV) or Mo(VI) can not be resolved because of the iron-sulfur absorptions.

4.3.2. EPR-spectra of acetylene hydratase

Meckenstock *et al.* (1999) purified acetylene hydratase both under air and under exclusion of dioxygen. The “as isolated” enzyme, prepared under air, showed a signal at $g_{av} = 2.01$ whereas the enzyme prepared under exclusion of dioxygen was EPR silent in the “as isolated” state. This axial signal is typical for a truncated [3Fe-4S] cluster as described for a variety of iron-sulfur proteins (Flint and Allen, 1996). Upon reduction with dithionite it disappeared, and both oxic and anoxic preparations of acetylene hydratase exhibited an intense rhombic signal ($g_{av} = 1.968$) that was assigned to a low-potential ferredoxin-type [4Fe-4S] cluster. When the enzyme was oxidized with $[Fe^{III}(CN)_6]^{3-}$ a new EPR signal with $g_{av} = 2.022$ appeared which disappeared on further addition of $[Fe^{III}(CN)_6]^{3-}$. The signal showed a temperature optimum around 5 K under non-saturating conditions of microwave power and was still detectable at 150 K. This signal was tentatively assigned to a W(V) center.

The redox potentials of the molybdenum centers in enzymes can vary significantly. For example, the redox potential ($E^{0'}$) of *Methanobacterium formicicum* formate dehydrogenase is about –400 mV (Pilato and Stiefel, 1999), of *E. coli* DMSO-reductase it is about –50 mV (Trieber *et al.*, 1996), and of *E. coli* respiratory nitrate reductase it is about +200 mV (Pilato and Stiefel, 1999). The redox potentials of W-complexes are much lower than the potentials of Mo-complexes, typically 300 – 400 mV more negative (Johnson *et al.*, 1996).

Acetylene hydratase activity of the W-enzyme was strongly dependent on the redox potential of the W-center (Meckenstock *et al.*, 1999). The midpoint redox potential was –340 mV, whereas at redox potentials higher than –300 mV no acetylene hydratase activity was detected. Further reduction at lower potentials led to the reduction of the [4Fe-4S] cluster but did not change the activity. Therefore, acetylene hydratase is active with the iron sulfur center in either the reduced or the oxidized form (Meckenstock *et al.*, 1999).

(a) W-acetylene hydratase

Acetylene hydratase of this work, purified under a N_2/H_2 atmosphere, showed a weak signal of a [3Fe-4S] cluster. The signal disappeared upon reduction with dithionite and an intense rhombic signal of a [4Fe-4S] (g_{av} = 2.022) cluster appeared. The $[Fe^{III}(CN)_6]^{3-}$ oxidized enzyme showed a g_{av} = 2.022 signal of a putative W(V) center.

(b) ^{95}Mo-acetylene hydratase

The “as isolated” acetylene hydratase showed a signal of a [3Fe-4S] cluster and a weak rhombic signal of a [4Fe-4S] cluster. Upon reduction with dithionite the signal of the [3Fe-4S] cluster disappeared and only the intense signal of the [4Fe-4S] cluster remained with a g_{av} of 1.97. Therefore, the Mo-acetylene hydratase in the “as isolated” state was partially reduced whereas the W-acetylene hydratase was purified in a more oxidized state. Oxidation of the enzyme with $[Fe^{III}(CN)_6]^{3-}$ led to the complex multiline EPR spectrum resulting from hyperfine interaction with the ^{95}Mo nucleus with I = 1/2.

The specific activity of the purified Mo-acetylene hydratase is lower than the specific activity of the W-enzyme. It is likely that the redox potential of the Mo-center is not low enough to catalyze the conversion of acetylene to acetaldehyde as efficiently as the corresponding W-enzyme.

(c) Acetylene hydratase - vanadate cultivation

Acetylene hydratase from vanadate cultivation was purified under exclusion of dioxygen. The "as isolated" enzyme showed a signal of a [3Fe-4S] cluster (g_{av} = 2.01) and the rhombic signal of a [4Fe-4S] cluster (g_{av} = 1.97). After reduction with dithionite, the intensity of the rhombic signal increased slightly. Overall, the signal has much less intense compared to the enzymes isolated from cells grown either with tungstate or molybdate. ICP-MS analysis showed that acetylene hydratase from vanadate cultivation only contained 2.41 Fe per enzyme AH *versus* 3.11 Fe/Mo-AH, or 3.52 Fe/W-AH. After oxidation with $[Fe^{III}(CN)_6]^{3-}$ a signal with g_{av} = 2.022 appeared that had the shape of the W(V) signal of W-acetylene hydratase and corresponded to a small amount of incorporated tungsten (Table 3.4). Although molybdenum was also found in this preparation, the signals of a ^{95}Mo(V) center were not detected.

4.3.3. EPR-spectra of transhydroxylase

Transhydroxylase exhibited a minor resonance at low magnetic field (g = 4.3) due to adventitious iron and a signal of a [3Fe-4S] cluster with g_{av} = 2.01 that disappeared above 30 K (Cammack and Weiner, 1990; Reichenbecher *et al.*, 1996; Kisker *et al.*, 1999). Depending on the preparation a weak signal at $g \approx 1.98$ of a Mo(V) 'resting' species could be seen. The intensity of the [3Fe-4S] resonance corresponded to ≤ 0.1 spins per molecule. Most likely, it originated from a slightly acid labile [4Fe-4S] cluster as previously described for DMSOR (Weiner *et al.*, 1992). A preparation of transhydroxylase with rapid neutralization of the enzyme fractions after chromatofocussing led to an enzyme with no [3Fe-4S] signal (Sommer, 1995; Kisker *et al.*, 1999). Because of line broadening the [3Fe-4S] signal disappeared above 35 K and the pure Mo(V) 'resting' signal remained. Upon addition of dithionite two intense new signals appeared with g_z = 2.08, g_y = 1.946 and g_x= 1.869, and g_z = 2.057, g_y = 1.957 and g_x = 1.874, which are characteristic for Fe-S centers. The first signal broadened above 30 K, whereas the paramagnetic center with g_z = 2.057, g_y = 1.957 and g_x = 1.874 remained visible up to 70 K (Kisker *et al*, 1999). After addition of 10 reduction equivalents transhydroxylase was fully reduced (Sommer, 1995). The paramagnetic Fe-S sites did not reveal any significant influence on the Mo(V) EPR signal with regard to relaxation or lineshape. It was concluded that there must be at least two different types of [4Fe-4S] centers. Furthermore, the existence of [2Fe-2S] sites could not be excluded by Kisker *et al* (1999).

Transhydroxylase prepared in this work showed, in the "as isolated" state a signal of a [3Fe-4S] cluster with $g_{av} = 2.01$ that disappeared above 16 K (Figure 3.23). An intense Mo(V) 'resting' signal around $g \approx 1.98$ with hyperfine coupling from ^{95,97}Mo dominateds the EPR spectrum. When pure transhydroxylase was stored in a N_2/H_2 atmosphere for 17 h, the lines broadened or disappeared. After oxidation with $[Fe^{III}(CN)_6]^{3-}$ the observed spectrum was similar to the spectrum of "as isolated" transhydroxylase. Therefore, transhydroxylase became reduced, at least partially, when stored under a N_2/H_2. The fully reduced enzyme (10 equivalents dithionite) exhibited two intense new signals with $g_z = 2.08$, $g_y = 1.94$, and $g_x = 1.87$ and $g_z = 2.05$, $g_y = 1.96$, and $g_x = 1.87$ which were tentatively assigned to two magnetically interacting [4Fe-4S] clusters (Fritz *et al.*, 2000). The existence of [2Fe-2S] clusters remains also unclear after these studies.

BLASTP searches with the small subunit of transhydroxylase as template revealed that 12 of the 13 cysteines were highly conserved within related enzymes. Some of them were referred to as [4Fe-4S] ferredoxins. The 15 cysteines of the big subunit did not align with the cysteines of related iron-sulfur proteins. Therefore, it seems unlikely that one iron-sulfur center is located on the big subunit. It is more likely that there are three [4Fe-4S] clusters located on the small subunit. The cysteines do not fit into the classical consensus sequence (-Cys-x_2-Cys-x_2-Cys-x_3-Cys-Pro-; Cammack, 1992) but they are related to this motif and there is evidence that this binding motif can be varied (e.g. Kemper *et al.*, 1998; Leartsakulpanich *et al.*, 2000). Recently a preliminary X-ray analysis of *Desulfovibrio gigas* W-formate dehydrogenase was published (Raaijmakers *et al.*, 2001). It was shown by X-ray analysis that the small subunit contains three [4Fe-4S] clusters. This subunit can be a model for the small subunit of the transhydroxylase with respect to the iron-sulfur centers. Unfortunately, the amino acid sequence is not published until today.

4.4. Evolution of the DMSO-reductase family

4.4.1. Relationships of the tree domains of life

The DMSOR family is a heterogeneous group of enzymes of bacterial and archaeal origin that is forming two major clades. The upper clade consists of the DMSOR subfamily (Figure 3.25 A), the oxidoreductases with unknown activity subfamily (B), the polysulfide/thiosulfate-reductase subfamily (C), the acetylene hydratase subfamily (D), and the *Streptomyces* oxidoreductase subfamily (E). The nitrate-reductases (F) and the formate-dehydrogenases (G) form the second half. All subfamilies, except the formate-dehydrogenases (G), form monophyletic groups that are clearly supported by high bootstrap values. Despite the great number of different enzymes, no enzymes from eukaryotic organisms were found to be homologous to the DMSOR family. The absence of eukaryotic homologs is quite surprising regarding the fact that these enzymes probably originated very early in the evolution of cellular life on this planet and in the light of the current view of the relationships of the three domains of life (Bacteria, Archaea, Eukarya). In the following, the evolution of the different enzyme types and the relationships of the organisms in which they are found will be discussed.

The most commonly accepted hypothesis for the interrelationships between the three domains of life is that the bacterial lineage separated first from the common ancestor of Archaea and Eukaryotes (Figure 4.1 A; Iwabe *et al.,* 1989, Gogarten *et al.*, 1989). Therefore, the Bacteria are regarded by this hypothesis as the oldest existing group of organism, and only after their separation, Archaea and Eukarya further subdivided into two independent lineages (Figure 4.1 A; for a review see Forterre and Philippe (1999) and the references therein). The rapidly growing number of genome projects is making a wealth of sequence data available. Analyses of these data showed that for the majority of genes the current view (Figure 4.1 A) is not supported (Forterre and Philippe, 1999). Rather there are many genes in which either Prokaryotes (Bacteria + Archaea) were each others closest relatives to the exclusion of Eukarya, or in which only prokaryotic copies were found. An alternative view of the relationships of the three domains was proposed by Brinkmann and Philippe (1999), Forterre and Philippe (1999), and Philippe and Forterre (1999). They favor a scenario where the Prokaryotes are a monophyletic group and the first separation was the one between Prokaryotes and Eukaryotes. Only later did the Prokaryotes subdivide into the sistergroups Bacteria and Archaea (Figure 4.1 B). The results presented in this work support the alternative view of the “Tree of life”.

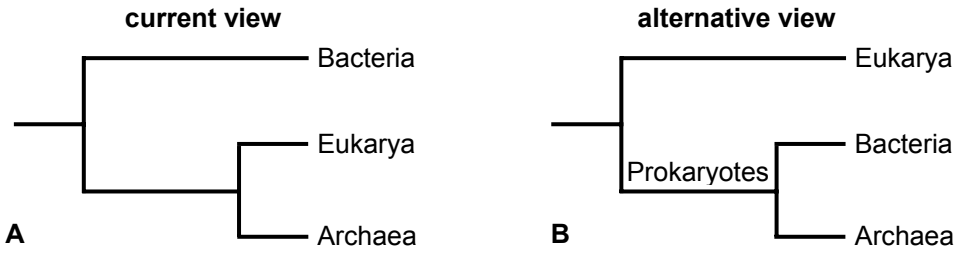

Figure 4.1 Phylogenetic trees of life.
Two alternative views on the relationship of the major lineages (omitting viruses).
A: The most commonly accepted hypothesis (Iwabe *et al.,* 1989, Gogarten *et al.*, 1989).
B: Alternative view (Brinkmann and Philippe, 1999).

The DMSOR family contains only enzymes from bacterial and archaeal origin. This is quite surprising and difficult to reconcile with the current view of the relationships of the three domains of life (Figure 4.1 A). It became clear very early that the evolution of the DMSOR-family is very complex with several ancient gene duplications in the common ancestor of the Prokaryotes (Figure 4.2). Within four of the seven defined subfamilies we can deduce at least one ancient gene duplication within the last common ancestor of Bacteria and Archaea. Therefore the majority of the enzyme types and perhaps even all of them seem to have originated in the last common ancestor of Bacteria and Archaea. Because all of these enzyme types are homologous to each other one must assume a common precursor enzyme out of which the different present types did evolve by several gene duplications. The duplication pattern observed in the DMSOR family can therefore be more easily explained under the assumption that the Prokaryotes are a monophyletic group (Figure 4.1 B). Under this scenario the observed pattern of gene duplications, which roughly correlates with the evolution of different enzyme activities, would be most easily explained by assuming a series of subsequent gene duplications correlated with the evolution of different enzyme functions in the last common ancestor of the Prokaryotes. Whereas the current view of the relationships between the three domains would imply that each time when we find a common ancestor of Bacteria and Archaea (about 10 times in figure 3.25) it would be at the same time a common ancestor of all Eukaryotes and therefore of all three domains of life. In consequence, under this scenario one would need to postulate a high number of independent losses of these different enzyme types and isoforms in the Eukaryotes. This seems to be a highly unlikely scenario. In contrast, if the Prokaryotes were monophyletic, the observed pattern would be easily explained by assuming an expansion of this enzyme family accompanied by several gene duplications in the common ancestor of Bacteria and Archaea after the separation of the Eukarya. With respect to the Eukaryotes there are two possibilities. Either they never had this enzyme-type or they once had an enzyme homologous to the DMSOR family

and lost it after their separation from the Prokaryotes. Several eukaryotic genomes were sequenced without finding any homologue. It may be possible that these enzymes occur in anaerobic Eukaryotes that are up to date not very well characterized. But, even the identification of an eukaryotic homologue would not necessarily mean that this enzyme must be of eukaryotic origin because it may also have originated in a lateral gene transfer or could possibly descend from an endosymbiosis with a prokaryote.

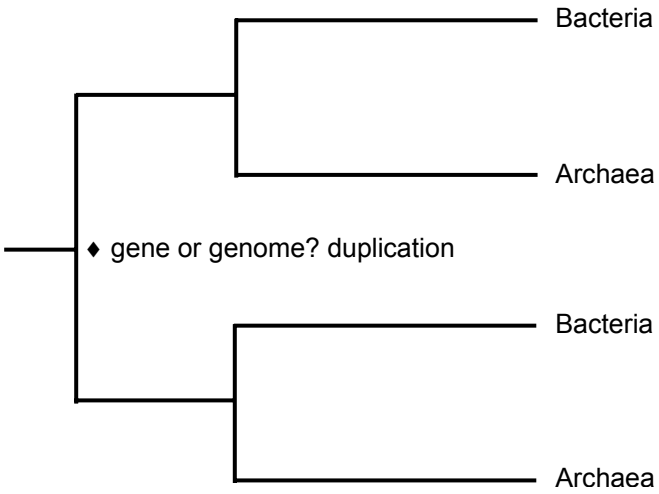

Figure 4.2 Widespread division pattern within the DMSO-reductase family.
♦: Gene or genome? duplication
Both branches contain sequences from archaea and bacteria.

Within the DMSOR family a division pattern is found that is characteristic for at least four of the seven subfamilies. This general pattern is shown in Figure 4.2. The subfamily of the oxidoreductases of unknown function is the best representative of this pattern (Chapter 3.3.1.). A gene duplication basal in the enzyme lineage leads to two branches that both contain sequences of archaeal and bacterial origin, forming two, highly supported, monophyletic groups. Each of these groups and therefore also the basal gene duplication has its origin at least in a common prokaryotic ancestor. To date there are no obvious explanations why this characteristic division pattern occurs in most of the subfamilies. One possible explanation, although difficult to prove, would be to assume a genome duplication in the common prokaryotic ancestor. Under the assumption of a genome duplication we would expect to find many duplicated genes that originated simultaneously in the common prokaryotic ancestor (Figure 3.25). This scenario would easily explain the pattern of basal gene duplications, observed within the majority of the enzyme types (Figure 4.2). The problem is that up to now nobody had postulated this kind of genome duplication and *a priori* there seems to be no other data supporting this scenario.

4.4.2. The DMSO-reductase subfamily

Only sequences from Bacteria belong to the DMSOR subfamily (Figure 3.26). Nevertheless although this group seems to be limited to bacteria we know from the above discussion that the gene duplication, that is at the origin of this enzyme subfamily, happened in a common prokaryotic ancestor. Therefore it cannot be excluded that Archaea once contained, or some of them still contain, enzymes homologous to the DMSOR subfamily. Furthermore the DMSOR subfamily also shows a basal gene duplication that is clearly older than the separation of all bacterial sequences studied. In this respect, the topology of the tree resembles the general pattern already described above (Figure 4.2).

Except for *M. tuberculosis* the sequences are all from proteobacteria with the γ-proteobacteria clearly dominating. A lateral gene-transfer to *M. tuberculosis* can therefore not be completely excluded but there are no data in favor of this assumption.

The DMSOR subfamily is deeply split into two monophyletic groups that are highly supported by bootstrap values. One half leads to the transhydroxylase and to the DMSO-reductases of the γ-proteobacteria, the other leads to the BSO/TMAO/*Rhodobacter*-DMSO-reductases. This separation originated in the above described ancient gene duplication. Under the assumption of a lateral gene-transfer to *M. tuberculosis*, the upper estimate of the split would correspond to an ancient gene duplication in at least the common ancestor of all Proteobacteria. Because this group is essentially limited to proteobacteria, their phylogenetic relationships are depicted in figure 4.3.

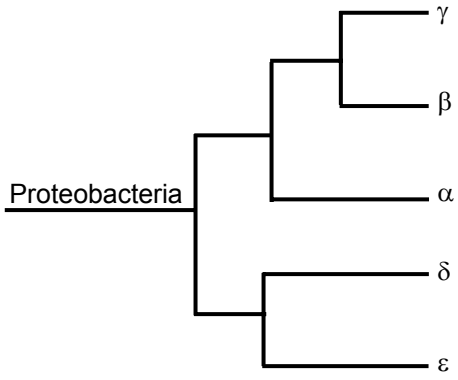

Figure 4.3 Phylogenetic tree of the proteobacteria (Schlegel, 1992).

The upper group of the DMSOR-subfamily consists of the *Rhodobacter* DMSO-reductases (Figure 3.26 a), the TMAO-reductases (b), and the BSO-reductases (c). The DMSO-reductases of the γ-proteobacteria (d), *M tuberculosis*, and the transhydroxylase (e) form the lower group. Most of the ancient gene duplications occurred at least basal within the proteobacteria and are

limited to the upper half of the tree of this subfamily (Figure 3.26). The BSOR is by far the most diverse group and contains for example enzymes from α, γ, and ε proteobacteria. The enzymes of this subfamily mostly prefer one substrate, but it was shown that e.g. *Rhodobacter* DMSOR and BSOR are able to use a variety of S- and N-oxides (Satoh and Kurihara, 1987; Pollock and Barber, 1997). Johnson and Rajagopalan (2001) showed that these functions are linked by a tyrosine, binding to the molybdopterin active site (Chapter 4.5.3).

The original enzyme of the DMSOR subfamily was presumably a DMSOR because enzymes from both, completely independent, groups are showing DMSOR activity. Although the transhydroxylase is the most basal member of the DMSO-reductases of the γ–proteobacteria it perhaps still maintains DMSO-reductase activity. Brune (1990) observed dimethylsulfide production when transhydroxylase was incubated with pyrogallol and DMSO (chapter 4.5.2.).

It is interesting that the γ-proteobacteria, especially *E. coli*, have an amazing number of proteins with similar function. *E. coli* for example possesses at least seven different DMSO-reductases plus three different BSO-reductases.

4.5. Towards the reaction mechanisms of acetylene hydratase and transhydroxylase

4.5.1. Acetylene hydratase

Acetylene hydratase has to be activated by a strong reductant such as titanium(III) citrate or dithionite to achieve full activity (Figure 1.6). Under these conditions, the ferredoxin-type iron-sulfur center is in its reduced state ($[4Fe\text{-}4S]^{+}$) and the tungsten center is in the tetravalent oxidation state as documented by EPR spectra (Meckenstock *et al.*, 1999). Oxic preparations of acetylene hydratase possess a [3Fe-4S] cluster but exhibit similar specific enzyme activity by comparison with the anoxic preparation, carrying the intact [4Fe-4S] cluster (Meckenstock *et al.*, 1999). Redox titrations of the iron-sulfur center and of the enzyme activity gave potentials of –410 mV and –340 mV, respectively (Figure 1.6). Thus, acetylene hydratase is active when the iron sulfur center is still oxidized in the $[4Fe\text{-}4S]^{2+}$ state. Setting the potential to ≤ –410 mV brought the iron sulfur center to the $[4Fe\text{-}4S]^{+}$ state but did not change the activity of the enzyme. Model studies demonstrated the likely participation of a W(IV) site in the catalysis of the hydration of acetylene, whereas the corresponding W(VI) remained inactive (Figure 4.4; Yadav *et al.*, 1997).

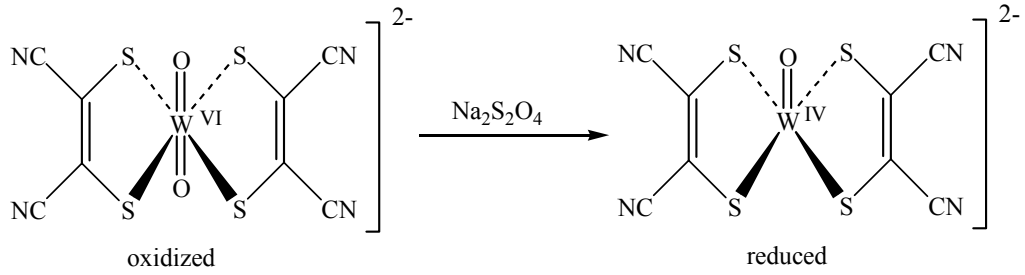

Figure 4.4 Reduction of $[Et_4N]_2[W^{VI}O_2(mnt)_2]$ (Yadav *et al.*, 1997).
mnt = 1,2-dicyanoethylenedithiolate

In addition to the classical Hg(II)/H^+-catalyzed Markownikoff hydration of alkynes (Figure 4.5 A), numerous transition metal catalysts have been developed in recent years for the synthesis of ketones via hydration of alkynes, including the anti-Markownikoff hydration of terminal alkynes catalyzed by a Ru(II)/phosphane mixture (Tokunaga and Wakatsuki, 1998). Figure 4.5 B shows an addition/elimination process of acetylene hydration according to Tokunaga and Wakatsuki's Ruthenium catalyzed hydration. Figure 4.5 C shows a vinyl-tungsten intermediate that could undergo a direct OH insertion to vinylalcohol and hence acetaldehyde.

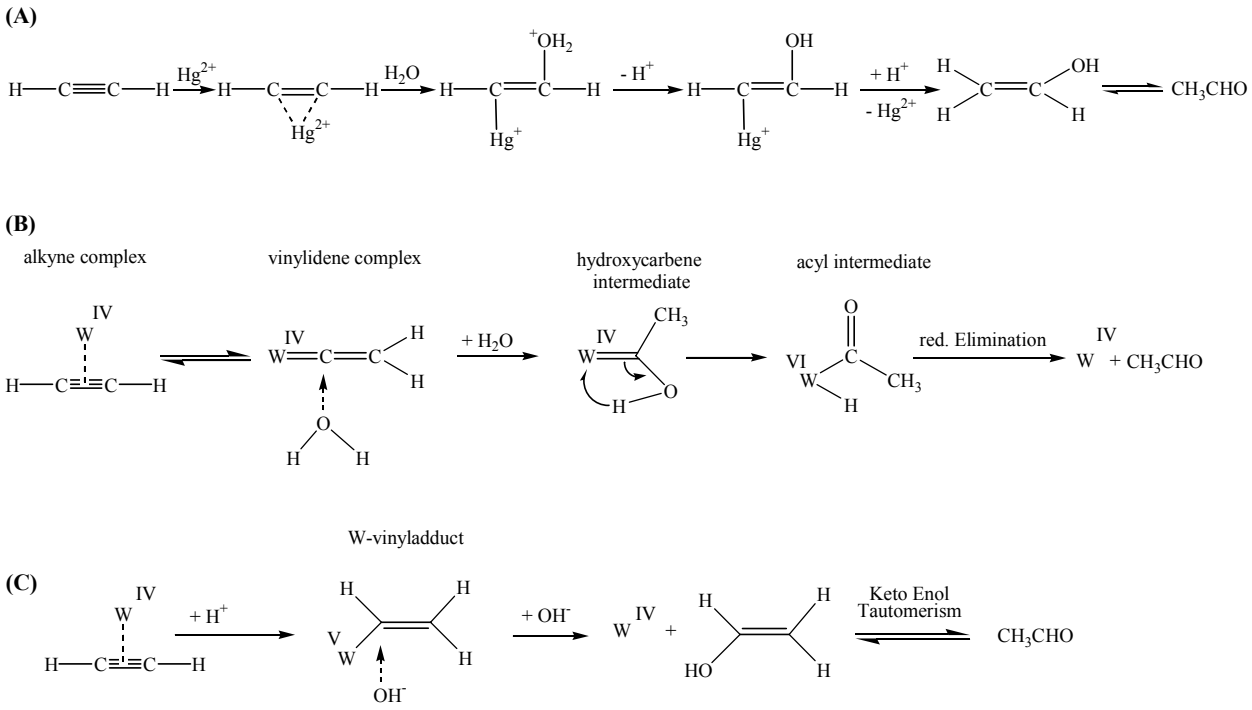

Figure 4.5 Possible reaction mechanisms of acetylene hydratase.
(A) Hg^{2+} catalyzed addition of water to alkynes (March, 1992).
(B) A putative mechanism, deduced from the anti-markownikoff hydration of terminal alkynes, catalyzed by a Ru(II)/phosphane mixture (Tokunaga and Wakatsuki, 1998).
(C) Vinyl intermediate-hydration of acetylene (B.T. Golding, personal comm.).

4.5.2. Transhydroxylase

Understanding the transhydroxylase reaction, converting pyrogallol to phloroglucinol, represents a chemical challenge. It was shown that 1,2,3,5-tetrahydroxybenzene was required in cell-free extracts at stoichiometric amounts to make the reaction run (Brune and Schink, 1990). When partially enriched transhydroxylase enzyme fractions were incubated with pyrogallol in the absence of tetrahydroxybenzene neither conversion of pyrogallol to phloroglucinol nor formation of tetrahydroxybenzene was detected in the standard assay of Brune and Schink (1990).

Reichenbecher and Schink (1999) showed a complete conversion of pyrogallol to phloroglucinol when the amount of enzyme was drastically increased and the pyrogallol concentration was decreased in the assay. Note that formation of tetrahydroxybenzene was not observed during the experiment. In one experiment of Reichenbecher and Schink (1999) as little as 0.7 µM (≈ 0.18 nmol) pyrogallol were incubated with 0.13 mg (≈ 1 nmol transhydroxylase) enriched enzyme preparation in a final volume of 0.25 ml. This was the only experiment in which formation of tetrahydroxybenzene was observed. Reichenbecher and Schink (1999) showed by an experiment in $^{18}OH_2$ that the pyrogallol-phloroglucinol transhydroxylase of *P. acidigallici* transfers hydroxyl substituents only between organic carriers. There was no exchange with free water. With this, the transhydroxylase differs from all other moco containing enzymes that catalyze hydroxylations by oxygen transfer between water and an organic substrate (Schultz *et al.*, 1995; Kisker *et al.*, 1997)

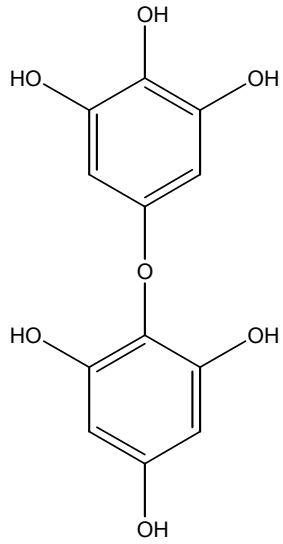

3,4,5,2',4',6'-Hexahydroxydiphenylether

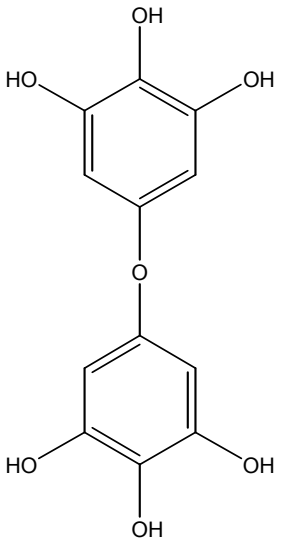

3,4,5,3',4',5'-Hexahydroxydiphenylether

Figure 4.6 Structure of two hexahydroxydiphenylethers (Hille *et al.*, 1999)

One putative mechanism (suggested by Hille *et al.*, 1999), a cyclic oxidation/reduction mechanism with the formation of two hexahydroxydiphenylethers (Figure 4.6) as intermediates, is depicted in figure 4.7. In the laboratory of J. Rétey (Universität Karlsruhe, Germany) the pure diphenylethers were synthesized and characterized (Hille *et al.*, 1999). In the presence of 3,4,5,2',4',6'-Hexahydroxydiphenylether and absence of tetrahydroxybenzene pure transhydroxylase catalyzed the conversion of pyrogallol into three new compounds. One of these compounds was phloroglucinol, the second one was not identified but it was formed only in the presence of transhydroxylase. The third one was not identified, it was formed non-enzymatically

and is probably an oxidation product of the 3,4,5,2',4',6'-Hexa-hydroxydiphenylether. When transhydroxylase was reduced with dithionite or glutathione and incubated with the hexahydroxydiphenylethers and pyrogallol, a slow conversion of pyrogallol into phloroglucinol was observed in the first three hours and overnight (18 h) the conversion was complete. A small, but significant, amount of tetrahydroxybenzene was formed during the reaction with a concomitant decrease of the used diphenylether (for details see Hille *et al.*, 1999). These results show that the diphenylethers interact with transhydroxylase and therefore can serve as donors of the hydroxyl group, but the slow conversion rate and the formation of free tetrahydroxybenzene render a possible function of the diphenylethers as intermediates questionable (Hille *et al.*, 1999).

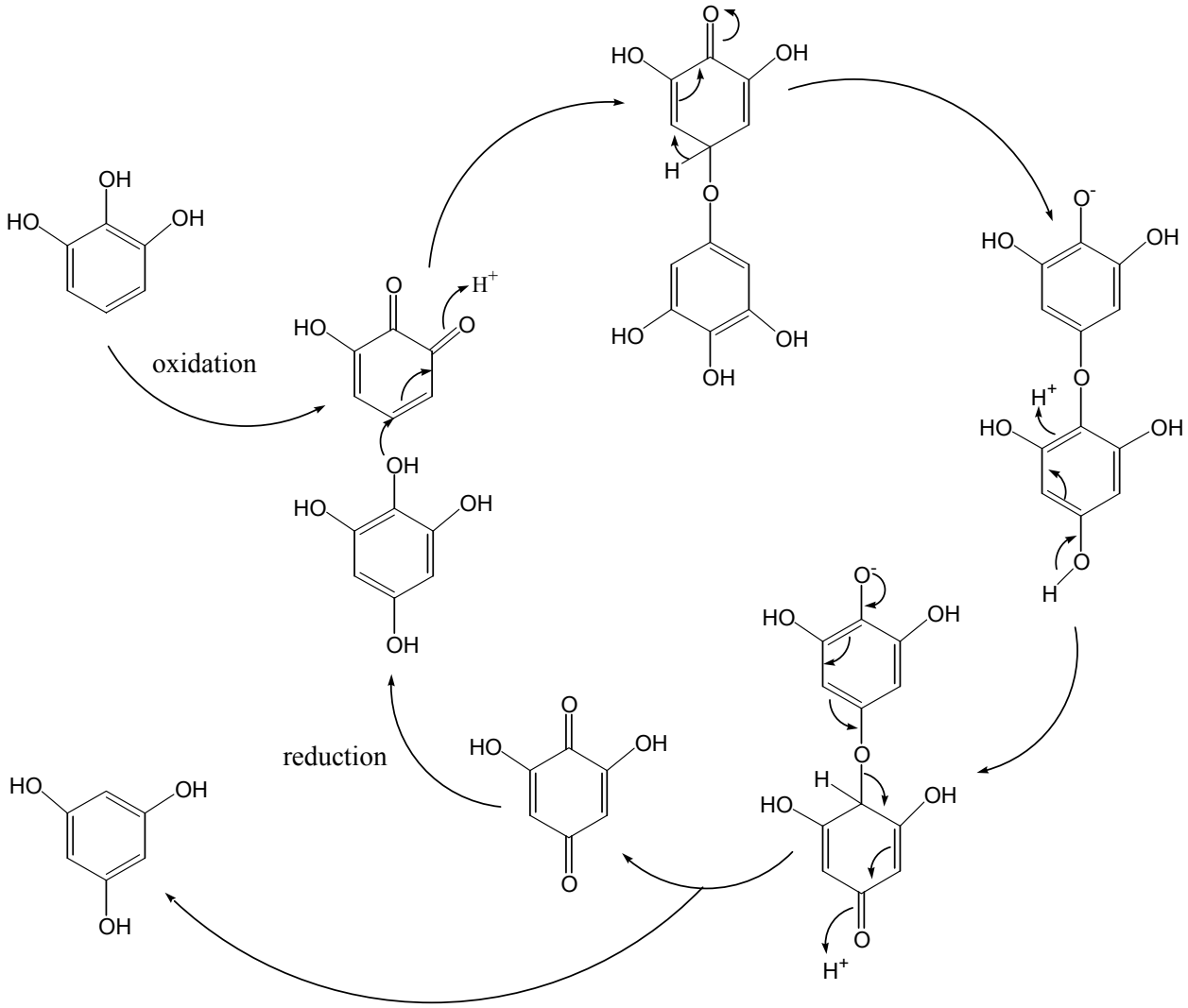

Figure 4.7 Putative mechanism for the pyrogallol-phloroglucinol conversion of trans-hydroxylase through a diphenylether intermediate (Hille *et al.*, 1999).

Widely accepted is the role of the molybdenum center of enzymes as an acceptor or donor of hydroxyl or oxo groups (Hille *et al.*, 1999). The reaction mechanism depicted in Figure 4.7 is also in conflict with this role. Two other mechanisms, implying the hydroxyl-donor/acceptor role of a molybdenum center, were suggested by Hille *et al.* (1999). In both mechanisms tetrahydroxybenzene is an intermediate that has to turn 180° during the reaction.

In the first mechanism a Mo(VI)-oxo group reacts by electrophilic substitution with the position 5 of pyrogallol, forming a tetrahydroxybenzene-Mo(VI) ether (Figure 4.8). The oxygen-Mo bond is cleaved and one molecule tetrahydroxybenzene is formed. The tetrahydroxybenzene undergoes a 180° turn and an oxidation to a para-quinone whereas the Mo(VI) center is reduced to a Mo(IV) center. In the following steps the Mo(IV) binds to the keto-group at position 2 of the ortho-quinone and a Mo(VI)-oxo is cleaved whereas the product phloroglucinol is formed.

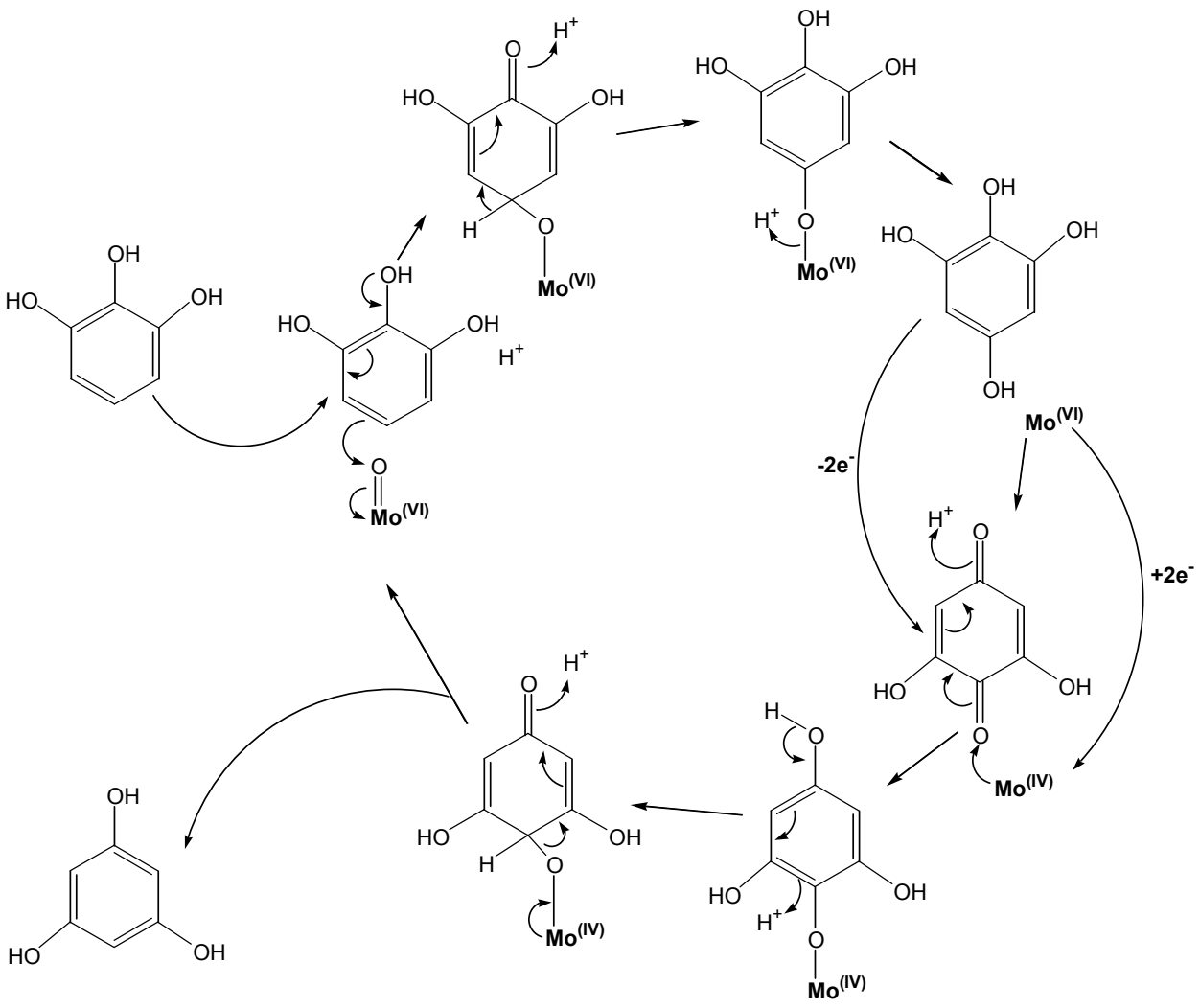

Figure 4.8 Putative mechanism for the transhydroxylase reaction via 'Umpolung' of the hydroxyl group by the molybdenum cofactor (Hille *et al.*, 1999).

In the second mechanism the substrate pyrogallol is oxidized to an ortho-quinone that is attacked by a nucleophilic Mo(IV)-OH center (Figure 4.9). One molecule tetrahydroxybenzene is formed that undergoes a 180° turn at the active site and reacts with the molybdenum center in a reverse way as described in the first half of the cycle (Hille *et al.*, 1999).

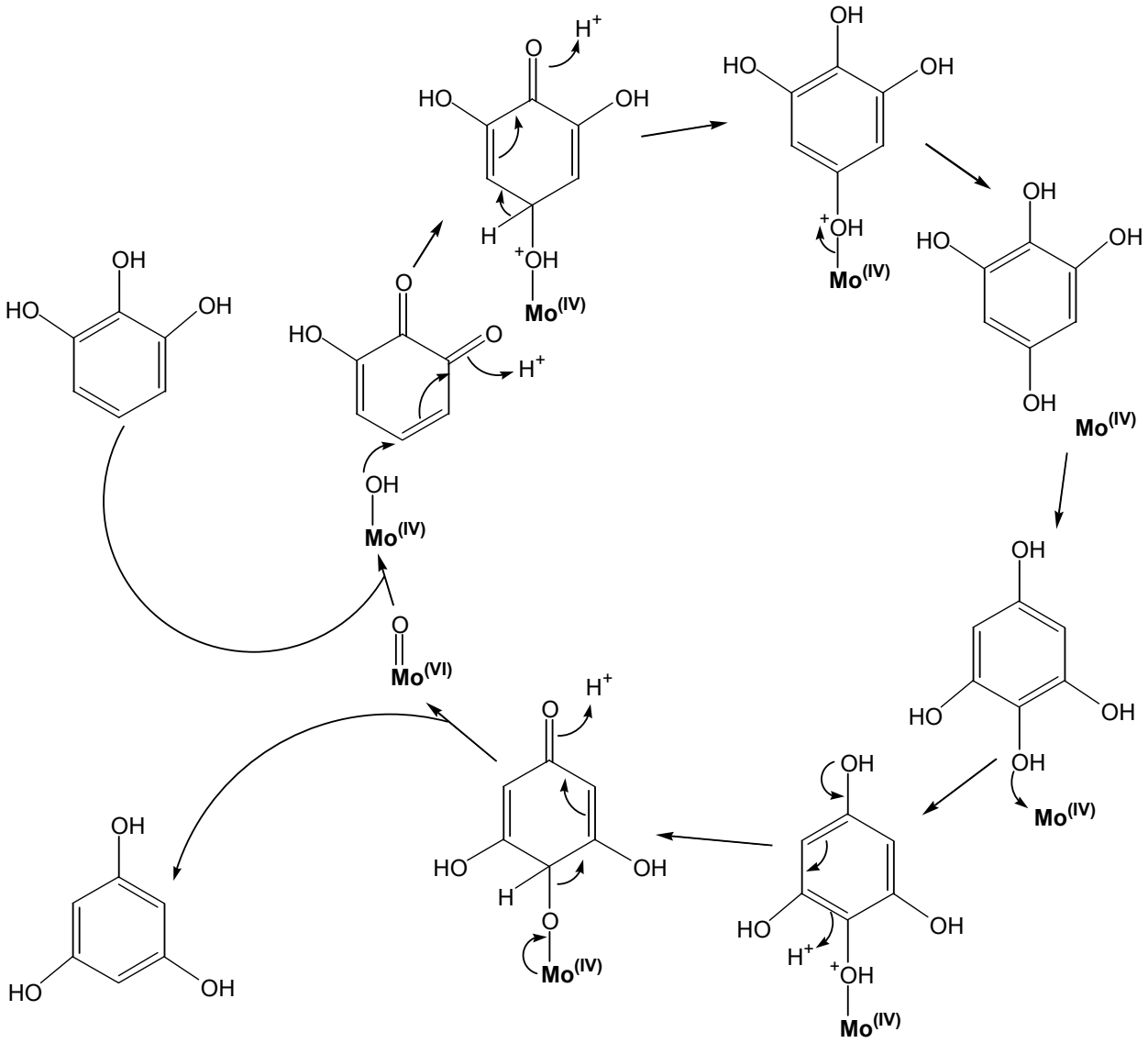

Figure 4.9 Putative mechanism for the transhydroxylase reaction via 'Umpolung' of the substrate by oxidation to an ortho-quinone and nucleophilic hydroxylation by a molybdenum-coordinated OH group (Hille *et al.*, 1999).

Though tetrahydroxybenzene is a potential intermediate in the last two mechanisms, it is not obvious why it is needed to start the reaction. One explanation is that the turning of tetrahydroxybenzene is only possible by a dissociation/reassociation process. After release from the enzyme it may compete with pyrogallol or phloroglucinol for the active site (Hille *et al.*, 1999). Consequently, a low intracellular pool of tetrahydroxybenzene originates that is hard to detect. This leads to inactive transhydroxylase, which has to be reactivated. About 10% of the

cell protein is transhydroxylase (Reichenbecher and Schink, 1999). This appears reasonable if (i) the transhydroxylating process is the rate-limiting step in the degradation of gallic acid, or (ii) transhydroxylase is inactivated by tetrahydroxybenzene formed in the reaction. The extreme substrate inhibition of transhydroxylase (Reichenbecher and Schink, 1999) can be a consequence of the in-activation of transhydroxylase by tetrahydroxybenzene being formed during the reaction. The specific activity under *in vitro* conditions can only be maximized by addition of equal amounts of pyrogallol and tetrahydroxybenzene (Brune and Schink, 1990) and running the reaction in a cycle with reactivation of the inhibited transhydroxylase by dehydroxylation of tetrahydroxybenzene. Reichenbecher and Schink (1999) demonstrated the formation of tetrahydroxybenzene when small amounts of pyrogallol and transhydroxylase were incubated without addition of tetrahydroxybenzene. In this experiment the molar transhydroxylase : pyrogallol ratio was about five. Brune (1990) observed dimethyl-sulfide production during incubation of transhydroxylase with pyrogallol and DMSO. He postulated that the effect of DMSO originates from an oxidative production of tetrahydroxy-benzene from pyrogallol. Because transhydroxylase belongs to the group of the DMSO-reductases (Figures 3.25, 3.26; Chapter 4.4), it is possible that transhydroxylase has a DMSO-reductase activity. The proposed mechanism of *R. sphaeroides* DMSOR (Garton *et al.*, 1997) suggests a Mo(IV) site that binds DMSO and that is oxidized to a Mo(VI)-oxo site during catalytic turnover. According to this mechanism transhydroxylase in the inactivated Mo(IV) state converts DMSO to dimethylsulfide and reactivates itself to the Mo(VI)-oxo species that is able to hydroxylate pyrogallol. Therefore, tetrahydroxybenzene is not formed by a direct reaction of DMSO and pyrogallol but can be formed after reactivation of transhydroxylase by DMSO.
If this interpretation is correct, then there is no need for an anaplerotic reaction to synthesize tetrahydroxybenzene de novo during growth as postulated by Hille *et al.* (1999). This hypothesis can be checked if transhydroxylase is incubated with pyrogallol and ^{18}O-marked DMSO. The ^{18}O should be found in the product phloroglucinol and in released tetrahydroxy-benzene. A control experiment incubating pyrogallol and DMSO under the same conditions will show that there is no oxidation of pyrogallol by DMSO.

This new reaction mechanism is summarized in figure 4.10. Activated transhydroxylase contains a Mo^{VI}-oxo species that can react with pyrogallol forming a molecule tetrahydroxybenzene and an inactivated transhydroxylase Mo^{IV} species. Tetrahydroxybenzene is released from the enzyme and reintegrated after a turn of 180°. Enzymatic cleavage of the hydroxyl group in position two of the tetrahydroxybenzene leads to the reactivation of transhydroxylase by forming the Mo^{VI}-oxo species and to a molecule of phloroglucinol. Because transhydroxylase is a putative DMSO-

reductase, it can be reactivated by reducing a molecule DMSO to dimethylsulfide (DMS) according to the proposed reaction mechanism of *R. sphaeroides* DMSO-reductase (Garton *et al.*, 1997). The involvement of the small subunit carrying the iron-sulfur clusters remains unclear.

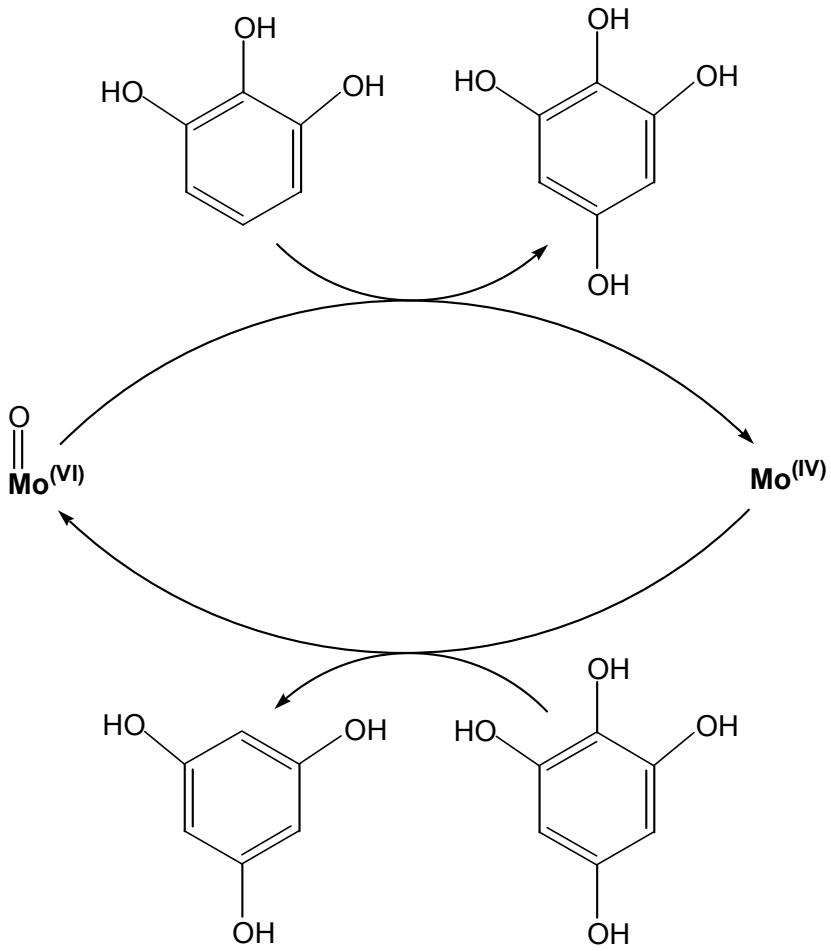

Figure 4.10 Proposed model for the conversion of pyrogallol to phloroglucinol by *P. acidigallici* transhydroxylase.

4.5.3. Is there a tyrosine at the active site?

The three dimensional structure of enzymes of the DMSO-reductase subfamily (Schneider *et al.*, 1996; Schindelin *et al.*, 1996; McAlpine *et al.*, 1997; Czjzek *et al.*, 1998; McAlpine *et al.*, 1998; Stewart *et al.*, 2000; Hung-Kei *et al.*, 2000) has generated interest in the role of a tyrosine during catalytic turnover of DMSO, TMAO, and BSO (Johnson and Rajagopalan, 2001). *R. sphaeroides* and *R. capsulatus* DMSOR are able to utilize a great variety of substrates including trimethylamine-N-oxide and dimethyl sulfoxide (Satoh and Kurihara, 1987). *R. sphaeroides* BSOR has been shown to use a variety of S- and N-oxides (Pollock and Barber, 1997). *E. coli*

and *S. massilia* TMAOR functions as the final enzyme in the anaerobic electron pathway and utilizes trimethylamine-N-oxide as terminal electron acceptor. Kinetic analyses of Iobbi-Nivol *et al.* (1996) have shown that *E. coli* TMAOR does not efficiently reduce S-oxides.

It has been postulated that the substrate specificity of the enzymes corresponds to a tyrosine near the active site (Czjzek *et al.*, 1998; Buc *et al.*, 1999). The DMSO-reductases and the BSO-reductases should have this residue whereas the TMAO-reductases do lack this tyrosine. Johnson and Rajagopalan (2001) showed, by site-directed mutagenesis, that insertion of a tyrosine in *E. coli* TMAOR results in a decreased preference for trimethylamine-N-oxide relative to dimethyl sulfoxide. Mutation or deletion of the tyrosine in recombinant *Rhodobacter* DMSOR results in a decreased specificity for S-oxides and an increased specificity for trimethylamine-N-oxide.

In chapter 3.3 the results of a phylogenetic analysis of DMSOR related enzymes were given. According to this analysis the DMSOR subfamily splits into five groups (Figure 3.26).

Figure 4.11 shows an alignment of selected members of the DMSOR subfamily. The *Rhodobacter* DMSOR group and the DMSO-reductases of the γ-proteobacteria as well as the BSO-reductases contain a residue equivalent to this tyrosine. The TMAO-reductases lack this tyrosine or have another amino acid at this position. Acetylene hydratase, as a member of another subfamily, does not fit into this alignment.

The enzymes of *S. putrefaciens* (CAA06794), *E. coli* (AAA23522), *M. tuberculosis* (E70916), *P. multocida* (AAK03838), and *P. acidigallici* (CAB50913) do not fit into this scheme although they belong to the DMSO-reductase subfamily. The alignment in the selected region is rather poor. It remains unclear if other residues can act in place of the tyrosine.

Not only tyrosine influences the substrate specificity. Buc *et al.* (1999) showed that a tungsten-substituted TMAOR (W-TorA) of *E. coli* could reduce a number of N-oxides as well as S-oxides. The corresponding Mo-TMAOR (Mo-TorA) is only able to reduce the N-oxides. The authors conclude that not only the tyrosine (Tyr-114) is a determining factor for the substrate specificity of TMAO-reductases and DMSO-reductases. In addition, the low potential and altered co-ordination situation in the case of W-TorA could circumvent the dependence on the tyrosine residue and would allow W-TorA to use DMSO as a substrate.

These questions should be checked by structural analysis of the enzymes from *S. putrefaciens*, *E. coli*, *M. tuberculosis*, *P. multocida*, *P. acidigallici* (transhydroxylase), and the *E. coli* W-TorA.

R. sphaeroides@Q57366	YGPTGTFGGS**Y**G-WKSPGRLHNCQ- 168	*Rhodobacter* DMSO reductases
R. sphaeroides@AAB94874	YGPTGTFGGS**Y**G-WKNPGRLHNCQ- 143	
R. capsulatus@3318672	YGPQGVFGGS**Y**G-WKSPGRLHNCT- 126	
R. capsulatus@2981909	YGPSGVFGGS**Y**G-WKSPGRLHNCT- 168	
P. multocida@AAK03877	YGPSGLHAGQTG-WRATGQLHSST- 159	TMAO reductases
V. cholerae@G82168	YGPSGLHAGQTG-WRATGQLHSST- 159	
S. putrefaciens@CAA06794	YGPTGTFGGS**Y**G-WRSPGRLHNCQ- 159	
S. massilia@O87948	REFLEKGVNA-D-RSTRGNGDFVR- 150	
E. coli@P33225	HGPSALLTAS-G-WQSTGMFHNAS- 170	
V. cholerae@H82137	YGPASIFAGS**Y**G-WRSNGVLHKAS- 136	BSO reductases
E. coli@AAA23522	HGPSALLTAS-GGWQSTGMFHNAS- 109	
E. coli@AAG58700	YGPASIFAGS**Y**G-WRSNGVLHKAS- 89	
C. jejuni@G81444	NGPSAIFAGS**Y**G-WRSSGVLHKAQ- 162	
H. influenzae@P44798	HGSTGIFAGS**Y**G-WFSCGSLHASR- 166	
R. sphaeroides@P54934	HGSTGIFAGS**Y**G-WFSCGSLHASR- 111	
H. pylori@G64570	KGASAIFGGS**Y**G-WKSSGNMQNSR- 152	
H. pylori@H71865	N----IFNAS**Y**GGWGHAGSLHRCN- 148	
M. tuberculosis@E70916	-PDRLKYPMKRVGKRGEGKFERIS- 103	DMSO-reductases of the γ-proteobacteria
P. multocida@AAK03838	DPDRLKYPMKRVGKRGEGKFERIS- 200	
H. influenzae@P45004	YGNEAVHVL-**Y**GTGVDGGNITNSN- 166	
Y. pestis@AAD37319	YGNEAVHVL-**Y**GTGVDGGNITNSN- 181	
E. coli@F64914	YGNEAVHVL-**Y**GTGVDGGNITNSN- 176	
E. coli@AAG56575	YGNESIYLN-**Y**GTGTLGGTMTRSW- 176	
E. coli@BAB34402	YGNEAVYIQ-**Y**SSGIVGGNITRSSP 143	
E. coli@P77374	YGNESIYLN-**Y**GTGTLGGTMTRSWP 174	
E. coli@E64914	YGNEAVYIQ-**Y**SSGIVGGNMTRSSP 173	
E. coli@P18775	YGNESIYLN-**Y**GTGTLGGTMTRSWP 181	
E. coli@AAG57632	YGNESIYLN-**Y**GTGTLGGTMTKSWP 113	
P. acidigallici@CAB50913	YGPSAILSTPSSHHMWGNVGYRHS- 155	Transhydroxylase

Figure 4.11 Partial sequence alignment of the members of the DMSO-reductase subfamily (Figures 3.25, 3.26). The highlighted Tyr (Tyr-156 in the *R. sphaeroides* alignment) is equivalent to the Tyr-114 of Johnson and Rajagopalan (2001) because the DMSOR-precursor protein was used in this alignment.

5. References

Achenbach-Richter L., Gupta R., Stetter K. O. and Woese C. R. (1987). Were the original eubacteria thermophiles? *Syst. Appl. Microbiol.*, **9**, 34 – 39

Adachi J. and Hasegawa M. (1996). MOLPHY version 2.3: programs for molecular phylogenetics based on maximum likelihood. *Comp. Sci. Monogr.*, **28**, 1 – 150

Appel R.D., Bairoch A. and Hochstrasser D.F. (1994). A new generation of information retrieval tools for biologists: the example of the ExPASy WWW server. *Trends Biochem. Sci.,* **19**, 258 – 260

Baas D. and Rétey J. (1999). Cloning, sequencing and heterologous expression of pyrogallol-phloroglucinol transhydroxylase from *Pelobacter acidigallici*. *Eur. J. Biochem.*, **265**, 896 – 901

Baker W., Nodzu R. and Robinson R. (1929). The Synthesis of Gossypetin and of Quercetagetin. *J. chem. soc*. 1929*,* 74 – 84

Baxter R.A. and Brown J.P. (1967). Preparation of 1,2,3,5-tetrahydroxybenzene. *Chem. Ind*., **27**, 1171

Baxter R.A., Ramage G.R. and Timson J.A. (1949). The Synthesis of Khellin. *J. chem.. soc.* 1949 (V)*,* S30 - S33

Beinert H., Holm R. H. and Münck E. (1997). Iron-sulfur clusters: nature's modular, multipurpose structures. *Science*, **277**, 653 – 659

Beinert H., Orme-Johnson W.H. and Palmer G. (1978). Special techniques for the Preparation of samples for low-temperature EPR spectroscopy. *Methods Enzymol*., **54**, 111 – 132

Bertram P.A., Schmitz R.A., Linder D. and Thauer R.K. (1994). Tungstate can substitute for molybdate in sustaining the growth of *Methanobacterium thermoautotrophicum*; Identification and characterization of a tungsten isoenzyme of formylmethanofuran dehydrogenase. *Arch. Microbiol.*, **161,** 220 – 228

Brinkmann H. and Philippe H. (1999). Archaea sister group of Bacteria? Indications from tree reconstruction artifacts in ancient phylogenies. *Mol. Biol. Evol.*, **16**, 817 – 825

Brune A. (1990). Der anaerobe Abbau von Trihydroxybenzolen. Dissertation, Universität Tübingen

Brune A. and Schink B. (1990). Pyrogallol-to-Phloroglucinol Conversion and Other Hydroxyl-Transfer Reactions Catalyzed by Cell Extracts of *Pelobacter acidigallici*. *J. Bacteriol.*, **172**, 1070 – 1076

Brune A. and Schink B. (1992). Phloroglucinol pathway in the strictly anaerobic *Pelobacter acidigallici*: fermentation of trihydroxybenzenes to acetate via triacetic acid. *Arch. Microbiol.*, **157**, 417 – 424

Brune A., Schnell S. and Schink B. (1992). Sequential Transhydroxylations Converting Hydroxyhydroquinone to Phloroglucinol in the Strictly Anaerobic, Fermentative Bacterium *Pelobacter massiliensis*. *Appl. Environ. Microbiol.*, **58**, 1861 – 1868

Buc J., Santini C.L., Giordani R., Czjzek M., Wu L.F. and Giordano G. (1999). Enzymatic and physiological properties of the tungsten-substituted molybdenum TMAO reductase from *Escherichia coli*. *Mol. Microbiol.*, **32**, 159 – 68

Bullock W.O., Fernandez J.M. and Short J.M. (1987). XL1-Blue: A high efficiency plasmid transforming *recA - E. coli* strain with ß-galactosidase selection. *Bio-Techniques,* **5**, 376

Cammack R. (1992). Iron-sulfur clusters in enzymes: themes and variations. *Adv. Inorg. Chem.*, **38**, 281 – 322

Cammack R. and Weiner J.H. (1990). Electron paramagnetic resonance spectroscopic characterization of dimethyl sulfoxide reductase of *Escherichia coli*. *Biochemistry*, **29**, 8410 – 8416

Cammack R., Patil D. S. and Fernandez V. M. (1985). Electron-spin-resonance/electron-paramagnetic-resonance spectroscopy of iron-sulphur enzymes. *Biochem. Soc. Trans.*, **13**, 572 – 578

Carter Jr., C.W. and Carter C.W. (1979). Protein crystallization using incomplete factorial experiments. *J. Biol. Chem.,* **254**, 12219 – 12223

Chan M.K., Mukund S., Kletzin A., Adams M.W.W. and Rees D.C. (1995). Structure of a hyperthermophilic tungstopterin enzyme, aldehyde ferredoxin oxidoreductase. *Science*, **267**, 1463 – 1469

Czjzek M., Dos Santos J.P., Pommier J., Giordano G., Mejean V. and Haser R. (1998). Crystal structure of oxidized trimethylamine N-oxide reductase from *Shewanella massilia* at 2.5 A resolution. *J. Mol. Biol.*, **284**, 435 – 447

De Renzo E.C., Kaleita E., Heytler P.G., Oleson J.J., Hutchings B.L. and Williams J.H. (1953). Identification of the xanthin oxidase factor as molybdenum. *Arch. Biochem. Biophys.*, **45**, 247 – 253

Diemann E. and Müller A. (1973). Thio and seleno compounds of the transition metals with the d^0 configuration. *Coord. Chem. Rev.*, **10**, 79 – 122

Dobbek H. and Huber R., in "Molybdenum and Tungsten. Their Roles in Biological Processes", Vol. 39 of 'Metal Ions in Biological Systems', A. Sigel and H. Sigel, eds.; M. Dekker Inc., New York, 2002, in press.

Eady R.R. (1996). Structure-Function Relationships of Alternative Nitrogenases. *Chem. Rev.*, **96**, 3013 – 3030

Ellis P.J., Conrads T., Hille R. and Kuhn P. (2001). Crystal Structure of the 100 kDa Arsenite Oxidase from *Alcaligenes faecalis* in two Crystal Forms at 1.64 Å and 2.03 Å. *Structure*, **9**, 125 – 132

Evans W.C. (1977). Biochemistry of the bacterial catabolism of aromatic compounds in anaerobic environments.. *Nature*, **270**, 17 – 22

Flint D.H. and Allen R.M. (1996). Iron-sulfur proteins with non redox functions. *Chem. Rev.,* **96**, 2315 – 2334

Forterre P. and Philippe H. (1999). Where is the root of the universal tree of life? *Bioessays*, **21**, 871 – 879

Foster J.F. and Sterman M.D. (1956). Conformation changes in bovine plasma albumin associated with hydrogen ion and urea binding. II. Hydrogen ion titration curves. *J. Am. Chem. Soc.*, **78**, 3656 – 3660

Fritz G., Büchert T., Huber H., Stetter K.O. and Kroneck P.M.H. (2000). Adenylylsulfate reductases from archaea and bacteria are 1:1 alphabeta-heterodimeric iron-sulfur flavoenzymes--high similarity of molecular properties emphasizes their central role in sulfur metabolism. *FEBS Lett.*, **473**, 63 – 66

Garton S.D., Hilton J.C., Oku H., Crouse B.R., Rajagopalan K.V. and Johnson M.K. (1997). Active Site Structures and Catalytic Mechanism of *Rhodobacter sphaeroides* Dimethyl Sulfoxide Reductase as Revealed by Resonance Raman Spectroscopy. *J. Am. Chem. Soc.*, **119**, 12906 – 12916

Goa J. (1994). A micro-biuret method for protein determination: determination of total protein in cerebrospinal fluid. *Scand. J. Clin. Lab. Invest*., **5**, 219 – 222

Gogarten J.P., Kibak H., Dittrich P., Taiz L., Bowman E.J., Bowman B.J., Manolson M.F., Poole R.J., Date T., Oshima T., Konishi, J., Denda, K. and Yoshida, M. (1989). Evolution of the vacuolar H^+-ATPase: implications for the origin of eukaryotes. *Proc. Natl. Acad. Sci. U.S.A*., **86**, 6661 – 6665

Greenwood N.N. and Earnshaw A. (1990). Chemie der Elemente, 1. korr. Auflage, VCH Verlagsgesellschaft mbH, Weinheim

Grunden A.M., Self W.T., Villain M., Blalock J.E. and Shanmugam K.T. (1999). An analysis of the binding of repressor protein ModE to modABCD (molybdate transport) operator/promoter DNA of *Escherichia coli*. *J. Biol. Chem.*, **274**, 24308 – 24315

Hagen W.R. and Arendson A.F. (1998). The bio-inorganic chemistry of tungsten. *Struct. Bonding*, **90**, 161 – 192

Hanahan D. (1983). Studies on transformation of *Escherichia coli* with plasmid. *J. Mol. Biol.,* **166**, 557 – 580

Heukeshoven J. and Dernick R. (1985). Simplified method for silver staining of proteins in polyacrylamide gels and mechanism of silver staining. *Electrophoresis*, **6**, 103 – 112

Hille R. (1996). The Mononuclear Molybdenum Enzymes. *Chem. Rev.*, **96**, 2757 –2816

Hille R. (1999). Molybdenum enzymes, In: Essays in Biochemistry **34** (Ballou D.P., Ed.) pp 125 – 137

Hille R. (2000). Molybdenum enzymes. *Subcell. Biochem.*, **35**, 445 – 485

Hille R., Rétey J., Bartlewski-Hof U., Reichenbecher R. and Schink B. (1999). Mechanistic aspects of molybdenum containing enzymes. *FEMS Microbiol. Rev.*, **22**, 489 – 501

Hung-Kei L., Temple C.A., Rajagopalan K.V. and Schindelin H. (2000). The 1.3 Å Crystal Structure of *Rhodobacter sphaeroides* Dimethyl Sulfoxide Reductase Reveals Two Distinct Molybdenum Coordination Environments. *J. Am. Chem. Soc.*, **122**, 7673 –7680

Imperial J., Hadi M. and Amy N.K. (1998). Molybdate binding by ModA, the periplasmic component of the *Escherichia coli* mod molybdate transport system. *Biochim. Biophys. Acta.*, **1370**, 337 – 346

Innis M.A., Myambo K.B., Gelfand D.H. and Brow M.A.D. (1988). DNA sequencing with *Thermus aquaticus* DNA polymerase and direct sequencing of polymerase chain reaction-amplified DNA. *Proc. Nat. Acad. Sci. USA,* **85**, 9436 – 9440

Inoue H., Nojima H. and Okayama H. (1990). High efficiency transformation of *Escherichia coli* with plasmids. *Gene*, **96**, 23 – 28

Iobbi-Nivol C., Pommier J., Simala-Grant J., Mejean V. and Giordano G. (1996). High substrate specificity and induction characteristics of trimethylamine-N-oxide reductase of *Escherichia coli*. *Biochim. Biophys. Acta*, **1294**, 77 – 82

Iwabe N., Kuma K., Hasegawa M., Osawa S. and Miyata T. (1989). Evolutionary relationship of archaebacteria, eubacteria, and eukaryotes inferred from phylogenetic trees of duplicated genes. *Proc. Natl. Acad. Sci. U.S.A.*, **86**, 9355 – 9359

Jancarik J. and Kim S.-H. (1991). Sparse matrix sampling: a screening method for crystallization of proteins. *J. Appl. Cryst*., **24**, 409 – 411

Johnson J.L., Rajagopalan K.V., Mukund S. and Adams M.W.W. (1993). Identification of molybdopterin as the organic component of the tungsten cofactor in four enzymes from hyperthermophilic Archaea. *J. Biol. Chem*., **268**, 4848 – 4852

Johnson K.E. and Rajagopalan K.V. (2001). An Active Site Tyrosine Influences the Ability of the Dimethyl Sulfoxide Reductase Family of Molybdopterin Enzymes to Reduce *S*-oxides. *J. Biol. Chem.*, **276**, 13178 – 13185

Johnson M., Rees D.C. and Adams M.W.W. (1996). Tungstoenzymes. *Chem. Rev.*, **96**, 2817 – 2839

Johnson M.K. (1994). Iron-sulfur proteins, in Encyclopedia of Inorganic Chemistry. (King B., Ed.), pp. 1896 – 1915, John Wiley & Sons, Chichester

Kemper M.A., Gao-Sheridan H.S., Shen B., Duff J.L., Tilley G.J., Armstrong F.A. and Burgess B.K. (1998). Delta T 14/Delta D 15 *Azotobacter vinelandii* ferredoxin I: creation of a new CysXXCysXXCys motif that ligates a [4Fe-4S] cluster. *Biochemistry*, **37**, 12829 – 12837

Kisker C., Schindelin H. and Rees D.C. (1997). Molybdenum-cofactor-containing enzymes: structure and mechanism. *Annu. Rev. Biochem.*, **66,** 233 – 267

Kisker C., Schindelin H., Baas D., Rétey J., Meckenstock R.U. and Kroneck P.M.H. (1999). A structural comparison of molybdenum cofactor-containing enzymes. *FEMS Microbiol. Rev.*, **22**, 503 – 521

Kletzin A. and Adams M.W.W. (1996). Tungsten in biological systems. *FEMS Microbiol. Rev.*, **18**, 5 – 63

Krieger R. (1997). Biochemische und spektroskopische Untersuchungen zur Struktur und Funktion der Acetylenhydratase aus *Pelobacter Acetylenicus* und der Transhydroxylase aus *Pelobacter Acidigallici*. Diplomarbeit, Universität Konstanz

Krumholz L.R and Bryant M.P. (1988). Characterization of the pyrogallol-phloroglucinol isomerase of *Eubacterium oxidoreducens*. *J. Bacteriol.*, **170**, 2472 - 2479.

Kumar S., Tamura K. and Nei M. (1994). MEGA: Molecular Evolutionary Genetics Analysis software for microcomputers. *Comput. Appl. Biosci.*, **10**, 189 – 191

Laemmli U.K. (1970). Cleavage of structural proteins during the assembly of the head of bacteriophage T4. *Nature,* **227**, 680 – 685

Leartsakulpanich U., Antonkine M.L. and Ferry J.G. (2000). Site-specific mutational analysis of a novel cysteine motif proposed to ligate the 4Fe-4S cluster in the iron-sulfur flavoprotein of the thermophilic methanoarchaeon *Methanosarcina thermophila*. *J. Bacteriol*., **182,** 5309 – 5316

Maniatis T. Fritsch E.F. and Sambrook J. (1987). Molecular cloning: a laboratory manual. Cold Spring Harbor Press, Cold Spring Harbor, N.Y., USA

March J. (1992). Advanced organic chemistry: reactions, mechanisms, and structure, 4. ed., Wiley & Sons, New York

McAlpine A.S., McEwan A.G. and Bailey S. (1998) The high resolution crystal structure of DMSO reductase in complex with DMSO. *J. Mol. Biol.*, **275**, 613 – 623

McAlpine A.S., McEwan A.G., Shaw A.L. and Bailey S. (1997). Molybdenum active centre of DMSO reductase from *Rhodobacter capsulatus*: crystal structure of the oxidized enzyme at 1.82-Å resolution and the dithionite-reduced enzyme at 2.8-Å resolution. *J. Biol. Inorg. Chem.*, **2**, 690 – 701

McPherson A. (1982). Preparation and analysis of protein crystals. Wiley & Sons, New York

Meckenstock R.U., Krieger R., Ensign S., Kroneck P.M.H. and Schink B. (1999). Acetylene Hydratase of *Pelobacter acetylenicus*. Molecular and spectroscopic properties of the tungsten iron-sulfur enzyme. *Eur. J. Biochem*., **264**, 176 – 182

Nomenclature Committee of the International Union of Biochemistry (NC- IUB) (1985). Nomenclature for incompletely specified bases in nucleic acid sequences. Recommendations 1984. *Eur. J. Biochem.*, **150**, 1 – 5

Pace N.R. (1997). A molecular view of microbial diversity and the biosphere. *Science*, **276**, 734 – 740

Peck H.D. Jr., Deacon T.E. and Davidson J.T. (1965). Studies on adenosine 5'-phosphosulfate reductase from *Desulfovibrio desulfuricans* and *Thiobacillus thioparus*, *Biochim. Biophys. Acta*. **96**, 429 – 446

Philippe H. (1993). MUST, a computer package of Management Utilities for Sequences and Trees. *Nucleic Acids Res.*, **21,** 5264 – 5272

Philippe H. and Forterre P. (1999). The rooting of the universal tree of life is not reliable. *J. Mol. Evol.*, **49**, 509 –523

Pilato R.S. and Stiefel E.I. (1999). Molybdenum and Tungsten Enzymes. In: Bioinorganic Catalysis, Second Edition, Revised and Expanded (Reedijk J. and Bouwman E., Ed.) pp 81 – 152, Marcel Dekker Inc., New York

Pollock V.V. and Barber M.J. (1997). Biotin sulfoxide reductase. Heterologous expression and characterization of a functional molybdopterin guanine dinucleotide-containing enzyme. *J. Biol. Chem.*, **272**, 3355 – 3362

Raaijmakers H., Teixeira S., Dias J.M., Almendra M.J., Brondino C.D., Moura I., Moura J.J. and Romao M.J. (2001). Tungsten-containing formate dehydrogenase from *Desulfovibrio gigas*: metal identification and preliminary structural data by multi-wavelength crystallography. *J. Biol. Inorg. Chem.*, **6**, 398 – 404

Rabilloud T. (1990). Mechanism of protein silver staining in polyacrylamide gels: a ten year synthesis., Burgess Publishing Company, Minneapolis. USA

Ramadoss C.S. (1979). The Effect of Vanadium on Nitrate Reductase of *Chlorella vulgaris*. *Planta*, **146**, 539 – 544

Rees D.C., Hu Y., Kisker C. and Schindelin H. (1997). A crystallographic view of the molybdenum cofactor. *J. Chem. Soc., Dalton Trans.*, 3909 – 3914

Reichenbecher W. (1995), Die Transhydroxylase aus *Pelobacter acidigallici*, Dissertation, Universität Konstanz.

Reichenbecher W. and Schink B. (1999). Towards the reaction mechanism of pyrogallol-phloroglucinol transhydroxylase of *Pelobacter acidigallici*. *Biochim. Biophys. Acta*, **35843**, 1 – 9

Reichenbecher W., Brune A. and Schink B. (1994). Transhydroxylase of *Pelobacter acidigallici*: a molybdoenzyme catalyzing the conversion of pyrogallol to phloroglucinol. *Biochim. Biophys. Acta*, **1204**, 217 – 224

Reichenbecher W., Rüdiger A., Kroneck P.M.H. and Schink B. (1996). One molecule of molybdopterin guanine dinucleotide is associated with each subunit of the heterodimeric Mo-Fe-S protein transhydroxylase of *Pelobacter acidigallici* as determined by SDS/PAGE and mass spectrometry. *Eur. J. Biochem.*, **237**, 406 – 413

Robson R.L., Eady R.R., Richardson T.H., Miller R.W. Hawkins M. and Postgate J.R. (1986). The alternative nitrogenase of *Azotobacter chroococcum* is a vanadium enzyme. *Nature*, **322**, 388 – 390

Rosner B. (1994). Reinigung und Charakterisierung der Acetylenhydratase aus *Pelobacter acetylenicus* und Vergleich mit Acetylen-umsetzenden Enzymen aus aeroben Bakterien. Dissertation, Universität Konstanz

Rosner B. and Schink B. (1995). Purification and characterization of acetylene hydratase of *Pelobacter acetylenicus*, a tungsten iron-sulfur protein. *J. Bacteriol.,* **177**, 5767 – 5772

Saiki R.K., Gelfand D.H., Stoffel S., Scharf S.J., Higuchi R., Horn G.T., Mullis K.B. and Erlich, H.A. (1988). Primer-directed enzymatic amplification of DNA with a thermostable DNA polymerase. *Science*, **233**, 1076 – 1078

Saitou N. and Nei M. (1987). The neighbor-joining method: a new method for reconstructing phylogenetic trees. *Mol. Biol. Evol.*, **4**, 406 – 425

Satoh T. and Kurihara F.N. (1987). Purification and properties of dimethylsulfoxide reductase containing a molybdenum cofactor from a photodenitrifier, *Rhodopseudomonas sphaeroides* f.s. denitrificans. *J. Biochem.* (Tokyo), **102**, 191 – 197

Sattler E. and Glombitza K.W. (1975). Synthesis of some polyhydroxyphenyl ethers. *Arch. Pharm.*, **308**, 813 – 818

Schindelin H., Kisker C., Hilton J., Rajagopalan K.V. and Rees D.C. (1996). Crystal structure of DMSO reductase: redox-linked changes in molybdopterin coordination. *Science*, **272**, 1615 – 1621

Schink B. (1984). Fermentation of 2,3-butanediol by *Pelobacter carbinolicus* sp. nov. and *Pelobacter propionicus*, sp. nov., and evidence for propionate formation from C_2 compounds. *Arch. Microbiol.*, **137**, 33 – 41

Schink B. (1985). Fermentation of acetylene by an obligate anaerobe, *Pelobacter acetylenicus* sp. nov. *Arch. Microbiol*., **142**, 295 – 301

Schink B. and Pfennig N. (1982). Fermentation of Trihydroxybenzenes by *Pelobacter acidigallici* gen. Nov. sp. nov., a New Strictly Anaerobic, Non-Sporeforming Bacterium. *Arch. Microbiol.*, **133**, 195 – 201

Schlegel H.G. (1992). Allgemeine Mikrobiologie, 7th edition, Thieme Verlag, Stuttgart

Schneider F., Löwe J., Huber R., Schindelin H., Kisker C. and Knäblein J. (1996). Crystal structure of dimethyl sulfoxide reductase from *Rhodobacter capsulatus* at 1.88 A resolution. *J. Mol. Biol.*, **263**, 53 – 69

Schultz B.E., Hille R. and Holm R.H. (1995). Direct oxygen atom transfer in the mechanism of action of *Rhodobacter sphaeroides* dimethyl sulfoxide reductase. *J. Am. Chem. Soc.*, **117**, 827 – 828

Smith P.K., Krohn R.I., Hermanson G.T., Mallia A.K., Gartner F.H., Provenzano M.D., Fujimoto E.K., Goeke N.M., Olson B.J. and Klenk D.C. (1985). Measurement of protein using bicinchoninic acid. *Anal. Biochem*. **150**, 76 – 85

Sommer S. (1995). Biochemische und spektroskopische Charakterisierung des Molybdoproteins Pyrogallol-Phloroglucin Transhydroxylase aus *Pelobacter acidigallici*. Diplomarbeit, Universität Konstanz

Stewart L.J., Bailey S., Bennett B., Charnock J.M., Garner C.D. and McAlpine A.S. (2000). Dimethyl sulfoxide Reductase: An Enzyme Capable of Catalysis with Either Molybdenum or Tungsten at the Active Site. *J. Mol. Biol.*, **299**, 593 – 600

Stiefel E.I. (1997). Chemical keys to molybdenum enzymes. *J. Chem. Soc., Dalton Trans.*, 3915 – 3923

Strimmer K. and von Haeseler A. (1996). Quartet puzzling: A quartet maximum likelihood method for reconstructing tree topologies. *Mol. Biol. Evol.*, **13**, 964 – 969

Strimmer K. and von Haeseler A. (1997). Likelihood-mapping: A simple method to visualize phylogenetic content of a sequence alignment. *Proc. Natl. Acad. Sci. (USA)*, **94**, 6815 – 6819

Swofford D.L. (1999). PAUP*. Phylogenetic analysis using parsimony (*and other methods). Version 4. Sinauer, Sunderland, Mass.

Temple C.A., George G.N., Hilton J.C., George M.J., Prince R.C., Barber M.J. and Rajagopalan K.V. (2000). Structure of the molybdenum site of *Rhodobacter sphaeroides* biotin sulfoxide reductase. *Biochemistry*, **39**, 4046 – 4052

Thompson J.D., Gibson T.J., Plewniak F., Jeanmougin F. and Higgins D.G. (1997). The ClustalX windows interface: flexible strategies for multiple sequence alignment aided by quality analysis tools. *Nucleic Acids Research*, **24**, 4876 – 4882

Tokunaga M. and Wakatsuki Y. (1998). The first anti-Markownikov hydration of terminal alkynes: formation of aldehydes catalyzed by a Ruthenium(II)/phosphane mixture. *Angew. Chem. Int. Ed.*, **37**, 2867 – 2869

Trieber C.A., Rothery R.A. and Weiner J.H. (1996). Consequences of removal of a molybdenum ligand (DmsA-Ser-176) of *Escherichia coli* dimethyl sulfoxide reductase. *J. Biol. Chem.*, **271**, 27339 – 27345

Van de Peer Y. and De Wachter R. (1993). TREECON: a software package for the construction and drawing of evolutionary trees. *Comput. Applic. Biosci.,* **9**, 177 – 182

Van de Peer Y. and De Wachter R. (1994). TREECON for Windows: a software package for the construction and drawing of evolutionary trees for the Microsoft Windows environment. *Comput. Applic. Biosci.,* **10**, 569 – 570

Van de Peer Y. and De Wachter R. (1997). Construction of evolutionary distance trees with TREECON for Windows: accounting for variation in nucleotide substitution rate among sites. *Comput. Applic. Biosci.,* **13**, 227 – 230

Wächtershäuser G. (1988). Pyrite formation, the first energy source for life: a hypothesis. *Syst. Appl. Microbiol.*, **10**, 207 – 210

Weiner J.H., Rothery R.A., Sambasivarao D. and Trieber C.A. (1992). Molecular analysis of dimethylsulfoxide reductase: a complex iron-sulfur molybdoenzyme of *Escherichia coli*. *Biochim. Biophys. Acta*., **1102**, 1 – 18

Widdel F. (1980). Anaerober Abbau von Fettsäuren und Benzoesäure durch neu isolierte Arten Sulfat-reduzierender Bakterien. Dissertation, Universität Göttingen

Widdel F. and Pfennig N. (1981). Studies an dissimilatory sulfate-reducing bacteria that decompose fatty acids. I. Isolation of new sulfate-reducing bacteria enriched with acetate from saline environments. Description of *Desulfobacter postgatei* gen. nov., sp. nov. *Arch. Microbiol.*, **129**, 295 – 400

Yadav J., Damar K.D. and Sabyasachi S. (1997). A Functional Mimic of the New Class of Tungstoenzyme, Acetylene Hydratase. *J. Am. Chem. Soc.*, **119**, 4315 – 4316

Yamamoto I., Saiki T., Liu S.M. and Ljungdahl L.G. (1983). Purification and properties of NADP-dependent formate dehydrogenase from *Clostridium thermoaceticum*, a tungsten-selenium-iron protein. *J. Biol. Chem.*, **258,** 1826 – 1832

Zehnder A.J.B. and Wuhrmann K. (1976). Titanium (III) citrate as a non-toxic oxidation-reduction buffering system for the culture of obligate anaerobes. *Science*, **194**, 1165 – 1166

Zehr B.D., Savin T.J. and Hall R.E. (1989). A one-step, low background coomassie staining procedure for polyacrylamide gels. *Anal. Biochem*., **182**, 157 – 159

Ziegenhorn J., Senn M. and Bücher T. (1976). Molar absorptivities of ß-NADH and ß-NADPH. *Clin. Chem*, **22**, 151 – 160

6. Appendix

6.1 Abbreviations

Å	Ångstrøm; 1 Å = 10^{-10} m
ADH	Alcohol dehydrogenase
AH	Acetylene hydratase of *Pelobacter acetylenicus*
bp	Basepair
BSA	Bovine serum albumin
BSO/BSOR	Biotin sulfoxide/Biotin sulfoxide reductase
Da	Dalton; 1 Da = 1 g mol^{-1}
DMSO/DMSOR	Dimethyl sulfoxide/ Dimethyl sulfoxide reductase
DNA	Deoxyribonucleic acid
EDTA	Ethylenediaminetetraacetic acid Tetrasodium salt dihydrate
EPR	Electron paramagnetic resonance
FPLC	Fast protein liquid chromatography
HEPES	N-[2-Hydroxy-ethyl]piperazine-N'-[ethanesulfonic acid]
HPLC	High performance liquid chromatography
Hz	Hertz [s^{-1}]
ICP-MS	Inductively coupled plasma mass spectrometry
KPi	Potassium phosphate
LB	Luria-Bertani medium
NADH	Nicotinamide adenine dinucleotide
orf	Open reading frame
PAGE	Polyacrylamide gel electrophoresis
PCR	Polymerase chain reaction
PEG	Polyethylene glycol
PVDF	Polyvinylidene difluoride
S-ADH	*Sulfolobus solfataricus* alcohol dehydrogenase
SDS	Sodium dodecyl sulfate
TEA	Triethanolamine = 2,2',2''-Nitrilotriethanol = Tris(2-hydroxyethyl)amine
TH	pyrogallol:phloroglucinol hydroxyltransferase, E.C. 1.97.1.2 = Transhydroxylase of *Pelobacter acidigallici*
TMAO/TMAOR	Trimethylamine-N-oxide/Trimethylamine-N-oxide reductase

Tris	Tris-(hydroxymethyl)-aminomethane
UV/Vis	Ultraviolet/Visible light
v/v	Volume per volume
w/v	Weight per volume
Y-ADH	Yeast alcohol dehydrogenase

6.2. Amino acids

A	Ala	alanine	M	Met	methionine
B	Asx	Asn or Asp	N	Asn	asparagine
C	Cys	cysteine	P	Pro	proline
D	Asp	aspartate	Q	Gln	glutamine
E	Glu	glutamate	R	Arg	arginine
F	Phe	phenylalanine	S	Ser	serine
G	Gly	glycine	T	Thr	threonine
H	His	histidine	V	Val	valine
I	Ile	isoleucine	W	Trp	tryptophan
K	Lys	lysine	Y	Tyr	tyrosine
L	Leu	leucine	Z	Glx	Gln or Glu

Adapted from *Eur. J. Biochem*. (1985), **150**, 1 – 5

6.3. Nucleic acid bases

A		*a*denine	S	G/C	*s*trong
G		*g*uanine	W	A/T	*w*eak
C		*c*ytosine	B	G/C/T	not A
T		*t*hymine	D	A/G/T	not C
R	A/G	pu*r*ine	H	A/C/T	not G
Y	C/T	p*y*rimidine	V	A/G/C	not T
K	G/T	*k*eto group	N	A/G/C/T	a*n*y
M	A/C	a*m*ino group	I	inosine	"wobble" to U/C/A/T

Adapted from *Eur. J. Biochem*. (1985), **150**, 1 – 5

6.4. International System of Units (SI)

In this work the *International System of Units SI*, shown in the standard DIN 1301 is used. Conversions to non-legal, historical units were done according to the Physikalisch Technische Bundesanstalt, Braunschweig. An overview on SI base units, SI prefixes, SI units, and non-legal units including conversion rates is available at http://www.ptb.de/english/misc/sie.pdf (English version) or http://www.ptb.de/deutsch/onlnpub/sid/sid.pdf (German version).

6.5. Acknowledgements

Danksagung

Mein besonderer Dank geht an Prof. Dr. Peter M.H. Kroneck für die Betreuung und Unterstützung der vorliegenden Arbeit, für die Förderung der Zusammenarbeit mit anderen Labors sowie für die Ermöglichung des Besuches von (inter)nationalen Tagungen und Kursen.

Prof. Dr. Bernhard Schink danke ich für die Übernahme des Coreferates dieser Arbeit und für die Möglichkeit, in seinem Labor die Anzucht von *Pelobacter acetylenicus* sowie *Pelobacter acidigallici* und die Reinigung der Acetylenhydratase erlernen zu können.

Bei Dr. Rainer U. Meckenstock möchte ich mich für die Hilfe bei der Bakterienanzucht, Proteinreinigung und die Einführung in die Biochemie der Acetylenhydratase bedanken.

Prof. Dr. Robert Huber danke ich für die Möglichkeit, in der Abteilung Strukturforschung am Max-Planck-Institut für Biochemie in Martinsried Kristallisationsexperimente durchführen zu können.

Ein Dank geht an Dr. Oliver Einsle und Dr. Holger Dobbek vom Max-Planck-Institut für Biochemie, die mich tatkräftig bei der Kristallisation der Transhydroxylase und der Acetylenhydratase unterstützt haben, und an alle anderen Mitglieder der Abteilung Strukturforschung, die jeden Aufenthalt in München zu einem unvergessenen Erlebnis machten.

Prof. Dr. Axel Meyer danke ich für die Möglichkeit, in seiner Arbeitsgruppe die DNA Sequenz der Acetylenhydratase aufklären und die phylogenetische Analyse durchführen zu können.

Dr. Henner Brinkmann danke ich für die vielfältige Unterstützung während der Sequenzierungsarbeiten und der Durchführung der phylogenetischen Analyse sowie für seine unendliche Geduld bei der Beantwortung meiner Fragen.

Diese Arbeit wurde durch das Schwerpunktprogramm „Radikale in der enzymatischen Katalyse“ der Deutschen Forschungsgemeinschaft (DFG) unterstützt.

Außerdem möchte ich mich bedanken bei …

meinen Eltern und Geschwistern, ohne deren Unterstützung ich nie soweit gekommen wäre.

allen, die mir bei der Erstellung der Doktorarbeit mit Rat und Tat geholfen haben, insbesondere bei den Mitgliedern der Arbeitsgruppe Kroneck:
Thomas Büchert, Dorrit Griesshaber, Hendrik Küpper, Frank Neese, Holger Nießen, Alexander Schiffer, Petra Stach, Alma Steinbach, Klaus Sulger und Anja Tabbert, sowie bei Norbert Huber, Andreas Kappler und Jens Seckinger.

meinen Vertiefungskursstudenten Jutta Hellstern, Susanne Buschke und Hans Zauner für ihre Hilfe und Mitarbeit bei zahlreichen Versuchen.

meinen Freunden aus den verschiedenen Fakultäten der Uni Konstanz für viele Feten, Fußballspiele, Fitnessgymnastiken, Joggingrunden und Praktikumsprotokolle.

Robert Bez und Reiner Schroff für viele Abende bei Bier und Wein sowie allen anderen Mitbewohnern in Hegne für die gute Atmosphäre im Haus.

dem Doschdeg Schdammdisch, dem Musikverein, dem TSV und allen anderen Freunden und Bekannten für geniale Oich-Feschde, Kegelabende, Fußballübertragungen, Zeltfeschde, Schdammdische, Ausflüge, Spiele, Urlaube, Geburtstagsfeten, Zockernachmittage, ...

6.6. Curriculum vitae

Personal Data:

Name: Dietmar Josef Abt

Born: 02.05.1970 (Albstadt Ebingen, Germany)

Education:

Since August 1998	Ph. D. Thesis in the group of Prof. P.M.H. Kroneck, Universität Konstanz: Tungsten-acetylene hydratase from *Pelobacter acetylenicus* and molybdenum-transhydroxylase from *Pelobacter acidigallici*. Two novel molybdopterin and iron-sulfur containing enzymes
May 1999	EU-ESF Advanced practical training course "Chemistry of metals in biological systems", Louvain-la-Neuve, Belgium
15.09.1998	Diploma in Biology
29.06.1998	Erstes Staatsexamen (secondary school teacher degree) in Biology and Chemistry
1997 - 1998	Diploma Thesis in the group of Prof. P.M.H. Kroneck, Universität Konstanz: Nitritreductase aus sulfatereduzierenden Bakterien: Reinigung, biochemische und spektroskopische Charakterisierung.
1991 - 1998	Student of Chemistry and Biology, Universität Konstanz, Germany
1989 - 1991	Army, Fernmeldebataillon 10, Sigmaringen, Germany
02.05.1989	Matriculation, Gymnasium Albstadt Ebingen, Germany
1980 - 1989	Gymnasium Albstadt Ebingen, Germany
1976 - 1980	Primary School at Harthausen, Germany

6.7. Publications

Kroneck P.M.H. and Abt D.J., in "Molybdenum and Tungsten. Their Roles in Biological Processes", Vol. 39 of 'Metal Ions in Biological Systems', A. Sigel and H. Sigel, eds.; M. Dekker Inc., New York, 2002, in press.

Abt D.J., Einsle O., Nießen H., Krieger R., Messerschmidt A., Schink B. and Kroneck P.M.H. (2001). Crystallization and preliminary X-ray analysis of the molybdenum dependent pyrogallol-phloroglucinol transhydroxylase of *Pelobacter acidigallici*. *Acta Cryst. D*, submitted.

Abt D.J., Brinkmann H., Meyer A., Schink B. and Kroneck P.M.H. (2001). Evolution of the Molybdopterin-containing proteins of the DMSO-reductase family. in preparation

Abt D.J. (1998). Nitritreductase aus sulfatereduzierenden Bakterien: Reinigung, biochemische und spektroskopische Charakterisierung. Diplomarbeit, Universität Konstanz

6.8. Conference abstracts

Abt D.J., Nießen H., Schink B. and Kroneck P.M.H. (2001). Novel bacterial molybdopterin enzymes: Mo-transhydroxylase and W-acetylene hydratase. 10th International Conference on Bioinorganic Chemistry (ICBIC 10), Florence, Italy

Abt D.J., Schink B. and Kroneck P.M.H. (2000). Structural characterization of two novel molybdopterin containing enzymes: W-acetylene hydratase and Mo-transhydroxylase. DFG-Priority Programme: Radicals in enzymatic catalysis, Schloß Rauischholzhausen

Abt D.J., Einsle O., Dobbek H., Huber R. and Kroneck P.M.H. (2000). Pyrogallol-phloroglucinol transhydroxylase of *Pelobacter acidigallici*. Crystallisation, biochemical and spectroscopic properties. *Biospektrum* (Sonderausgabe 2000)

Abt D.J., Dobbek H., Baas D., Reichenbecher W., Huber R., Rétey J., Schink B. and Kroneck P.M.H. (1999). The Mo-enzyme pyrogallol-phloroglucinol transhydroxylase of *Pelobacter acidigallici*. Crystallization, biochemical and spectroscopic properties. EU-ESF Advanced practical training course "Chemistry of metals in biological systems", Louvain-la-Neuve, Belgium

Abt D.J., Dobbek H., Baas D., Reichenbecher W., Huber R., Rétey J., Schink B. and Kroneck P.M.H. (1999). Pyrogallol-phloroglucinol transhydroxylase of *Pelobacter acidigallici*. New aspects in crystallization, biochemical and spectroscopic properties. *Biospektrum* (Sonderausgabe 1999).